Simulation of non-linear response of a shear wall and foundation comparing finite- and macro element techniques

by
Aðalsteinn Már Ólafsson

Thesis
**Master of Science in Civil Engineering
with specialization in Structural Design**

February 2012

Simulation of non-linear response of a shear wall and foundation comparing finite- and macro element techniques

Aðalsteinn Már Ólafsson

Thesis submitted to the School of Science and Engineering
at Reykjavík University in partial fulfillment
of the requirements for the degree of
**Master of Science in Civil Engineering
with Specialization in Structural Design**

February 2012

Supervisors:

   Eyþór Rafn Þórhallsson,
   Associate Professor, Reykjavík University, Iceland
   Dr. Jónas Þór Snæbjörnsson,
   Professor, Reykjavík University, Iceland

Examiner:

   Dr. Rajesh Rupakhety,
   Adjunct Professor, University of Iceland, Iceland

Abstract

Reinforced concrete shear walls have proven to be very effective in resisting lateral loads produced in structures during earthquake action. To ensure reliability in the design of such walls, the response to earthquake induced actions should ideally be analyzed using the non-linear properties of the wall as well as considering external non-linearity effects such as soil-structure interaction. Preferably a range of earthquake records should be used in the analysis process to get a good overview of the structural response since the structure and the substructure can be sensitive to the magnitude, load pattern and frequency content of the earthquake. This type of analysis is only possible using computer models. The most common method used for computer modeling of structures is the finite element method. The use of the finite element method to solve earthquake response of the models when considering all the involved non-linearities is a time consuming process. Therefore designers generally rely on simplified formulations and empirical methods provided within design codes. The shortcomings of using design codes is that the formulas provided rely on a rather limited set of shape functions and spectral charts to determine the earthquake induced responses. Non-linear effects are mostly considered indirectly through estimated behavior factors and soil classifications.

To address the need for improved earthquake design process there is an ongoing development of macro elements that can replace the use of standard finite elements for non-linear analysis. The use of macro elements instead of finite elements can reduce the scope of the model and thus reduce the time needed to calculate the earthquake induced response. The drawback of using macro elements are that the equations are based on certain assumptions and simplifications which engineers must be aware of to be able to choose the appropriate elements for their analysis and as a result macro elements are less versatile than the standard finite elements.

This study compares the use of finite and macro elements utilized to model a squat shear wall resting on a soil bed to be used for simulation of earthquake induced response. The programs used are Ansys for the finite element modeling and OpenSees for macro element modeling.

The results show that for a lateral pushover test the macro elements response to loading still lacks non-linear capabilities when using the finite element calculations as a baseline. For the soil modeling the macro element model is found to be much simpler in setup than the finite element model but needs special care in calibration of the end stiffnesses. The simulation of granular soil in the finite element model was problematic and could use further investigation.

In all the tests performed the non-linear macro element model calculations were solved within minutes from executing the analysis while the non-linear finite element models required from few hours to some days to solve.

Based on the comparison of these case studies, a simulation trying to capture non-linear behavior of material and deformation of the wall is still somewhat lacking when using these macro elements, the setup of the BNWF is simple enough but the end stiffness needs to be

attuned so as the both models would yield similar results. The benefit in reduced calculation time is however apparent and a reason enough to continue the development of macro elements for earthquake response calculations.

Útdráttur

Járnbentir steinsteyptir skerveggir hafa sannað gildi sitt þegar kemur að því að standast lárétta áraun í jarðskjálftum. Til að tryggja að hönnun slíkra veggja sé fullnægjandi ætti svörun þeirra við jarðskjálftaáraun að vera greind með tilliti til ólínulegra eiginleikja veggjarins sem og ólínulegra áhrifa vegna víxlverkunar milli jarðvegs og byggingar. Til að fá góða mynd af svöruninni er æskilegt að nota fjölda af jarðskjálftaröðum þar sem stærð, stefna og tíðni innihald jarðskjálfta hefur áhrif á svörun veggjar. Helsta aðferðin til að reikna svörun við jarðskjálftaáraun er að nota tölvulíkön sem nýta sér einingaraðferðina til útreikninga, en hún getur orðið bæði flókin og seinleg þegar um ólínulega greiningu er að ræða. Þess í stað nota hönnuðir hönnunarstaðla og reynslujöfnur sem gefnar eru upp í þeim. Þessar reynslujöfnur eiga þó aðeins við um takmarkað sett af formum byggginga og svörunarrófa, sem er ókostur. Þar kemur ólínuleg hegðun einungis óbeint við sögu í gegnum val á hegðunarstuðli. Jafnframt þá gilda staðalleiðbeiningar fyrst og fremst fyrir einföld regluleg mannvirki auk þess sem form svörunarrófs er staðlað og eingöngu háð vali á grunnhröðunargildi og jarðvegsflokki. Þessi tvö skilyrði henta oft illa raunverulegum óreglulegum mannvirkjum nálægt upptökum jarðskjálfta.

Til þess að hagkvæmt sé að hanna veggi með ólínulegum tölvulíkönum þarf að stytta þann reiknitíma sem núverandi einingaraðferð tekur, sérstaklega þegar tekið er tillit til áhrifa grundunnar. Til þess hafa verið hannaðar fjöleiningar (macro elements) sem herma eftir afmörkuðum þáttum í hegðun burðareininga. Takmörkun á hegðun fækkar þeim jöfnum sem þarf að reikna og þar af leiðandi taka slíkir útreikningar skemmri tíma. Aftur á móti þarf hönnuðurinn að gera sér grein fyrir takmörkunum fjöleininganna þannig að viðeigandi fjöleiningar séu valdar fyrir viðeigandi burðareiningu. Niðurstöðurnar eru einnig takmarkaðri þar sem ekki er lengur hægt að fylgjast með hegðun einstakra eininga í líkaninu.

Í þessari rannsókn er gerður samanburður á lágum skerveggjum þar sem svörun líkana sem notast við einingar- og fjöleiningaraðferð eru borin saman. Tekið er tillit til ólínulegra eiginleika steinsteyptra veggja og svo jarðvegs og þeirrar víxlverkunar sem á sér stað milli jarðvegs og veggjar. Einingarlíkön eru sett upp í forritinu ANSYS en fjöleiningarlíkön í OpenSees.

Fjöleiningarlíkönin þar sem veggirnir urðu fyrir hliðaráraun sýndu að ólínulegum eiginleikum fjöleininganna er ábótavant þegar miðað er við niðurstöður einingaraðferðarinnar. Þegar jarðvegshluti líkansins var skoðaður kom í ljós að fjöleiningaraðferðin var heppilegri til að herma eftir svörun jarðvegs en þó þarf að stilla endastífleika líkansins til að samræmast betur niðurstöður einingarlíkansins. Það er nokkrum erfiðleikum háð að herma eftir efniseiginleikum kornótts jarðvegs þegar notast er við einingaraðferð og þarfnast frekari skoðunar.

Líkön sem voru gerð með fjöleiningaraðferð voru yfirleitt reiknuð á fáeinum mínútum, aftur á móti líkön gerð með einingaraðferð voru reiknuð á nokkrum klukkustundum og upp í nokkra daga.

Þegar báðar aðferðirnar eru bornar saman kemur í ljós að fjöleiningarnar skila ekki nógu góðum niðurstöðum þegar þær eru notaðar til að herma eftir broti veggjar. Hinsvegar er munur í reiknitíma það mikill að það réttlætir frekari rannsóknir til að fá fjöleiningar til að ná að herma betur eftir hegðun skerveggja.
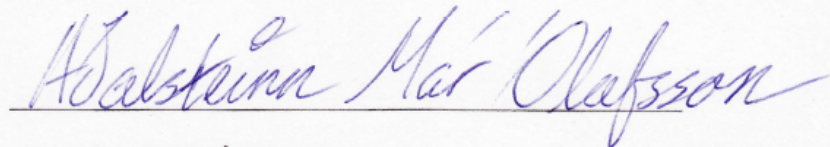
Simulation of non-linear response of a shear wall and foundation comparing finite- and macro element techniques

Aðalsteinn Már Ólafsson

Thesis submitted to the School of Science and Engineering
at Reykjavík University in partial fulfillment
of the requirements for the degree of
**Master of Science in Civil Engineering with
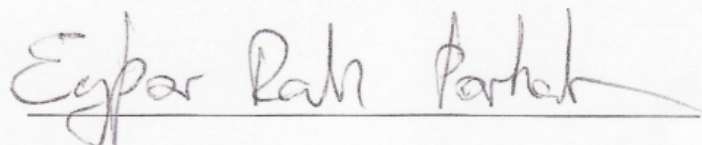Specialization in Structural Design**
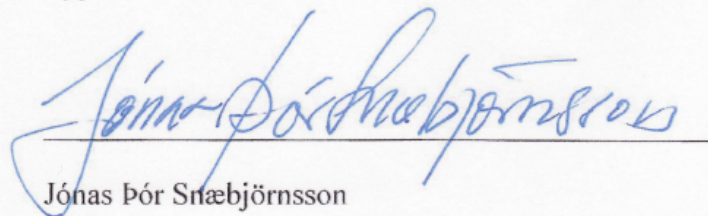
February 2012
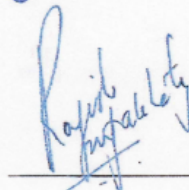
Student:

Aðalsteinn Már Ólafsson

Supervisors:

Eyþór Rafn Þórhallsson

Jónas Þór Snæbjörnsson

Examiner:

Rajesh Rupakhety

Contents

List of Figures

List of Tables

List of Symbols

Capital symbols

A_n, A_{t1}, A_{t2}	Area of soil interfaces, normal, horizontal and vertical respectively.
A_g	Gross cross sectional area of a wall.
B	Characteristic length of a foundation.
B_f	Breadth of footing.
C_n, C_{t1}, C_{t2}	Damping acting at soil interface, normal, horizontal and vertical damping respectively.
C_r	Elastic range of the BNWF soil springs.
D_f	Depth of the embedment of the BNMWF footing.
E, E_c, E_s	Young's modulus and subscript for concrete and steel respectively.
E'_s, E_t	Young's modulus of steel after yielding.
G, G_c	Shear modulus and shear modulus of concrete respectively.
I_0	Rotational inertia of a rocking block.
K	Stiffness matrix.
K_{0ij}	Static stiffness component such as K_z and K_h etc.
K, K_x, K_ϕ	Flexural stiffness of a member the foundation and rotational stiffness of the foundation respectively. K is also a factor used in the Kent and Park concrete model but is not related to stiffness.
K_p	Post-yield stiffness of the BNWF soil springs.
K_{unl}	Unloading stiffness of the BNWF soil springs.
K_z, K_r, K_t, K_h	Vertical, rocking, torsional and horizontal stiffnesses respectively.
$K_{ij}(\omega)$	Component of stiffness as a function of frequency.
$\Re(K_{ij})$	Real part of a stiffness component, the actual stiffness.
$\Im(K_{ij})$	Imaginary part of a stiffness component, damping properties of the stiffness.
L	Length of the footing.

L_{end}	Length of the end regions in the BNWF model.
M	Mass.
M_ω	Earthquake magnitude on the Richter scale.
N_n, N_{t1}, N_{t2}	Forces acting on faces of soil interfaces, normal, horizontal and vertical respectively.
P_{ult}	Passive resistance capacity of the BNWF model.
Q_{ult}	Vertical bearing capacity of the BNWF model.
$\mathbf{R}$	Force matrix.
R_e	Ratio of the length of footing that denotes the end regions where stiffer springs are placed in the BNWF model.
R_k	Stiffness ratio of the end springs in the BNWF model.
T_{ult}	Sliding resistance capacity of the BNWF model.
TP	Tension capacity of soil in the BNWF model.
Z	Factor used in the Kent and Park concrete model.

Lower case symbols

a, r_0	Radius of a rigid massless disc.
a_0	Kinematic damping component.
c	Cohesion of soil.
c_{ij}	Frequency dependent coefficient.
c_{rad}	Radiational damping properties.
c_p, c_s	Pressure and shear wave velocity respectively.
c_p^L, c_p^R	Velocity of dilational pressure wave in soil layer and rock respectively.
d	Depth of a soil layer.
f_c'	Compressive cylinder strength.
f_{cr}	Factor for how much of the cracked concrete section is effective as a shear spring.

f_t	Tensile yield strength concrete.
f_y	Tensile yield strength of steel.
f_{yh}	Yield strength of transverse reinforcement in Kent and Park concrete model.
f_x	Force acting in local x-direction of finite element.
h	Height.
h'	The width of concrete core measured to the outside of the stirrups in the Kent and Park concrete model.
i	Imaginary number $\sqrt{-1}$.
ij	The subscript$_{ij}$ refers to the ij'th component in a matrix.
k_{ij}	Frequency dependent coefficient.
s_h	The spacing of stirrups in the Kent and Park concrete model.
t	Time.
$\mathbf{u}$	Displacement matrix.
$u,\ u_g,\ u_f,\ u_e$	Displacement of the SSI system, the ground, the foundation and flexural displacement.
$\dot{u}_n,\ \dot{N}_{t1},\ \dot{N}_{t2}$	Velocities of the nodes at soil interfaces in normal, horizontal and vertical direction respectively.
$\ddot{u},\ \ddot{u}_g,\ \ddot{u}_f,\ \ddot{u}_e,\ \ddot{\phi}_f$	Acceleration of the SSI system, ground, foundation and acceleration of the flexure respectively.
z	Displacement of a massless disc in the vertical direction.
$z_0^L,\ z_0^R$	Opening angle for a cone in the soil layer and rock respectively.

Greek symbols

α	Angle that a line from the corner to center of gravity makes with the vertical edge of a rocking block.
α_s	Geometrical factor that determines the shear coefficient for sections.
$-\alpha$	Reflection coefficient for waves.

β	Factor used to calculate Drucker-Prager yield surface in relation to ϕ.
β_t, β_c	Open and closed coefficients respectively for shear transfer of concrete cracks.
γ	Unit weight.
ϵ, ϵ_{20}	Strains in the concrete and 20% of the strain at peak compressive strength in the Kent and Park concrete model.
ζ	Damping ratio to account for material damping of the soil.
θ	The changing angle of a rocking block to the ground.
ν	Poisson's ratio.
π	Ratio of a circle's circumference to its diameter.
ρ, ρ_L	Density, subscript denotes soil layer density.
ρ_s	Ratio of steel reinforcement for Kent and Park concrete model.
$\sigma_{1,2,3,11,22,33,12,13,23}$	Stress tensor components.
σ_c, f'_c	Compressive strength of concrete and compressive cylinder strength respectively.
σ_n, τ_{t1}, τ_{t2}	Stresses in soil interface normal, and shear respectively.
$\sigma_{xx,zz,yx,zx}$	Stresses action on planes of a finite element.
υ	Poisson's ratio.
ϕ	Angle of friction of granular soil.
ϕ_f	Rotation of a foundation.
ψ	Dilation angler of granular soil.
ω_n^2	Natural frequency of a system.

Abbreviations

BEM	Boundary element method.
BNWF	Beam on non-linear Winkler foundation.
DOF	Degrees of freedom.

DP	Drucker-Prager.
EC8	Eurocode 8.
FE	Finite element.
FEM	Finite element method.
ÍST-13	Íslenskur staðall (outdated Icelandic design code).
ME	Macro element.
MVLEM	Multiple-vertical-line-element model.
PEER	Pacific Earthquake Engineering Research Center.
SSI	Soil-structure interaction.

1 Introduction

1.1 Earthquakes and Earthquake Engineering

One of the primary tasks of a structural engineer in the design process of a structure is to guarantee the load bearing capacity of the structural components while keeping the cost to a minimum. Many different factors play a role in such design process such as type of structure, function, life span and location to name but a few. For example, geographical location determines if a structure has to be designed to withstand earthquakes.

Earthquakes are generally caused by fault movements between tectonic plates. Body waves travel in all directions from the center of the earthquake. There are two types of body waves; the primary or pressure wave (P-wave) travels from the center by alternating compression and rarefaction in the conducting medium. The secondary or shear wave (S-wave) is a transverse wave traveling perpendicularly to its propagation causing shear deformation in the conducting medium. The traveling pattern of these waves can be seen in figure 1a. At the earth's surface these two body waves are polarized and become surface waves, named Rayleigh and Love waves. The motion of these waves can be described as follows; Rayleigh wave is a vertical wave and moves similarly to ripples in water while Love waves cause lateral movements of the earth in a motion like a moving snake, see figure 1b [38]. The waves cause ground movements, inertia of structures and their mass inevitably produces lateral loads and rotational moments in response to the ground movements. Therefore the vertical bearing components of structures such as shear walls and columns must be designed to endure these lateral loads [11].

(a) Body waves   (b) Surface waves
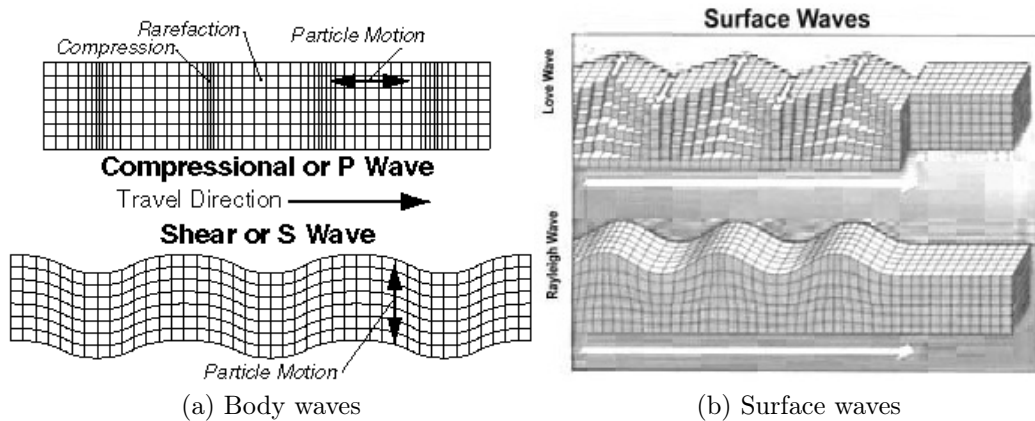
Figure 1: Two dimensional picture of body waves and surface waves.

To estimate these loads engineers need to understand the response of the ground as well as the response of the structural components during an earthquake. Soil properties play a big part when determining the speed of the body waves and the frequency and acceleration of the polarized counterparts. The ductility of the structure and masses define its inertia and therefore the forces generated. Rocking and translation of the foundation also affects the response of the structure. The impinging of the footing of the structure on the soil when rocking occurs can also alter the

earthquake wave pattern in the medium beneath it. All of the above is commonly referred to as soil-structure interaction (SSI).

In the $M_\omega = 6.3$ earthquake in Olfus, Iceland in the year 2008, foundation rocking as described above is believed to have occurred. Many buildings in the earthquake affected area were damaged in the earthquake but reports of collapse were almost none. Many of the buildings of the area were designed and built prior to the introduction of the earthquake design codes ÍST-13 and Eurocode 8 (EC8) [16] and were therefore not built to the specifications of those codes. If the assumptions made in EC8 are used to calculate the design force of the Olfus earthquake many of the buildings should have collapsed entirely. The fact that the buildings did not collapse indicates that the simplifications within the code do not capture the actual behavior of the buildings during the earthquake.

Rocking and translational movement of the foundation has been shown to lower base shear loads made from the assumptions made by the formulation provided by EC8 [42] which could explain why the buildings did not collapse.

Eurocode 8 allows the designer to deviate from the prescribed methods providing that full scale earthquake testing is performed on either a computational or a scaled model to guarantee that the design fulfills the code requirements. Such a testing of a simple computational model that is able to simulate SSI and non-linear material behavior is a time consuming project when using the conventional finite element method (FEM). A multitude of earthquake records must be tested to get a good estimation of the performance of the structure and that increases the time needed to check the intended design of the structure. This type of testing of a design project is therefore still mostly confined to academic projects and design of important structures such as nuclear power plants, dams and bridges. With increased computational power made available in the recent years and recent advances in the design of macro elements (ME) used to represent structural models the time needed to perform a computational earthquake testing can be reduced enough to make it a viable design option. The macro elements are, however, not as versatile as finite elements and the limitations of ME puts extra demand on the engineer to choose the right elements to use for a given structural component as well as in interpreting the results correctly.

1.2   Aim and Objectives of the Research

In this study an attempt will be made to use macro elements available in OpenSees to mathematically model a squat shear wall subjected to earthquake induced loads. At the foundation level SSI will be taken into consideration. To verify the performance of the ME models the same models will be analyzed using ANSYS and finite elements (FE). The analysis will be done in the following steps to assess the performance of the macro elements representing the wall and the macro elements representing the SSI system.

1. A case of a squat shear wall rigidly connected to the ground subjected to lateral pushover test.

2. A comparison of a SSI system where the wall rests embedded in sand with an inverted T-type footing using cyclic load test comparison.

1.3 Thesis outline

This paper is divided into five chapters. The first chapter outlines the reasons and structure of the research done.

Second chapter covers some aspects of SSI such as the static and dynamic response of the soil using fundamental solutions. Rocking of structures is briefly discussed. The finite element method is described as well as the division of the model domain into near- and far-field. At last the cone model method to derive dynamic stiffness of soil is described to show how methods of simplification can be made to capture the complex SSI behavior.

The third chapter the choice of programs is explained. The macro elements and their function are described. The elements used for Ansys are listed and material models are described.

Fourth chapter covers the attuning of the finite element and macro element models.

The fifth chapter displays the results and comparison of lateral pushover tests of the wall models and the results for soil-structure interaction model subjected to vertical harmonic loading of 1 Hz and 5 Hz.

In the sixth chapter the results are discussed as well as future research possibilities.

1.4 Tools used for this study

In this study Ansys version 12.1 is used and OpenSees version 2.3.1 and 2.2.2. The analysis of the finite element models are done on a machine with an Intel dual-core 2.4 MHz processor and 8.0 GB ram utilizing both cores. The macro element models are solved on a machine with an Intel dual-core 3.0 GHz processor and 16.0 GB ram utilizing one of the cores. Data processing is done with Excel 2007 and Visual Basics. The paper is written with LaTeX.

2 Review of Literature

This chapter provides insight into how to mathematically represent a model of a structure subjected to earthquake loads. The main focus is on the fundamental solutions for the response of the soil, then the finite element method is briefly described and the discretization between near- and far-field. At last the cone model method is described to show how analytical methods can be used to replace complex fundamental solutions.

2.1 Soil-Structure Interaction

Soil-structure interaction can be summarized in short as how a structure and the soil on which it's built behave as a coupled system when subjected to an earthquake. Several different aspects affect the system such as the soil composition, which may cause amplification of seismic waves [19], rocking of a structure and the feedback by a structure's inertia as well as reflection of earthquake waves back into the soil domain at the free-field and structure interface. To capture this complicated behavior with a mathematical model is a difficult procedure. A common practice is to separate the structure and the ground, simplifying the model and to allow for a better insight for each part and then find a compliance function at the interface to couple the whole model through superimposition of the separate parts [43].

2.1.1 A case of Soil-Structure Interaction

To realize the importance of SSI let us consider lateral movement of a mass in a two degrees-of-freedom (DOF) system where the structure is free to move laterally and to rotate at its foundation such as in figure 2.

$$u = u_g + u_f + \phi_f h + u_e \tag{1}$$

The total displacement of the mass u is the sum of the ground displacement u_g, the horizontal displacement of the foundation u_f, displacement due to the foundation rotation ϕ_f and the flexural deformation of the column supporting the mass u_e. The acceleration of the mass $\ddot{u}$ is then the sum of the rate of change of all the components:

$$\ddot{u} = \ddot{u}_g + \ddot{u}_f + \ddot{\phi}_f h + \ddot{u}_e \tag{2}$$

Equilibrium states that the restoring forces that are stored in the column due to a displacement are equal to the acceleration of the mass M, the restoring force is related to the flexural stiffness K of the column:

$$M\ddot{u} + Ku_e = 0 \tag{3}$$
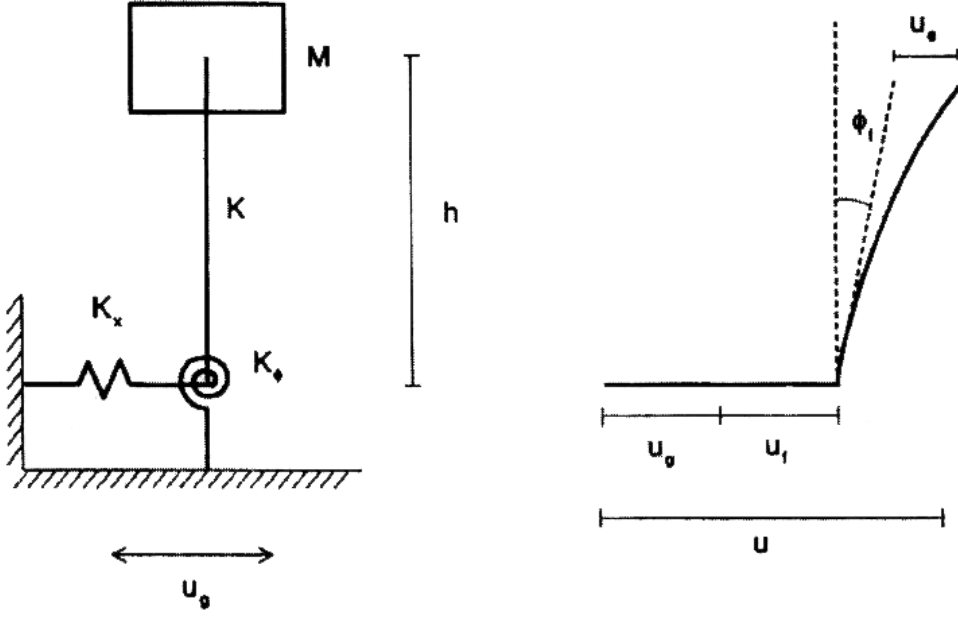
Figure 2: Illustrative picture to describe SSI compliance (from Dominguez [9]).

The two equilibrium equations of the flexural member:

$$K_x \ddot{u}_f = K \ddot{u}_e \tag{4}$$

$$K_\phi \ddot{\phi}_f = K \ddot{u}_e h \tag{5}$$

By rearranging equations 4 and 5 the following relationship can be made:

$$\ddot{u}_f = \frac{K}{K_x} \ddot{u}_e \tag{6}$$

$$\ddot{\phi}_f = \frac{Kh}{K_\phi} \ddot{u}_e \tag{7}$$

K_x is the lateral stiffness of the foundation, K_ϕ is the rotational stiffness and $\ddot{\phi}_f$ the rate of change of the rotation, $\ddot{u}_g$ and $\ddot{u}_f$ are the acceleration of the ground and foundations respectively. Substituting into equation (2) the acceleration of the system becomes:

$$\ddot{u} = \ddot{u}_g + \left(\frac{K}{K_x} + \frac{Kh^2}{K_\phi} + 1 \right) \ddot{u}_e \tag{8}$$

Thus the equilibrium equation (3) becomes:

$$M \left(\frac{K}{K_x} + \frac{Kh^2}{K_\phi} + 1 \right) \ddot{u}_e + K u_e = -M \ddot{u}_g \tag{9}$$

6

If this is compared to a system with a rigid foundation i.e. infinite stiffness of K_x and K_ϕ the above equation is simplified to:

$$M\ddot{u}_e + Ku_e = -M\ddot{u}_g \tag{10}$$

The natural frequency of the SSI system is:

$$\omega_n^2 = \frac{K}{M} \frac{1}{\left(\frac{K}{K_x} + \frac{Kh^2}{K_\phi} + 1\right)} \tag{11}$$

And the natural frequency with a rigid base is:

$$\omega_n^2 = \frac{K}{M} \tag{12}$$

It is clear that the foundation flexibility has impact on the acceleration of the mass and the natural frequency ω_n^2 of the system [9].

2.2   Fundamental Solutions

In the early twentieth century the soil stiffness had to be determined by fundamental solutions. The displacements in the soil due to excitation at an arbitrary location had to be determined. The solution for the displacement within solid elicited by static force at an arbitrary location was first posed by Lord Kelvin in 1848. Further advances in the field were made by Stokes who calculated the response due to a harmonic force in 1849. These solutions considered a infinite solid but the involved integrals were later used to obtain solutions for stresses in a soil by load on a circular disc resting on at the top of a half-space layer. The following equations mathematically represent the soil stiffness for translation, rocking and torsion when the load is applied to a rigid circular disc resting at the top of the soil;

The vertical stiffness K_z obtained by Boussinesq in 1885:

$$K_z = \frac{4Ga}{1 - \upsilon} \tag{13}$$

Rocking stiffness K_r discovered by Borowicka in 1943 (same as k_ϕ in the previous chapter):

$$K_r = \frac{8Ga^3}{3(1 - \upsilon)} \tag{14}$$

Torsional stiffness K_t derived in 1944 by Erich Reissner:

$$K_t = \frac{16Ga^3}{3} \tag{15}$$
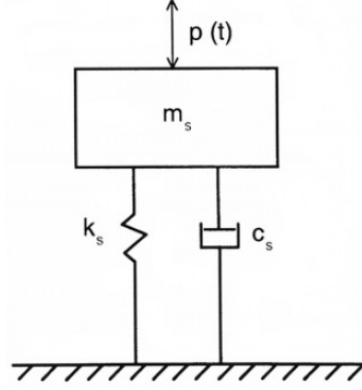
Figure 3: Mass-spring-damper analog system (from Dominguez [9]).

And finally horizontal stiffness K_h discovered by Mindlin in 1949 (same as K_x in the previous chapter):

$$K_h = \frac{8Ga}{2 - \upsilon} \tag{16}$$

In the above equations a is the radius of the plate, G the shear modulus of the soil and υ the Poisson's ratio [19].

Prior to discovering torsional stiffness Reissner had come up with as solution for the dynamic vertical response for a said massless disc in 1936. Although his solution was incomplete his insight regarding radiation damping and the use of equivalent mass-spring-damper analog system seen in figure 3 are still used as the foundation for the boundary element method (BEM) [19, 9].

In 1971 Veletsos and Wei completed the expression for dynamic stiffness of a circular rigid foundation. Their solution considers a harmonic moment and horizontal loads [43]. The response of such a disc is summarized as:

$$\mathbf{R} = \mathbf{K}\mathbf{u} \tag{17}$$

$\mathbf{R}$ is the force matrix, $\mathbf{K}$ is the dynamic stiffness matrix and $\mathbf{u}$ the corresponding matrix consisting of displacements and rotations. The same notation is used when describing a static case except here the stiffness matrix $\mathbf{K}$ is a function of the load frequency ω. Each stiffness component of the matrix is expressed as:

$$K_{ij}(\omega) = \Re(K_{ij}) + i\Im(K_{ij}) \tag{18}$$

The real part is the actual stiffness and inertia of the soil while the imaginary part is the corresponding damping. The main damping is due to radiation, material damping is included later in the formulation. Since the radiation damping is frequency dependent the stiffness component is usually taken as:

$$K_{ij} = K_{0ij}(k_{ij} + ia_0c_{ij}) \tag{19}$$

K_{0ij} is the static value of the stiffness as in equations (13,14,15,16), the subscript ij refers to the stiffness component in the matrix, k_{ij} and c_{ij} are coefficients dependent on the frequency of the
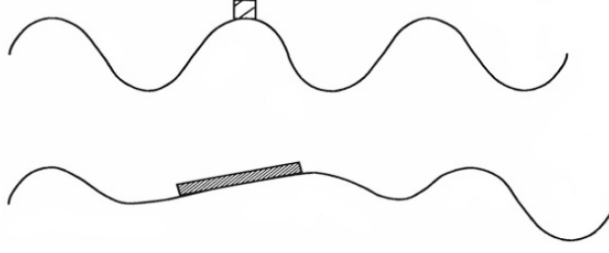
Figure 4: Simplified image of kinematic interaction, a small structure does not alter the wave input like a large structure (from Dominguez [9]).

soil. Kinematic interaction is determined by $a_0 = \omega B/c_s$ where B is the characteristic length of the foundation and c_s is the shear wave velocity in the soil[1]. Kinematic interaction is described by Dominguez as where the size of the foundation can alter the traveling wave in the soil. A very idealized case of kinematic effects is shown in figure 4. Finally, material damping properties of the soil are accounted for by including a damping ratio ζ:

$$K_{ij} = K_{0ij}(k_{ij} + ia_0 c_{ij})(1 + 2i\zeta) \tag{20}$$

Equation 20 shows how to calculate each stiffness component of the stiffness matrix in equation 17 and thus foundation response to dynamic excitation can now be obtained [9, 43, 46]. The coefficients need to be evaluated for different size of foundations and type of soil as well as frequency of the load and involve complex integrals omitted from this thesis. The solutions are frequency dependent, therefore a transformation is needed to use them in the time domain. Such conversions do not provide extra insight to SSI as such and are therefore omitted from this literature overview.

With the introduction of computers the focus changed from idealized analytical problems to more practical ones. Solving cases with elements of irregular shape and flexibility became possible. The finite and the macro element methods both emerged almost simultaneously. The finite element method has been more used since the stiffness is derived from continuity and connectivity of the elements and the material data whereas the appropriate macro elements needs to be chosen for each given individual problem, providing that they exist. Further research of impedance functions describing soil reaction when using other types of foundations such as rectangular and strip foundations and the manipulation of discretization to solve complex integrals has enlarged the library of macro/boundary elements available and the use of those elements has gained increased popularity.

In this context, it is specially mentioned, that macro elements are a more general term for boundary elements. Macro elements are elements designed by analytical equations but are not necessarily confined to the boundaries of the domain of a model.

---

[1]Different symbols are used for the shear wave velocity and the disc radius as well as damping coefficients in [9, 43] but the equations are the same whereas Dominguez's approach is more general.

2.2.1 Relaxed and non-relaxed boundaries

The concept of relaxed and non-relaxed boundary conditions is usually presented when considering macro/boundary element calculations. Relaxed boundaries as the term suggests is a less rigorous approach to solve the stress pattern in a macro element. Only the stresses that are primarily related to a given mode of excitation are considered and the remaining part of the stress tensors are truncated. Therefore only a part of the actual force pattern are used in the results. The non-relaxed boundary conditions however couples the modes of excitation resulting in a complete stress pattern [27]. It is clear that the coupling of the excitations result in a more complete stress pattern that is more difficult to formulate and is more computationally expensive than the relaxed boundaries.

2.3 Rocking and sliding

A structure supported on shallow foundations can undergo sliding, settling and rocking when subjected to earthquake loads. For a stiff structure such as shear wall building this translation and rocking will influence the structural response when subjected to earthquake induced excitation.

For flexible structures the overall displacements of the the structure are mainly attributed to the deflections of structural components whereas foundation displacements and rotations can be considered negligible [6, 11].

Rocking of structures was first studied by Housner in 1963. His research followed the Chilean earthquake of May 1960 where slender structures of inverted pendulum type survived the ground shaking better than structures expected to be more stable. In his initial observation a rigid block on a rigid foundation was subjected to acceleration load at the base as shown in figure 5. The basic equation for a rigid block rocking can be taken as:

$$I_0 \frac{d^2\theta}{dt^2} = -WRsin(\alpha - \theta) \tag{21}$$

The block's inertia, I_0 times the rate of the angular change $\ddot{\theta}$ equals the restoring moment due to the block's weight. Furthermore equations for the natural period of the block were devised and its response to sinusoidal pulse acceleration and sequential pulses with alternating directions to simulate earthquake load. His final conclusion was that the stability of structures subjected to an earthquake motion is greater than the stability when subjected to a single lateral force [17].

Since neither the block nor ground can be perfectly rigid, studies have been made to expand the application of rocking models such as the one proposed by Spanos and Koh [36, 15]. They consider a similar rocking block but the foundation is represented by Winkler foundation springs with no tension capacity, see figure 6. The center of the structure is used as a fixed pivot point. To rectify this, the assumption was made that the deformation of the soil springs should result in the pivot points moving from the ends of the block towards the center. Their findings were that rocking can be beneficial in terms of lowering base shear. Further studies where the block is
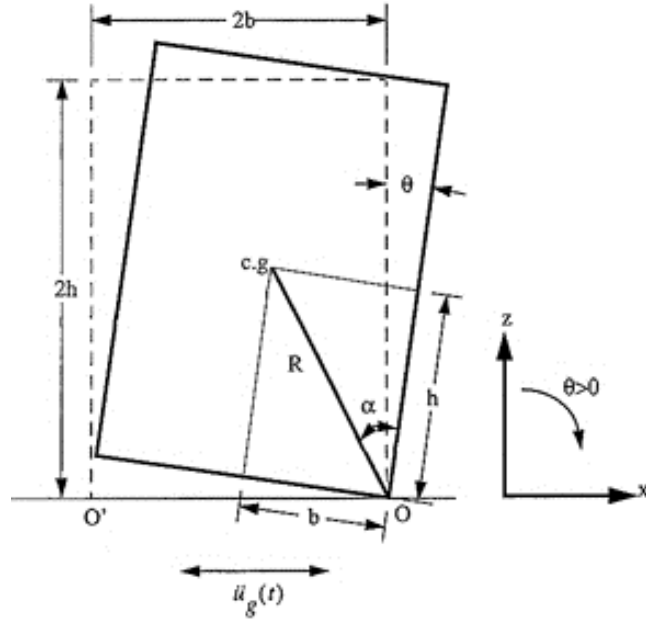
Figure 5: Rocking of a rigid block on rigid foundation (from Housner [17]).
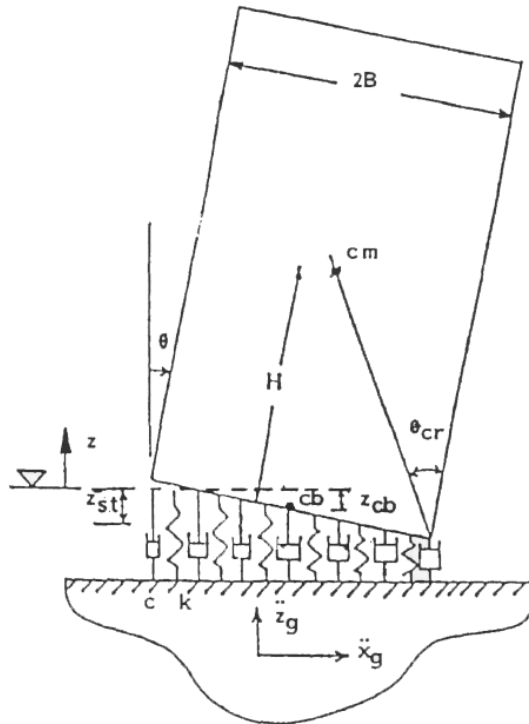
Figure 6: Rocking of a rigid block on Winkler foundation (from Spanos and Koh [36]).

replaced by flexible elements have shown beneficial results in terms of lower base shear and less tensile stresses while total displacements increase due to uplift and drift at the foundation level [6, 42, 30, 3].

11

2.4 The Finite Element Method

The finite element method is a tool used to solve the distribution of a field variable such as displacement at an point in a domain due to excitation at an arbitrary location. This is achieved by dividing the domain into elements, such as the ones shown in figure 7, that are tied together at nodes. Physical laws are then applied to each element which have simpler geometry than the domain itself. The field variable is then approximated by solving a set of simultaneously tied equations. For structural engineering these physical laws are shape functions determined by the given geometry and the degrees-of-freedom for each element [22]. By keeping the elements and the shape functions simple, a domain can be discretized so that a numerical solution can replace the complex integrals used when deriving fundamental solutions.
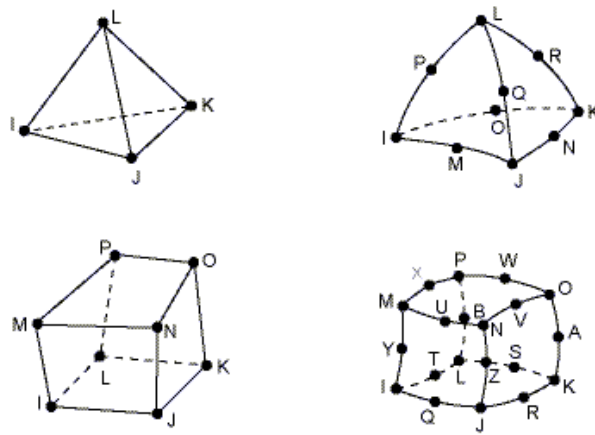
Figure 7: Two different solid elements (from Liu and Quek [22]).
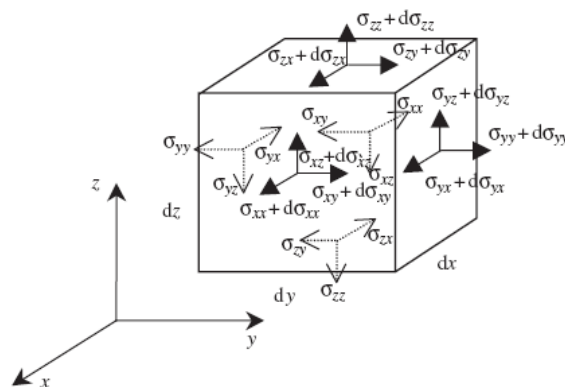
Figure 8: State of stress on an element of infinitesimal size (from Liu and Quek [22]).

A typical procedure to solve a field variable for an element in the x-direction for an element shown in figure 8 is to form an equilibrium equation describing the state of the element stresses and deformations:

$$(\sigma_{xx} + d\sigma_{xx})dydz - \sigma_{xx}dydz + (\sigma_{yx} + d\sigma_{yx})dxdz - \sigma_{yx}dxdz$$
$$+ (\sigma_{zx} + d\sigma_{zx})dxdy - \sigma_{zx}dxdy + f_x = \rho \ddot{u}dxdydz \qquad (22)$$

Here f_x is the force acting in the x-direction. The σ denotes stresses for appropriate faces and ρ is the density of the material that makes up the element. For time history analysis such as earthquakes the FEM uses a time step based approach where the state of the model is calculated for each step stored for use in the next consecutive step. At first glance the FEM seems ideal to solve a SSI system as the need for fundamental solutions is omitted. By looking at equation (22) the continuity of the elements and equilibrium laws incorporate a non-relaxed method where full coupling exists between stresses. On the other hand the numerical stability of the FEM requires the time interval between each step, when performing time history analysis, to be small in order to achieve convergence in the solution. This interval between steps is determined either by a fraction of the highest mode period that contributes to the response of the structure [4] or the time it takes the propagating wave to transverse the smallest element present in the model. With few elements present this type of analysis can be solved with modern desktops. Considering that the normal time step is of the magnitude of $0.001 - 0.002$ seconds, thousands of calculations are needed when analyzing a full time history earthquake record which typically ranges between 10 and 60 seconds in length. When using non-linear calculations a new tangent stiffness matrix needs to be evaluated from the previous step. This is an iterative process which makes the solution time when carrying out time history analysis very sensitive to changes in the size of the domain and the number of elements.

2.4.1 Treatment of the truncated soil boundaries

When using FE to model the soil of the domain one needs to deal with truncation of the soil at the boundaries. The dynamic equilibrium (22) generates a reflective wave at the the boundaries that travels back into the domain of interest. In practice the domain is usually split into near- and far-field as shown in figure 9. The near-field is the actual model of interest while the far-field is usually the continuum of the soil. Some methods have been devised to simulate the infinite media in such a way that wave radiation back to the domain of interest does not occur. The most notable are the ones that use infinite elements or viscous boundaries. Infinite elements are elements made by a shape function that approximates a sequence of a decaying form [18]. That means that one element can represent infinity of the far-field at the truncated boundaries. Infinite elements are limited for the reason that the input of the excitation must follow a certain form. Therefore the use of direct earthquake records is impossible [39]. Viscous boundaries are simpler in use but are less accurate. They are designed in a way that makes the damping equal to the
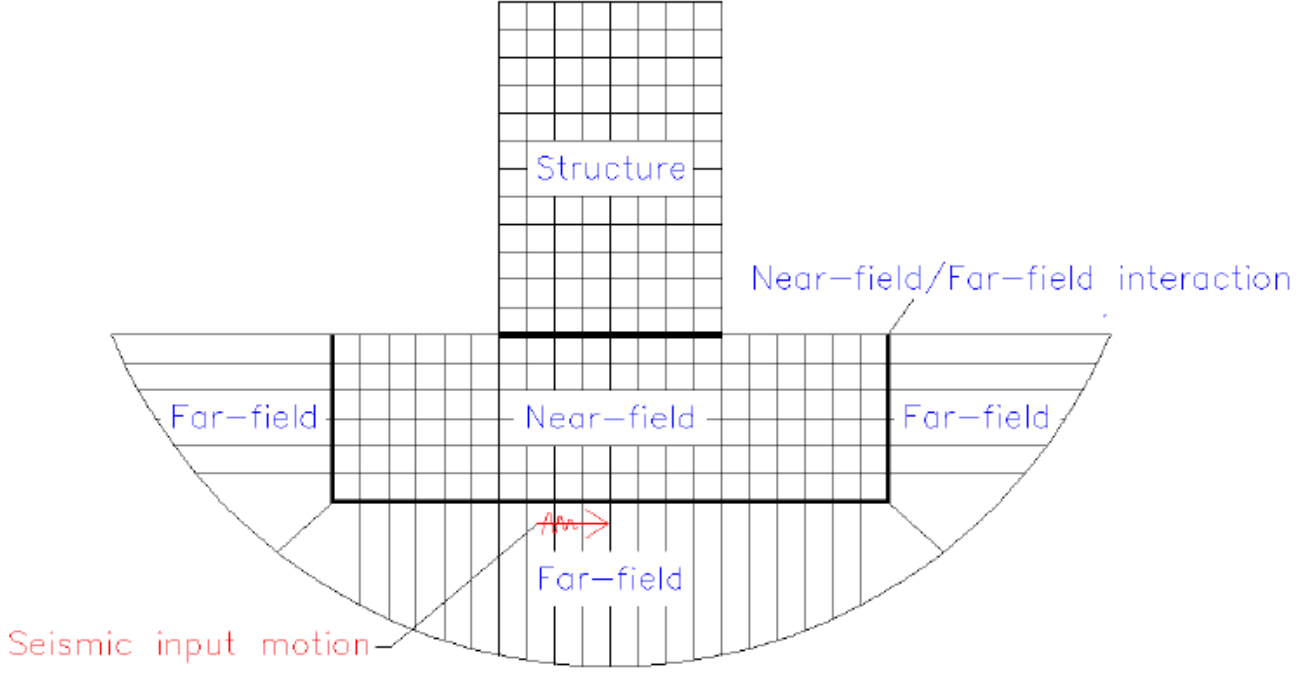
Figure 9: Model domain displaying near and far-field (from Olafsson [30]).

speed of the node where the damping element is connected:

$$
\begin{aligned}
N_n &= A_n * \sigma_n && \rightarrow && N_n + C_n * \dot{u}_n = 0 \\
N_{t1} &= A_{t1} * \tau_{t1} && \rightarrow && N_{t1} + C_{t1} * \dot{u}_{t1} = 0 \\
N_{t2} &= A_{t2} * \tau_{t2} && \rightarrow && N_{t2} + C_{t2} * \dot{u}_{t2} = 0
\end{aligned}
\tag{23}
$$

N denotes the normal and shear forces, A is the area of the truncated boundaries (attributing to each node), σ and τ are the normal and shear stresses, C is the normal and shear damping and $\dot{u}$ is the velocity of the node located at a boundary in the normal and shear directions. The damping matrix becomes:

$$
\mathbf{C} =
\begin{bmatrix}
A_n * \rho * c_p & 0 & 0 \\
0 & A_{t1} * \rho * c_s & 0 \\
0 & 0 & A_{t2} * \rho * c_s
\end{bmatrix}
\tag{24}
$$

Here the c_p and c_s are the pressure and shear wave velocity respectively and are related to the soil's density, elasticity and the Poisson's ratio. The reason why the damping matrix are less accurate is that they do not simulate the elastic recovery of the soil at the boundaries. The damping matrix $\mathbf{C}$ does not account for rotational damping. Errors in damping and elastic recovery are reduced by keeping the soil part of the near-field relatively big compared to the foundation of the structures resting on it [39].

The damping matrix in equation (24) can be applied to the horizontal boundaries to represent the continuum of the soil. The bottom boundary of the FE model needs to be fixed [9] or given some other kind of boundaries that populates the displacement matrix with initial conditions. This approach does not always depict reality since the soil layering can be complicated and long way down to a bedrock. The input motion in form of earthquake records are usually placed at the bottom of the model inducing another inaccuracy to the model where the recording usually takes place at the free field of the soil.

2.5   Other SSI deterministic methods

Previously in this chapter the BEM was described as a mass-spring-damper analog system where the stiffness properties of the springs, and the damping as well, was derived from fundamental solutions. The need of a fundamental solution can be an obstacle when determining SSI effects and the involved mathematical expressions can obscure the nature of dynamic stiffness. Other methods have been devised to calculate the dynamic stiffness such as the cone model.

A cone model as presented by Wolf [45, 33] is a straightforward method to obtain the dynamic stiffness as opposed to the fundamental solution integrals needed for the fundamental solutions given by Wolf and Dominguez [46, 8]. The cone model uses the approach of introducing a massless, rigid disc shown in figure 10. Once the disc is subjected to a harmonic vertical load $P_0(t)$ a dilational wave propagates downwards with the velocity c_p^L. This applies so long as the Poisson's

Figure 10: Cone model response of a massless disc (from Wolf and Zhang [45]).

ratio is less than 0.33. This wave follows a cone (apex 1) which shape is determined by the opening angle z_0^L and the soil's mass density ρ_L. The displacement of the soil can be taken as equal to that of a half space and such is inversely proportional to the distance of the apex

$$u(z,t) = \frac{z_0^L}{z_0^L + z} f\left(t - \frac{z}{c_p^L}\right) \tag{25}$$

where z is the distance measured from the free surface downwards. To determine the apex and z_0^L the cone static stiffness $\rho(c_p^L)^2 \pi r_0^2 / z_0^L$ is adjusted to yield the same static stiffness as a disc on a homogeneous half space as the one in equation (13) resulting in:

$$\frac{z_0^L}{r_0} = \frac{\pi}{2} \frac{(1 - v_L)^2}{1 - 2v_L} \tag{26}$$

The incident wave f will refract at the soil/rock interface ($z = d$). The refracted wave h will continue through the rock causing continued downwards displacements:

$$u_R(z,t) = \frac{\frac{z_0^L z_0^R}{z_0^L + d}}{z_0^R - d + z} h\left(t - \frac{d}{c_p^L} + \frac{d}{c_p^R} - \frac{z}{c_p^R}\right) \tag{27}$$

This equation shows the propagation of the wave in the rock that follows apex 2 and z_0^R can be determined by equation (26). From the rock layer a reflective wave g propagates through the soil layer upwards along another cone (apex 3). The displacement in the layer $u_L(z,t)$ now equals:

$$u_L(z,t) = \frac{z_0^L}{z_0^L + z} f\left(t - \frac{z}{c_p^L}\right) + \frac{z_0^L}{z_0^L + 2d - z} g\left(t - \frac{2d}{c_p^L} + \frac{z}{c_p^L}\right) \tag{28}$$

At the interface where the cones coincide the arguments of all the wave functions f, g and h are the same for the given time that takes the pressure wave to travel from the surface to the interface between the layers $t - d/c_p^L$. The upwave g will reflect towards the free surface along a cone (apex 4) and from the surface back to the rock layer and so forth. A reflection coefficient $-\alpha$ is defined to determine the amount of the original wave reflected. Sufficient accuracy for $-\alpha$ can be gained by replacing the cone with a prismatic bar and using the equilibrium and compatibility criteria at the layer interface.

$$-\alpha = \frac{\rho_L c_p^L - \rho_R c_p^R}{\rho_L c_p^L + \rho_R c_p^R} \tag{29}$$

All these waves contribute to the displacement within the soil and the dynamic stiffness can be obtained from the sum of these contributions. Suppose that the incident wave is subjected at the top of the disc as $\bar{u}_0(t)$ which was the original wave f in equation (25) the displacement $u_L(z,t)$

may be described as:

$$u_L(z,t) = \underbrace{\frac{z_0^L}{z_0^L + z} \bar{u}_0 \left(t - \frac{z}{c_p^L} \right)}_{\text{incident wave}}$$

$$+ \sum_{j=1}^{\infty} (-\alpha)^j \left[\underbrace{\frac{z_0^L \bar{u}_0 \left(t - \frac{2jd}{c_p^L} + \frac{z}{c_p^L} \right)}{z_0^L + 2jd - z}}_{\text{up wave from rock}} + \underbrace{\frac{z_0^L \bar{u}_0 \left(t - \frac{2jd}{c_p^L} - \frac{z}{c_p^L} \right)}{z_0^L + 2jd + z}}_{\text{down wave from surface}} \right] \quad (30)$$

The sum integer k represents the largest j while the arguments of $\bar{u}_0$ for z and t remain positive.

Further simplifications for this cone model exist such as *unfolded layered cone* where the unfolded cones represent a wave pattern with decaying amplitude and the associated reflections and refractions. Other simplification have also been made through the use of non-radiating cone frustum. More detailed description in use of these cones and application to SSI problems can be found in Wolf [45].

17

3 Shear wall dimensions and the programs and elements used

The focus of this study are squat shear walls with an aspect ratio lower than 2.0 resting on a soil substructure to be subjected to earthquake loads (figure 11). Their length and height range is between 3 and 5 meters. The programs for numerical modeling of these walls should be able to handle the non-linearities that occur once the system is subjected to the earthquake loads. The following non-linearities are considered:

1. Geometric non-linearities due to deformations that can change the geometric configuration and thus cause non-linear behavior.

2. Material non-linearities due to stress-strain relationship such as plasticity and hysteresis.

3. Contact non-linearities where a changed status of contact between bodies changes the stiffness of the model.

Based on these non-linearities ANSYS was chosen to model the system using conventional FE techniques while OpenSees is used to make a macro element representation of the system.

An inverted T-type footing is chosen to stabilize the wall against overturning where as the numerical approximations in the FE model can produce unwanted loads in the direction perpendicular to the load of the earthquake action. The Beam on non-linear Winkler foundation (BNWF) that is used to represent the soil and footing in OpenSees is designed for the same type of footing as the FE model. The wall is reinforced with a double c/c 200 mm S10[2] grid in both vertical and horizontal direction.

_____

[2]A common steel reinforcement bar 10 mm in diameter.
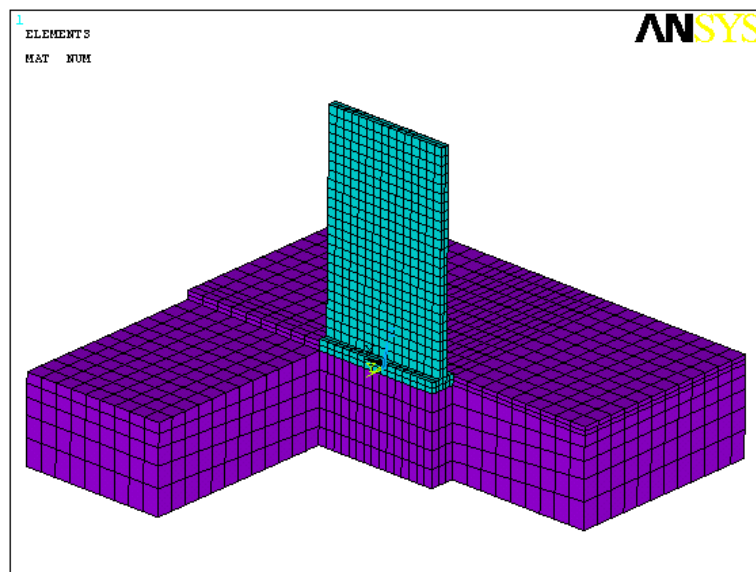
Figure 11: Setup of a squat shear wall resting on soil layer where parts of the soil is hidden to show the meshing.

3.1 OpenSees modeling options

OpenSees is a framework for earthquake engineering simulation developed by the collaborative environment of the Pacific Earthquake Engineering Research Center (PEER) [25]. The framework is object oriented so computer codes describing new functions can be added as packages without compromising the library of elements and solvers that already exist. These packages are called or activated by text commands and the programming language used to access these packages is TCL (Tool Command Language). Since the framework is embedded within a program language, common programming commands are available. With proper syntaxes making loops, such as what-if and while analyses is simple procedure.

The framework can be divided into three main categories; the model builder where the packages describing elements/nodes/materials/load patterns are stored, the output/recorder package where the user specifies the type of the output required for post processing and finally the analysis package where the type of analysis is specified and the methods used to solve the model and convergence criteria are determined. All these packages can be implemented into program routines in such as way that if the iteration method used should fail a routine can be created to change the iterative method and/or the convergence criteria.

The SSI system in OpenSees will be represented by macro elements, the wall itself will be modeled with a Flexure-Shear Interaction Displacement-Based Beam-Column Element (flexure-beam element) and with a Force-Based Beam-Column Element (force-beam element). The footing of the wall is a multi node elastic beam resting on BNWF spring/dashpot foundation. The input files used to call the necessary packages used to describe and solve the wall model are supplemented in appendix B.

3.1.1 Force-Based Beam-Column Element

Macro elements have been designed to capture the behavior of beams and columns with good results. Wall segments have been shown to be more complicated in formulation. With the work of Vulcano et al. [44] Multiple-Vertical-Line-Element Model (MVLEM) was developed to model walls. For walls with aspect ratio over 3.0 that mainly undergo flexure displacement a MVLEM such as the Force-Based Beam-Column Element in OpenSees has predicted wall response to lateral loads with good results [51]. If displacements are significant due to shear lagging, as in shear walls with low aspect ratio, the force-beam element has to be aggregated with a shear spring to account for the shear deformation. The configuration for such aggregation is summarized in figure 12. The equation for this spring over the height of the wall is:

$$k_{shear} = f_{cr} G_c \alpha_s A_g \tag{31}$$

Here the f_{cr} is the ratio of the fully cracked shear modulus to the uncracked one, G_c is the shear modulus of the concrete, α_s is the shear coefficient for a rectangular section taken as 5/6 and A_g
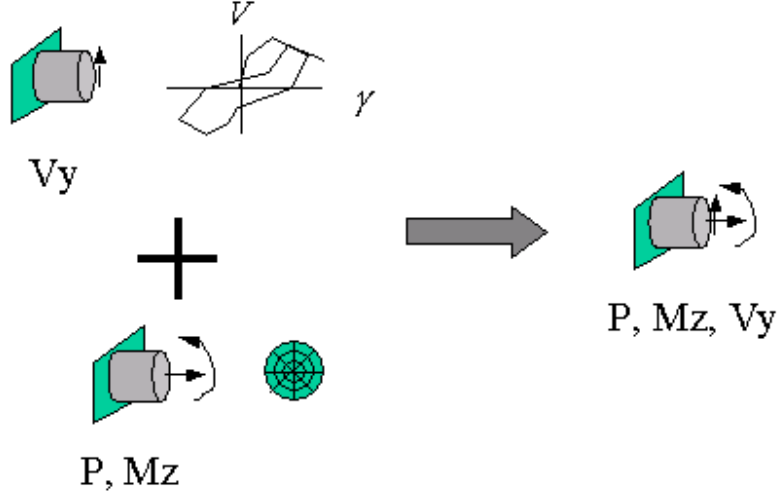
Figure 12: Section aggregator combines two stiffness models into one (from the OpenSeesWiki website [25]).

denotes the gross section area. The f_{cr} is often taken as 0.01 but for this research it is calibrated specifically to account for horizontal reinforcement since it is not accounted for in the description of the force-beam element section.

3.1.2 Flexure-Shear Interaction Displacement-Based Beam-Column Element

A MVLEM with built in shear deformation was created by Petrangeli et al. [32]. L. M. Massone refined the element based on their work and coded it into OpenSees as the Flexure-Shear Interaction Displacement-Based Beam-Column Element [24]. The element has two nodes and multiple elements can be connected together at the nodes to model a wall of specific cross section and height. The wall cross section is divided into strips defined by location in a local coordinate system with the corresponding cross section area of the contributing materials of each strip. The layout for the strips/fibers is shown in figure 13. Contribution of each strip/fiber is then summed up in the middle of the element (figure 14). The shear and flexure is coupled by monitoring deformation and strains in the elements. Iterative methods using compatibility, material laws and equilibrium are used to find the ratio of the coupling between the shear and the flexure. A flowchart describing the iterative process is shown in figure 15. The exact method of the coupling is beyond the scope of this research but can be found in L. M. Massone's thesis [24].

3.1.3 Beam on non-linear Winkler Foundation

The BNWF is a two-dimensional shallow foundation model where the foundation is taken as an elastic beam supported on number of discrete non-linear Winkler springs. The implementation of the model in OpenSees is made possible due to the work of Raychowdhury [35]. Three nodal degrees of freedom are used to capture translation for horizontal and vertical movements as well as rotational directions. The springs act independently of each other and are modeled as zero

21
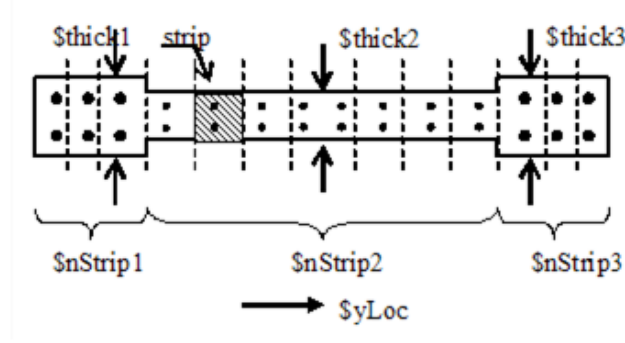
Figure 13: Strips and fibers making a wall cross section (from the OpenSeesWiki website [25]).
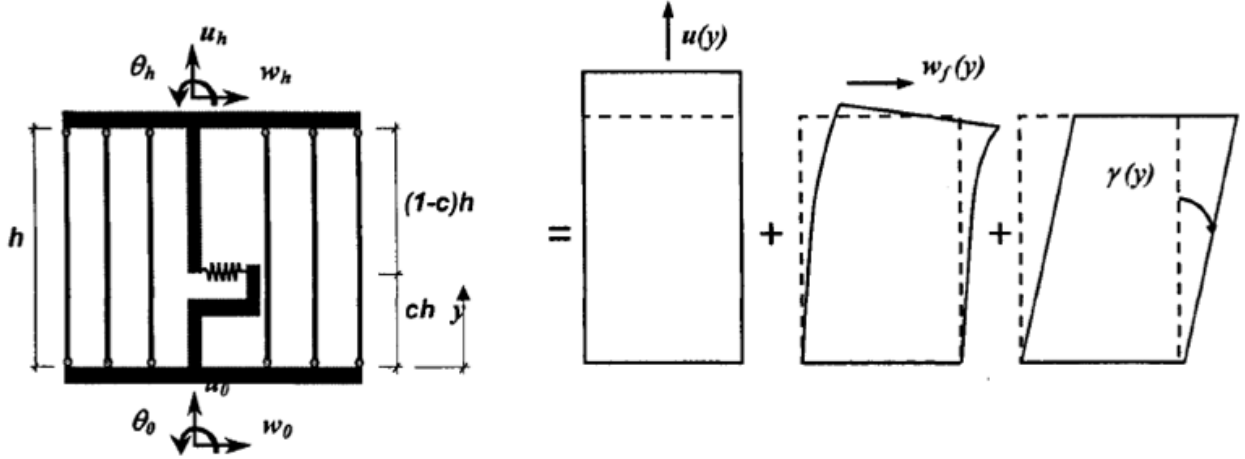
Figure 14: MVLEM with a built in shear spring such as the flexure-beam element (from Massone [24]).

length elements in OpenSees that can capture near- and far-field behavior. The setup of a zero length element can be seen in figure 16.

Three set of zero length elements are used to model the soil compliances *PySimple1* which is the passive resisting force due to embedding of the foundation, *TzSimple1* is used for the sliding resistance and *QzSimple1* for vertical stiffness. Figure 17 shows the setup of the foundation.

The vertical and lateral stiffnesses K_v and K_h for both *QzSimple1* and *TzSimple1* are calculated using the expressions provided by Gazetas [14] and shown in figure 18. The BNWF can be created by a command in OpenSees, the user has to define an input file that contains the required soil properties, footing dimensions and meshing properties. The input parameters required are shown in table 1, some of the parameters are hard-coded into OpenSees and cannot be modified.

Note that the kinematic interaction is not included in the formulas provided by Gazetas but since the wall foundation is relatively small compared to the earthquake wave the kinematic effects should be negligible. The frictional spring does not account for the reduced friction whilst the foundation is rocking. The springs are all independent of each other making the model follow the relaxed form of the BEM.

Global Trial Deformation stage at section (j): u_x u_y θ

Global Trial Strains stage at strip (i) in section (j): ε_y γ_{xy}

Variable set up

Material prop.: f_c, ε_{cr} f_{cr} E_c f_y ε_{sy} ...
Reinforcement ratios: ρ_x ρ_y

Starting point (var.)

$\varepsilon_x = \varepsilon_x + \Delta\varepsilon_x$

Compatibility

$\varepsilon_1\left(\varepsilon_x,\varepsilon_y,\gamma_{xy}\right)$ $\quad$ $\varepsilon_2\left(\varepsilon_x,\varepsilon_y,\gamma_{xy}\right)$ $\quad$ $\alpha\left(\varepsilon_x,\varepsilon_y,\gamma_{xy}\right)$

+

Material Laws

Steel $\qquad\qquad$ **Concrete**
$\varepsilon_x \rightarrow \sigma_{sx}$ $\qquad\qquad$ $\varepsilon_1, \varepsilon_2 \rightarrow \sigma_{c1}$ $\left.\right\}$ σ_{cx}
$\varepsilon_y \rightarrow \sigma_{sy}$ $\qquad\qquad$ $\varepsilon_2, \varepsilon_1 \rightarrow \sigma_{c2}$ $\left.\right\}$ σ_{cy}

+

Equilibrium

$\sigma_{x\_Trial} = \sigma_{cx} + \rho_x{}^* \sigma_{sx}$

Convergence ?

Error $= abs(\sigma_{x\_Trial} - \sigma_x) <$ TOL

$\sigma_x = 0$ (or other function)

NO $\qquad$ **YES**

Stresses at strip (i) in section (j)

$\tau_{yx}{}^{ij} = -(\sigma_{c1} - \sigma_{c2})^*\sin(2^*\alpha)/2$
$\sigma_y{}^{ij} = \sigma_{cy} + \rho_y{}^* \sigma_{sy}$

Global Equilibrium at trial deformation at section (j) (upper node)

$N^j = \Sigma \sigma_y{}^{ij} * A^{ij}$
$V^j = \Sigma \tau_{xy}{}^{ij} * A^{ij}$
$M^j = \Sigma \sigma_y{}^{ij} * A^{ij} * x_{ij} - V^{j*}(1-c)^*h$

(j) (i)

Figure 15: Flow chart for the element iteration procedure to couple the flexure and the shear deformations of the flexure-beam element (from Massone [24]).
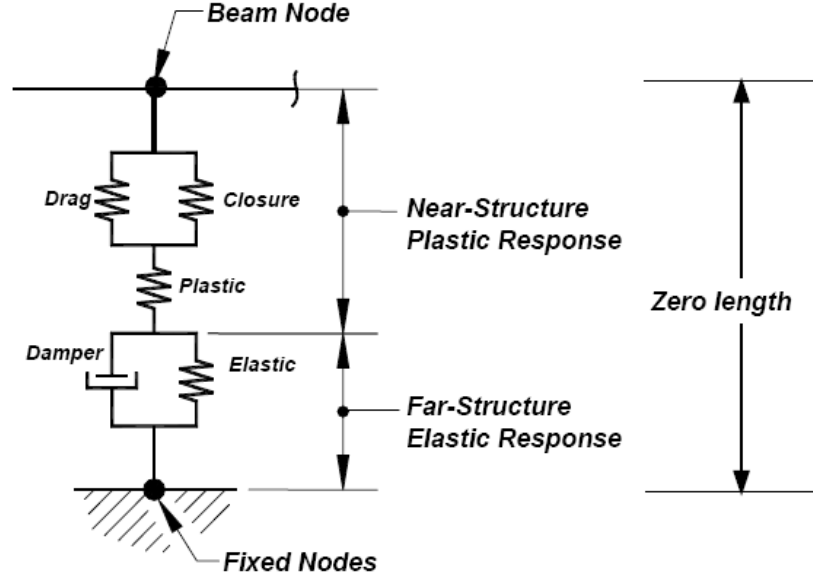
Figure 16: Zero length elements capturing near and far-field behavior (from Raychowdhury [35]).

Table 1: Model parameters used for the BNWF.

User-defined parameters	Hard-coded parameters
Capacity of footing (Q_{ult}, P_{ult} or T_{ult})	Elastic range (C_r)
Stiffness of footing (K_v or K_h)	Post-yield stiffness (K_p)
Soil type (sand or clay)	Unloading stiffness (K_{unl})
Footing dimensions (L, B, H and D_f)	
Tension capacity (TP)	
End-length ratio (R_e)	
Stiffness intensity ratio (R_k)	
Spring spacing (l_e/L)	

3.2 ANSYS modeling

The modeling in ANSYS follows a traditional method in the sense that the model is represented by its geometry which is then discretized into finite elements. The wall is represented by SOLID65 elements that are special concrete elements that can crush and crack and follow a William-Warnke failure criteria. Other parts, such as the soil and the foundation are modeled using SOLID95 elements. To separate the foundation from the soil CONTA174 elements are used. To capture the viscous damping a user specified matrix is made with the DAMP MATRIX 27 element. The exact formulation of these elements have been covered in many studies and are available within the ANSYS help utility. The setup of the models are done using the ANSYS parametric design language and the wall types changed by manipulating the input files. The input files used to run the models can be found in appendix A.
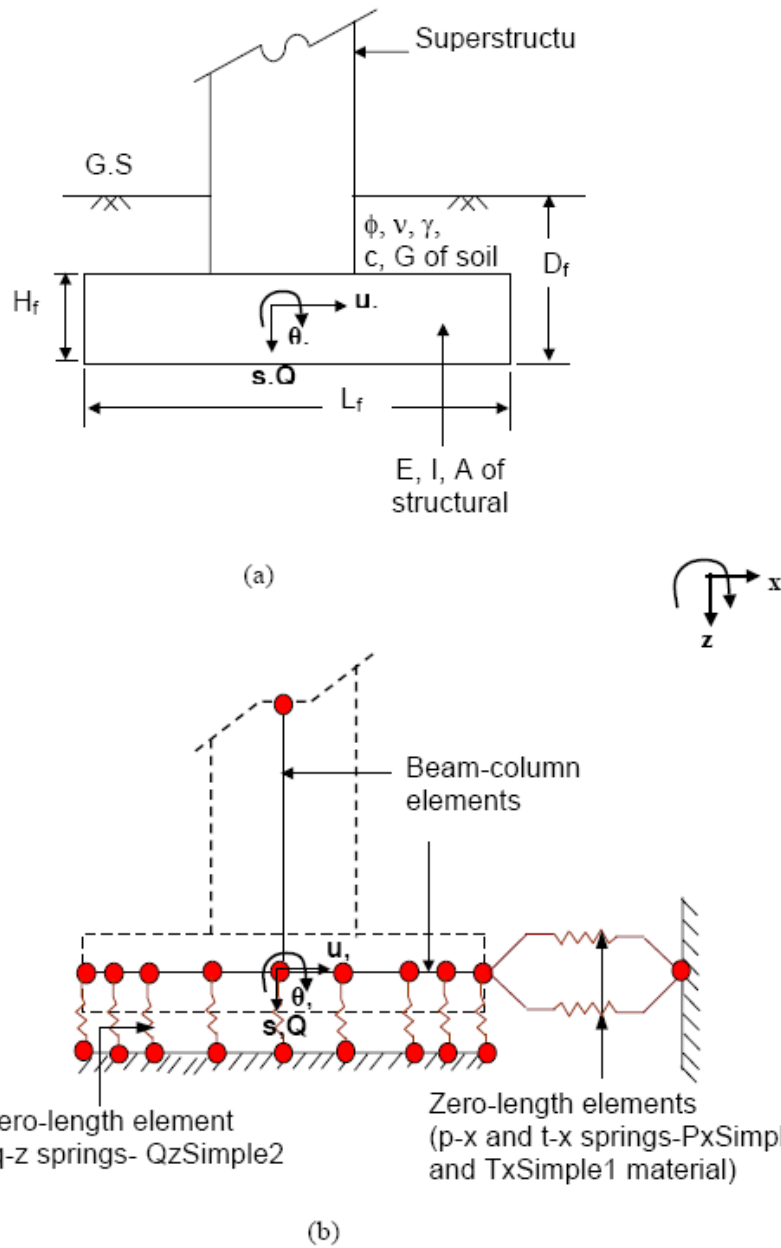
Figure 17: Setup of a Beam on non-linear Winkler foundation (from Raychowdhury [35]).
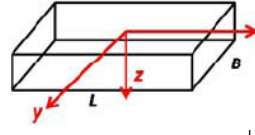
Stiffness	Equation
Surface Stiffness	
Vertical Translation	$K_Z' = \dfrac{GL}{1-v}\left[0.73 + 1.54\left(\dfrac{B}{L}\right)^{0.75}\right]$
Horizontal Translation (toward long side)	$K_Y' = \dfrac{GL}{2-v}\left[2 + 2.5\left(\dfrac{B}{L}\right)^{0.85}\right]$
Horizontal Translation (toward short side)	$K_X' = \dfrac{GL}{2-v}\left[2 + 2.5\left(\dfrac{B}{L}\right)^{0.85}\right] + \dfrac{GL}{0.75-v}\left[0.1\left(1-\dfrac{B}{L}\right)\right]$
Rotation about x-axis	$K_{\theta x}' = \dfrac{G}{1-v}I_X^{0.75}\left(\dfrac{L}{B}\right)^{0.25}\left(2.4 + 0.5\dfrac{B}{L}\right)$
Rotation about y-axis	$K_{\theta y}' = \dfrac{G}{1-v}I_Y^{0.75}\left[3\left(\dfrac{L}{B}\right)^{0.15}\right]$
Stiffness Embedment Factors	
Embedment Factor, Vertical Translation	$e_Z = \left[1 + 0.095\dfrac{D_f}{B}\left(1 + 1.3\dfrac{B}{L}\right)\right]\left[1 + 0.2\left(\dfrac{2L+2B}{LB}H\right)^{0.67}\right]$
Embedment Factor, Horizontal Translation (toward long side)	$e_Y = \left[1 + 0.15\left(\dfrac{2D_f}{B}\right)^{0.5}\right]\left\{1 + 0.52\left[\dfrac{\left(D_f - \dfrac{H}{2}\right)16(L+B)H}{BL^2}\right]^{0.4}\right\}$
Embedment Factor, Horizontal Translation (toward short side)	$e_X = \left[1 + 0.15\left(\dfrac{2D_f}{L}\right)^{0.5}\right]\left\{1 + 0.52\left[\dfrac{\left(D_f - \dfrac{H}{2}\right)16(L+B)H}{LB^2}\right]^{0.4}\right\}$
Embedment Factor, Rotation about x axis	$e_{\theta X} = 1 + 2.52\dfrac{H}{B}\left(1 + \dfrac{2H}{B}\left(\dfrac{d}{D_f}\right)^{-0.2}\left(\dfrac{B}{L}\right)^{0.5}\right)$
Embedment Factor, Rotation about y axis	$e_{\theta Y} = 1 + 0.92\left(\dfrac{2H}{L}\right)^{0.60}\left(1.5 + \left(\dfrac{2H}{L}\right)^{1.9}\left(\dfrac{H}{D_f}\right)^{-0.60}\right)$

Where, K_i = Uncoupled Total Surface Stiffness for a rigid plate on a semi-infinite homogeneous elastic half-space, e_i = Stiffness Embedment Factor for a rigid plate on a semi-infinite homogeneous elastic half-space, L = foundation length, B = foundation width, D_f = depth of embedment, H = foundation thickness, G = Shearing Modulus, v = Poisson's ratio.

Figure 18: Foundation stiffnesses by Gazetas (from Raychowdhury [35]).

3.3 Material properties

3.3.1 Concrete

Material models are chosen with the objective to have as similar properties as possible within OpenSees and ANSYS. As OpenSees has some predefined models a predefined model with least complexity was chosen while keeping the non-linear nature of concrete. Concrete 2 in OpenSees is a modified Kent and Park model following a loading and unloading rule by Yassin[3] (OpenSees wiki [25]). The same model is then implemented by using a multi-linear kinematic hardening curve in ANSYS formulated by equations (32) through (38) and a concrete model following a William-Warnke failure criteria[4]. The Modified Kent and Park model can be seen in figure 19 showing the slope equations and figure 20 showing the material definition within OpenSees.

The formulations for the modified Kent and Park model were found within Orakcal et al. [31]. The model is a stress-strain relation compression curve divided into three regions: The first region is an initially elastic region under compression that experiences increasing non-linearity, reaching the peak compressive stress $f'c$ ($\epsilon_c \leq \epsilon_0$):

$$\sigma = Kf'_c \left[2 \left(\frac{\epsilon_c}{\epsilon_0} \right) - \left(\frac{\epsilon_c}{\epsilon_0} \right)^2 \right] \tag{32}$$

where ϵ is the strain. The second region is the softening of the material ($\epsilon_0 < \epsilon_c \leq \epsilon_{20}$):

$$\sigma_c = Kf'_c[1 - Z(\epsilon_c - \epsilon_0)] \tag{33}$$

The last region accounts for failure of the concrete. This happens at ϵ_{20} when the slope from equation (33) has reached 20% of the ultimate compressive stress ($\epsilon_{20} < \epsilon_c$):

$$\sigma_c = 0.2Kf'_c \tag{34}$$

$$\epsilon_0 = 0.002K \tag{35}$$

$$K = 1 + \frac{\rho_s f_{yh}}{f'_c} \tag{36}$$

$$Z = \frac{0.5}{\frac{3+0.29f'_c}{145f'_c-1000} + 0.75\rho_s \sqrt{\frac{h'}{s_h}} - 0.002K} \tag{37}$$

$$E_c = \frac{2kf'_c}{\epsilon_0} \tag{38}$$

---

[3]Mohd Hisham Mohd Yassin, "Nonlinear Analysis of Prestressed Concrete Structures under Monotonic and Cycling Loads", PhD dissertation, University of California, Berkeley, 1994. not listed in the references. The reference is given within the OpenSees wiki that describes the material model and is accessible at: http://opensees.berkeley.edu/wiki/index.php/Concrete02_Material_-_Linear_Tension_Softening

[4]This is the only concrete model available in ANSYS. Details for the model can be found in the ANSYS help.

The various symbols in the previous equations are:

$K =$ a factor that accounts for the increase in concrete strength due to confinement.

$\epsilon_0, \epsilon_{20} =$ strains in the concrete and 20% of the strain at peak compressive strength.

$f'_c =$ the concrete compressive cylinder strength.

$Z =$ calculated constant, use MPa for the compressive cylinder strength for correct results.

$f_{yh} =$ the yield strength of transverse reinforcement.

$\rho_s =$ the ratio of the volume of the transverse reinforcement to the volume of the concrete core measured to the outside of the stirrups.

$h' =$ the width of concrete core measured to the outside of the stirrups.

$s_h =$ the spacing between the stirrups.
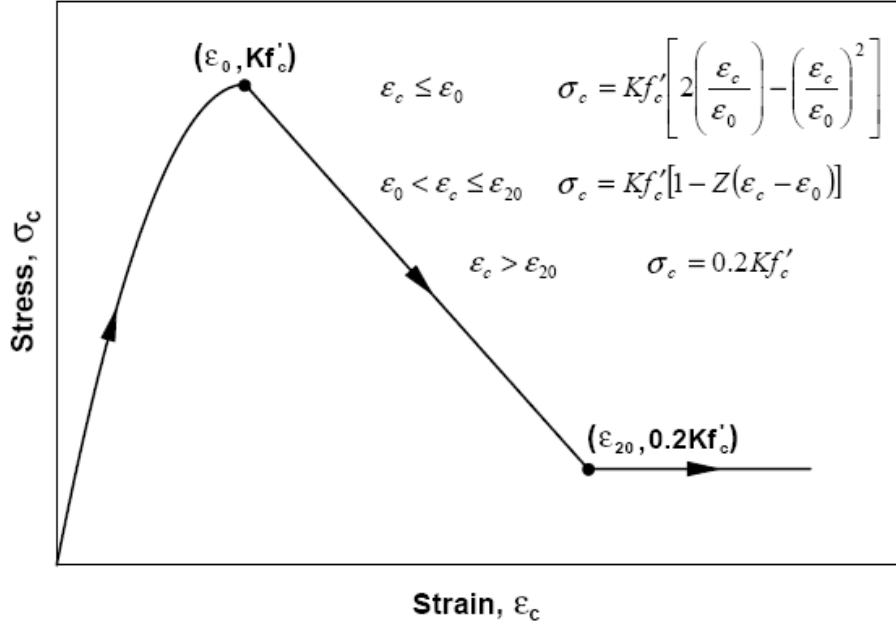
Figure 19: Modified Kent and Park model (from Orakcal et al. [31]).

For the particular walls in this research the extra strength of the concrete due to refinement will be discarded making $K = 1$ and $\rho_s = 0$. The tension capacity f_t will be taken as 10% of the compression capacity. Concrete properties are summarized in table 2 where ϵ_{20} was calculated by given formulas.

Table 2: Properties of concrete.

E_c [Pa]	f'_c [Pa]	ϵ_0	$0.2f'_c$ [Pa]	ϵ_{20}	f_t [Pa]	v
25e9	25e6	0.002	5	0.005	2.5e6	0.2

The more specific values of β_t and β_c needed for crack shear transmittance needed for the William-Warnke failure model. λ is the ratio between the unloading slope of the Concrete 2
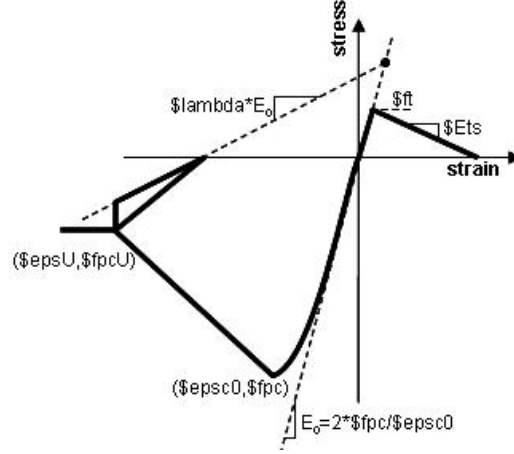
Figure 20: Modified Kent and Park model developed by Mohd Hisham Mohd Yassin (from the OpenSeesWiki [25]).

Table 3: More specific parameters needed for each program.

ANSYS	β_t	β_c
	0.4	0.8
OpenSees	λ	E_t [Pa]
	0.1	$2.5e9$

material and should not effect the model when only subjected to lateral pushover load, E_t is used for the tensile unloading slope of the Concrete 2 model can be found in table 3.

3.3.2 Steel

Steel is modeled as a bilinear isotropic material in ANSYS and Steel 1 in OpenSees as shown in figure 21, using the same parameters. The strain-hardening ratio of steel is taken as 0.01 to derive the tangent modulus E'_s. The steel parameters can be found in table 4.
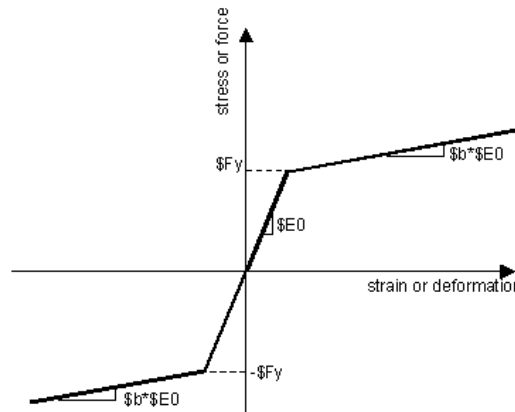
Figure 21: Bilinear curve of steel (from the OpenSeesWiki [25]).

Table 4: Properties of steel.

E_s [Pa]	f_y [Pa]	E'_s [Pa]	v
$210e9$	$410e6$	$2.1e9$	0.3

3.3.3 Soil

The modeling of the soil was limited to the BNWF properties. The soil model is calibrated to capture the response of clay or sand. The input is therefore based on the mechanical properties of these materials. These properties are the cohesion of the soil c, the angle of friction between the material particles ϕ, the unit weight of the soil γ, the shear modulus G, Poisson's ration ν, radiational damping properties of the soil c_{rad} and the tension capacity TP. For this particular model the values for sand used in the experiment by Zhang and Tang [51] were adopted[5] and can be found in table 5.

Table 5: Properties of soil used in OpenSees.

c [Pa]	ϕ	γ [N/m^3]	G [Pa]	ν	c_{rad}	TP
0.01	29	18849.3	155959410	0.25	0.05	0.1

The soil simulation in Ansys is a bit different. The simulation of granular materials is done by using a linear-elastic perfectly-plastic Drucker-Prager (DP) model. A DP model is dependent on the hydrostatic pressure acting on the elements. That is the increase in compression/tension capacity when one or more of the forces acting on the element caue compression and vice versa. If the yield surface is plotted in principal stress space the surface is represented by a cone as shown in figure 22.
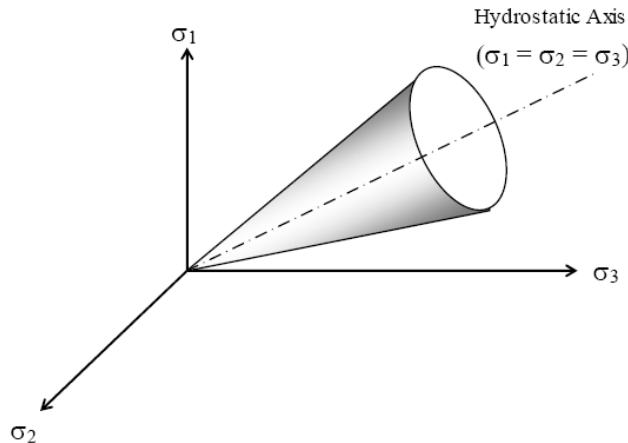
Figure 22: Drucker-Prager failure criterion for a granular material (from Lacey et al. [20]).

---

[5]The shear modulus for the sand model given there is quite high resulting in a very high Young's modulus, this high value has possibly had some effect on the Drucker-Prager material model in the Ansys FE model causing difficulties in convergence.

A DP model only relies on few parameters such as the Yong's modulus E, Poisson's ratio ν, the angle of friction ϕ and a dilation angle ψ and fits well with available data. The yield criteria of a cohesionless DP material model is taken as:

$$f = \beta * I_1 + \sqrt{J_2} \tag{39}$$

where I_1 is the first invariant of the stress tensor given as

$$I_1 = \sigma_1 + \sigma_2 + \sigma_3 \tag{40}$$

and J_2 is the section invariant of deviatoric stress tensor

$$J_2 = \frac{1}{6}[(\sigma_{11} - \sigma_{22})^2 + (\sigma_{22} - \sigma_{33})^2 + (\sigma_{33} - \sigma_{11})^2] + \sigma_{12}^2 + \sigma_{13}^2 + \sigma_{23}^2 \tag{41}$$

In the above equations σ with corresponding subscript denotes a stress tensor component. β is

$$\beta = \frac{2\sin\phi}{\sqrt{3}(3 - \sin\phi)} \tag{42}$$

Equation 39 represents the cone shown in figure 22. The third parameter is the dilation angle ψ of the soil that predicts the flow rule, that is how the plastic strains develop beyond the yield of the material. The exact value of the dilational angle for this sand example is not known but based on the work of Lacy et al. [20] a value that equals to half of the friction angle is chosen. The parameters for the soil in ANSYS are summarised in table 6.

Table 6: Properties of soil used in ANSYS.

E [Pa]	ν	ρ [kg/m³]	c [Pa]	ϕ	ψ	Damping
389898525	0.25	1921.44	0.0	29	14.5	5%

4 Attuning the computational models

In order to obtain reliable results the FE and ME models need to be attuned. Both these methods are dependent on the number of elements in the model. The number of elements has to be chosen to find balance between calculation time and accuracy. For the attuning a 3.0 m by 3.0 m wall model is used. The FE model is used as a baseline for the calibration of the ME models. For simplicity, force and deformation are used as a reference for the attuning. The displacements of the FE model is the average displacement of all the nodes located at the top of the wall and for the ME models the average displacement is measured at the top node of the wall where all the displacements of the fibers are averaged.

4.1 Attuning the FE models

The attuning was controlled by changing variables in the APDL (appendix A). For example the element size is controlled by a global command meaning that all the model is meshed using elements of specific edge length. The application of load is quite convenient since the node numbering follows a scheme where nodes of elements at the bottom and top areas of the wall are numbered first in consecutive order. Thus it is easy to calculate the number of nodes on each area and find the range of the nodes at the top of the wall to apply the load.

4.1.1 Material definition check and mesh dependence

The FE model is subjected to a 1.0 MN lateral load distributed evenly between the top nodes of the wall. The load is applied in steps of 1.0 kN by using ramped loading scheme. For each step the response of the wall due to an increase of the load is solved. Once convergence fails for a given step it is assumed the wall has reached peak load resistance.

The softening branch that is shown in figure 19 of the concrete material could not be simulated as a material property in the FE model. However, it is somewhat accounted for with the crack generation of the William-Warnke model as formation of cracks account for degeneration of strength in the model.

To verify that the material model was working properly when coupling kinematic hardening model with a William-Warnke failure criteria, a cylinder compression test of the concrete as well as a tensile test was simulated. Special care is needed when testing the cylinder so that the elements do not experience extra pressure due to constraints against expansion. The results matched the desired data as can be seen in figure 23, note that the displacement is given for a 10 cm high cylinder. The concrete follows the kinematic hardening model while it uses the ultimate tensile capacity from the William-Warnke model.

After verifying the material definition the effect of changing the mesh discretization with using different element sizes was examined. The element size was confined to elements with 0.2 m, 0.1 m and 0.05 m edge length, the results of changing element size is shown in figure 24. The calculation

time increased with the number of elements as expected, for the model with a mesh of elements with edge length 0.2 m the calculation time was about 4 minutes. For the model with a mesh of elements with edge length 0.2 m the calculation time was about 40 minutes and lastly the model with mesh of elements with edge length 0.05 m the calculation time was around 9 hours. The increase in calculation time is almost linear considering that halving the element size increases the number of elements by 2^3 in the model. Based on these calculations a mesh of elements with edge length 0.1 m is used for further calculations.
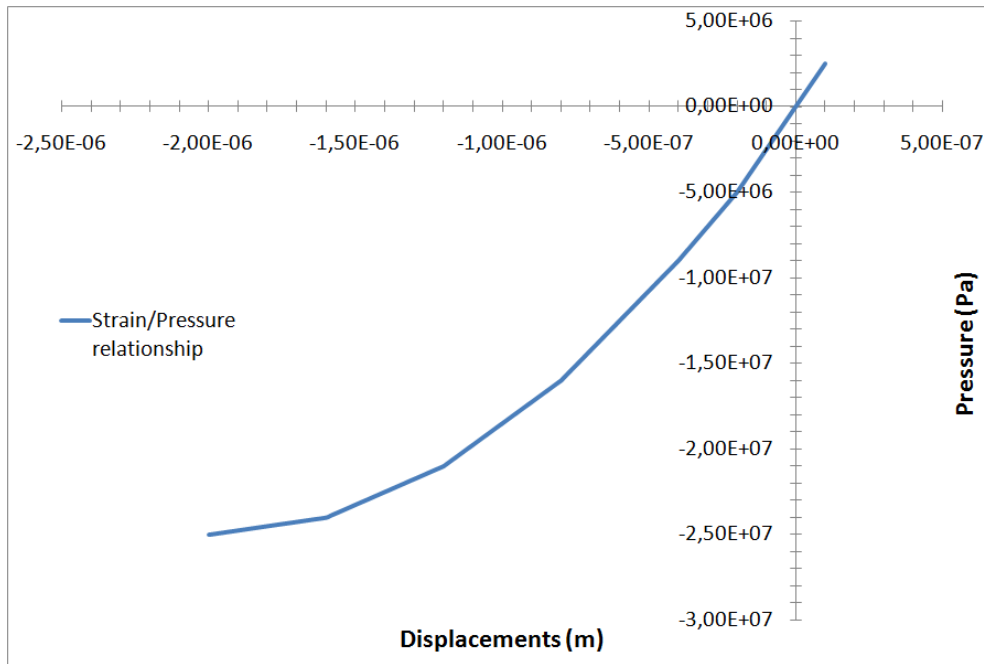
Figure 23: Concrete properties in ANSYS verified by FE cylinder compression and tension test.
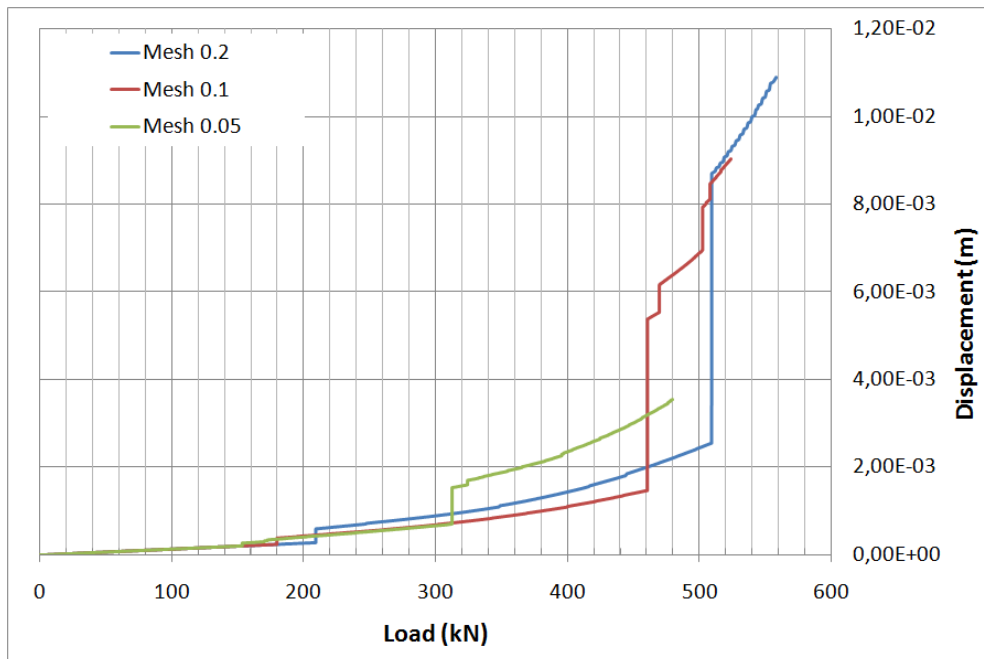
Figure 24: The effect of a finer mesh on finite element wall in ANSYS

4.2 Attuning of the ME models

As previously mentioned the OpenSees is used within a program language environment. To see what effect of changing the number of elements, fibers, center of rotation has on the model the Source.txt (appendix B) file is run in a loop and the counter is then used to change the desired parameter.

4.2.1 Attuning of the flexure-beam element

The setup of the flexure-beam element used to represent a shear wall is tested to evaluate suitable discretization of fibers in the section and elements in the height. For discretization of fibers in the local Y direction the division ranges from 1 to 18 in the section. For the discretization in the height the number of elements ranges from 1 to 57. Discretization in the local Z direction of the section does not affect the results. The ratio of the height from the bottom to the centroid of the curvature distribution c (shown in figure 14) is lastly attuned to follow the FE model as closely as possible.

Discretization of fibers in the Y local direction of the section changes the results for the ultimate force and displacement drastically to begin with but becomes stable in the deflection for eleven elements in the section as seen in figure 25. The fiber division used for the section is four elements per each meter of the wall.

The effects of increasing the number of elements in the height are shown in figure 26. To balance the time needed to calculate the wall response and for obtaining accurate results, four elements are used per meter over the height of the wall.

Based on Massone's experiments [24] the flexure-beam element using centroid of the curvature distribution $c = 0.4$ of the element height provides the best results for his experiments. The effects of changing the center of rotation values for c ranging between 0.1 and 1.0 were tested for the flexure-beam element and the model response calculated. The results are shown in figure 27a. Models with values of c ranging between 0.25 and 0.45 using smaller intervals were also tested and the results are shown in figures 27b and 27c. Based on these tests $c = 0.36$ is used for this study.
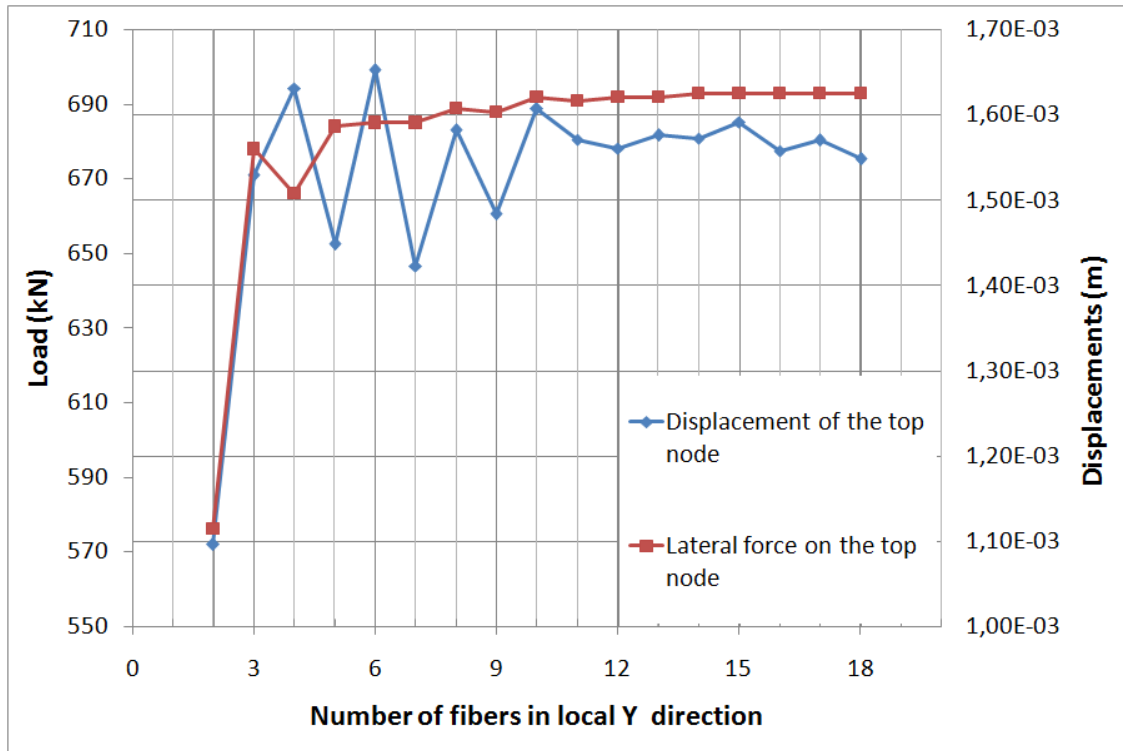
Figure 25: Force and displacement relationship in increasing number of fibers in the local Y direction of the flexure-beam element section.
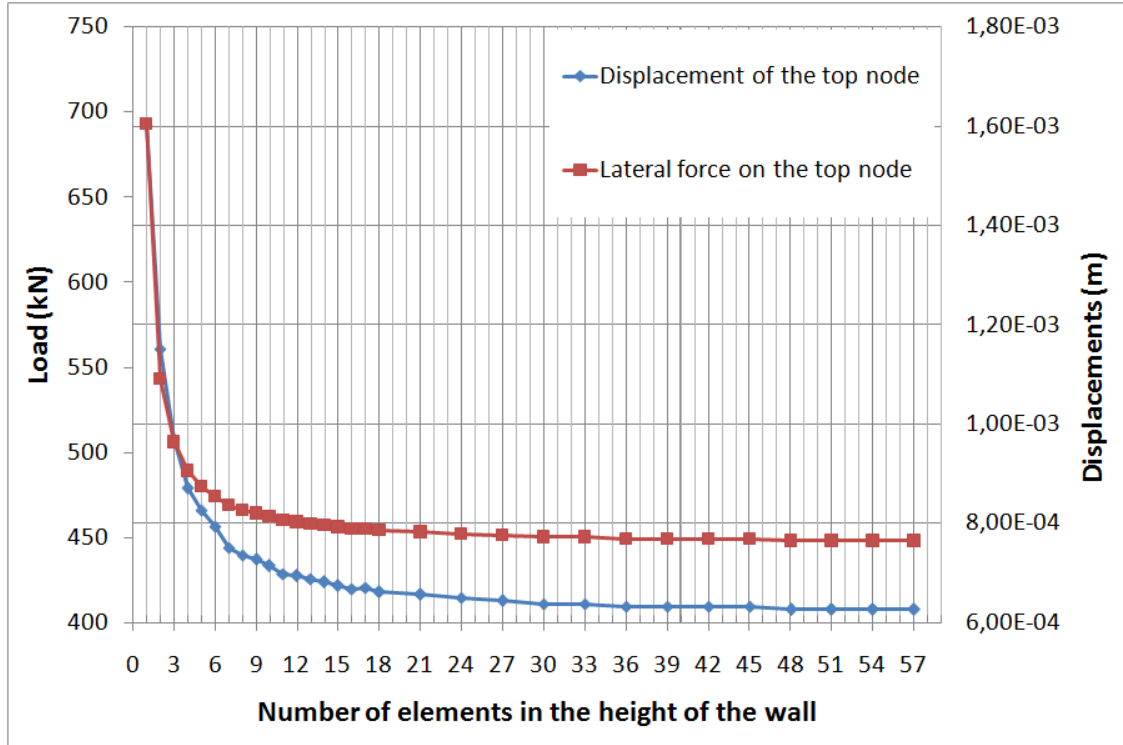
Figure 26: The difference between number of elements in height for a wall modeled with the flexure-beam element.
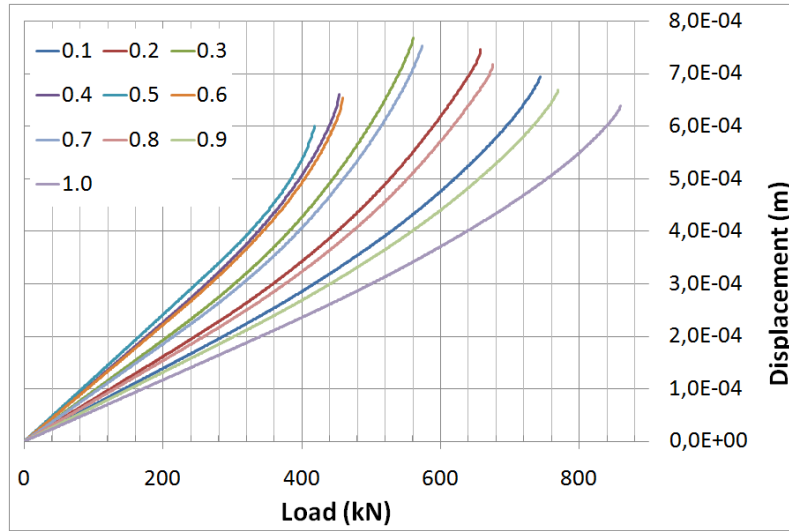
(a) Coarse values between 0.1-1.0.
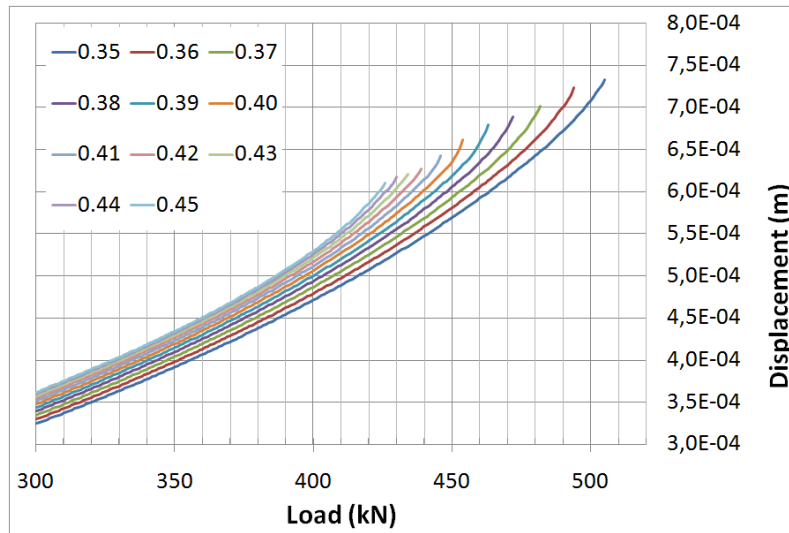
(b) Fine values between 0.35-0.45.
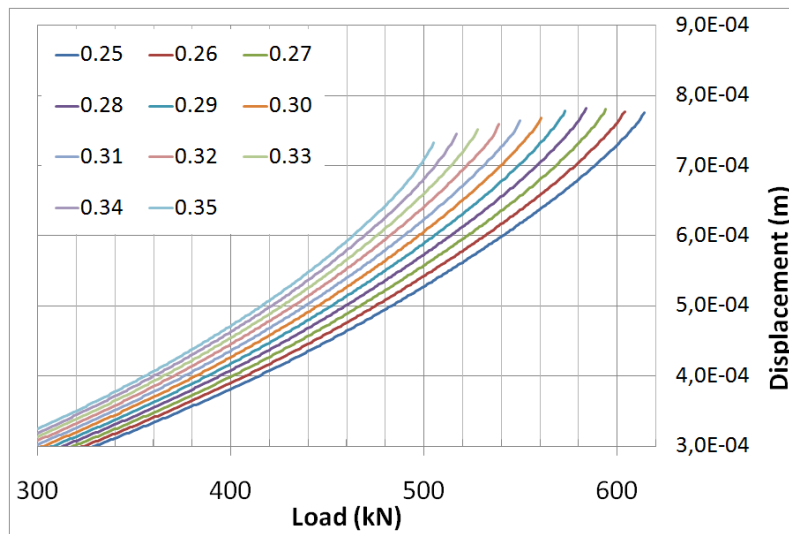
(c) Fine values between 0.25-0.35.

Figure 27: The effects of changing the center of rotation c in the flexure-beam element.

4.2.2 Attuning of the force-beam element

The force-beam element relies on displacement as an input. The solver will calculate the necessary forces needed to produce specified displacements. For calibration purposes target displacement was specified as 0.0035 m with a displacement load step of 0.0001 m. Instead of calculating displacements for a given load the solver, when using displacements as an input, provides the load as a fraction of the input load needed for the target displacement. Therefore, a lateral load of 1.0 N was used as a base for the force-beam elements.

The model showed some unexpected behavior, when testing it with few elements and few integration points of each element, showing random behavior. Instead of the proposed looped approach used for the calibration of the flexure-beam element section the force-beam element section was tested using 1 to 18 fibers in the local Y direction and 1, 3 and 12 elements in the height. Each element has seven integration points. The results are shown in figure 28. When not supplied with sufficient number of elements the section behavior is unstable (figures 28a and 28b). Discretization of four elements per meter in the height and five fibers in the length is chosen based on these results.
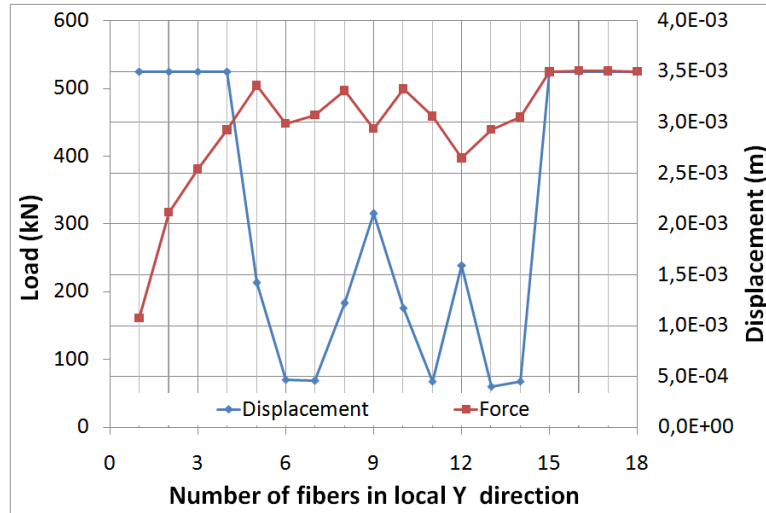
(a) One element in the height.
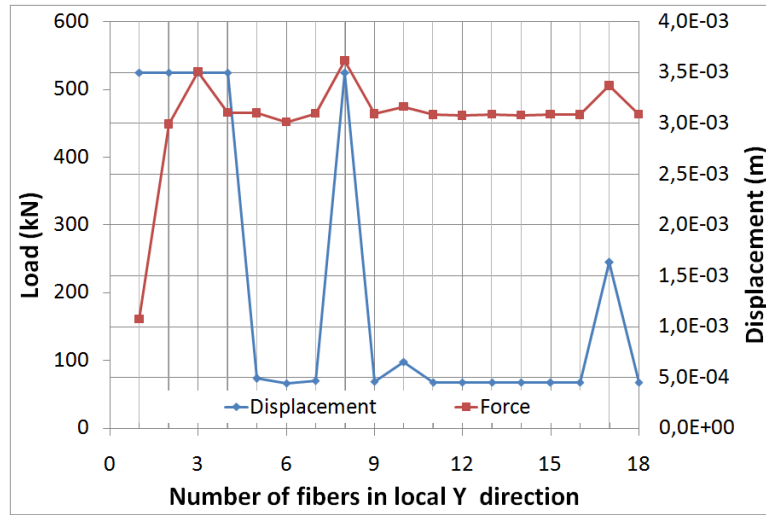
(b) Three elements in the height
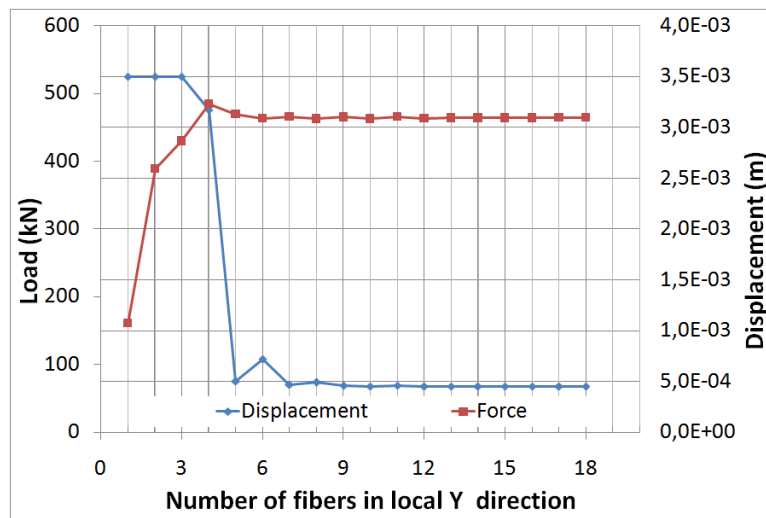
(c) Twelve elements in the height.

Figure 28: Force and displacements as a function of the number of sections in the force-beam element.

4.3 Attuning the Open and Closed Shear transfer coefficients for the FE model

At this stage the FE models using open and closed shear transfer coefficients of 0.8 and 0.4 did not exhibit response that was similar to the responses of the flexure- and force-beam elements. In order to obtain different results these coefficients were changed and given values listed in table 7. The results for each model are shown figure 29. The model with an open coefficient of 0.1 and a closed one of 0.2 are the ones that agree best with the ME models.

Table 7: New coefficients used for open and closed shear transfer of cracks in ANSYS.

β_t	0.4	0.2	0.1	0.05	0.0
β_c	0.8	0.4	0.2	0.1	0.15
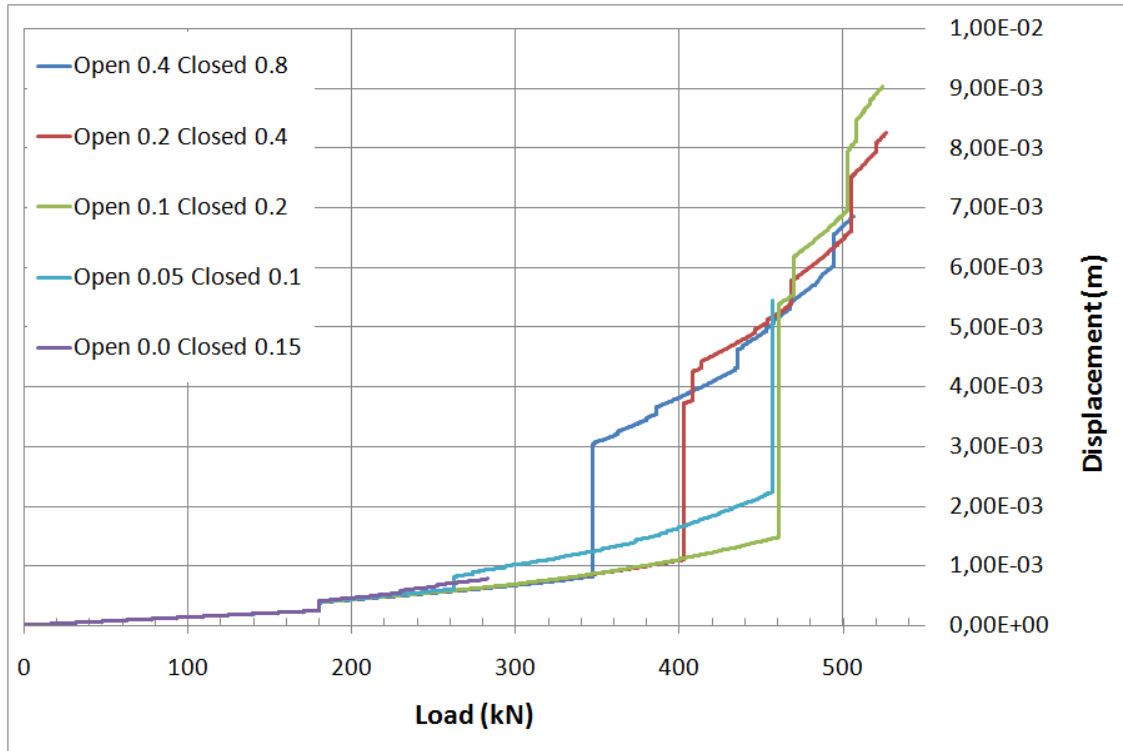
Figure 29: The force displacement relationship using the new coefficients for open and closed shear transfer of cracks in ANSYS.

4.4 Attuning the shear-spring for the force-beam element

As a final stage of experimenting with element attributes and parameters the force-beam element is aggregated with a shear spring. The ratio of the fully cracked section shear modulus to the uncracked shear modulus f_{cr} is calibrated to match the new FE model. For this particular case $f_{cr} = 0.08$ fits best to the FE results. The coarse values for f_{cr} varying from 0.1 and 1.0 are shown in figure 30 and for finer values varying from 0.01 to 0.1 are shown in figure 31.

40
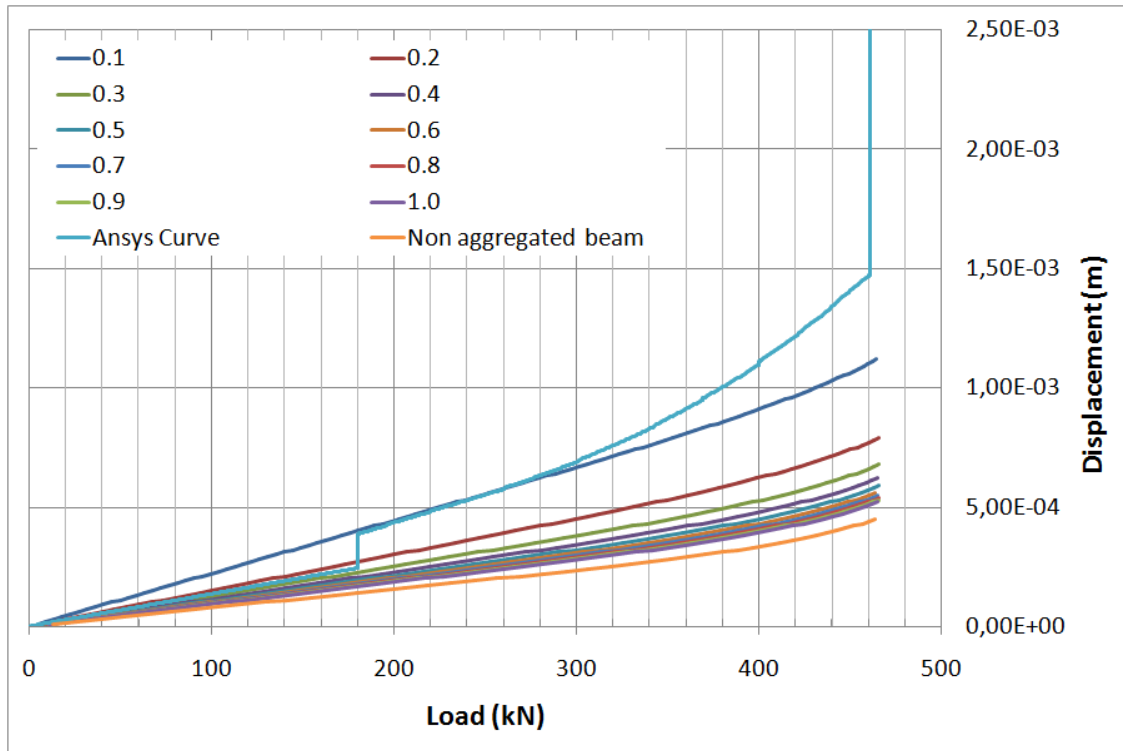
Figure 30: Effects of coarse changes in the values ranging from 0.1-1.0 of f_{cr} for section aggregation spring.
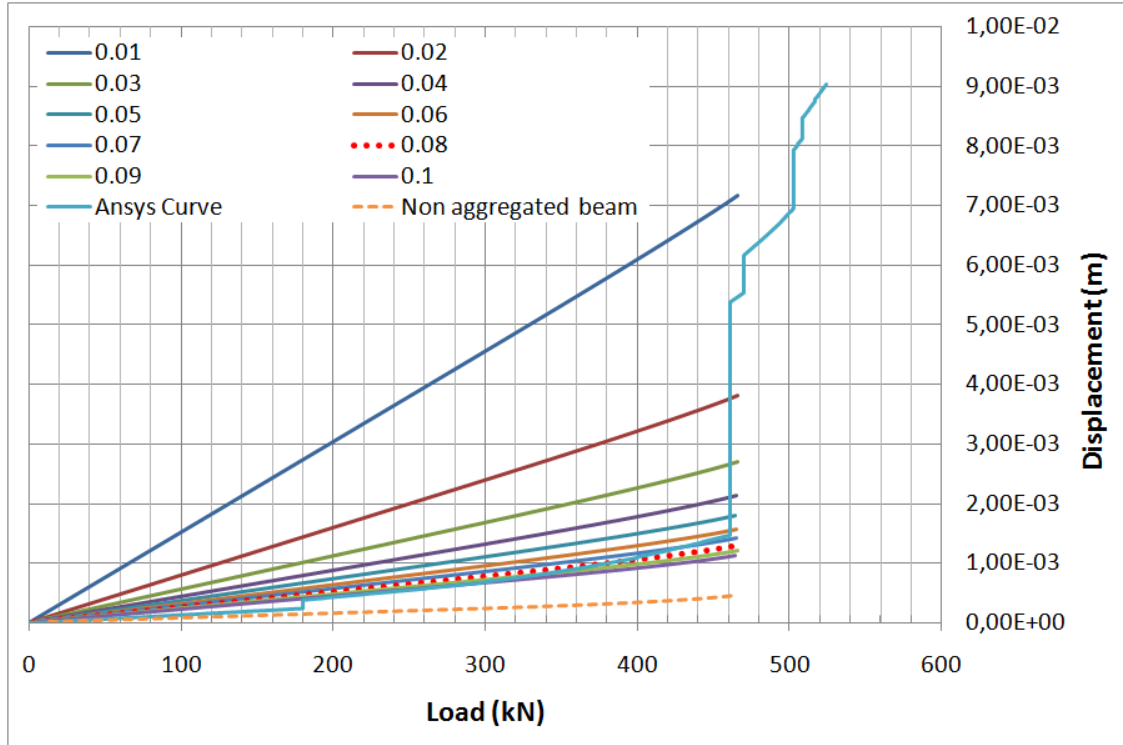
Figure 31: Effects of fine changes in the values ranging from 0.01-0.1 of f_{cr} for section aggregation spring.

5 Analysis and results

In this chapter the results from lateral pushover loading of a simple squat shear wall are displayed. Both linear and non-linear results cases are considered. An in depth look is taken into the FE model and the development of cracks and stress distribution. The results for vertical frequency loading on a wall with footing resting on a sand soil layer are also presented for the FE and ME models.

5.1 Walls without footing subjected to lateral pushover load

The models in this section are squat shear walls. They have no footing and are fixed at the bottom level. This setup is to assess the response of the flexure and force-beam elements when they are used to model a shear wall. Two larger models 5x10 and 5x15 are also analyzed to see if the flexure- and force-beam element response is closer to the FE response with increased slenderness ratio.

5.1.1 Linear tests

The linear test only serves to show the difference between the FE and ME response, where the ME response lacks shear deformation. The flexure-beam element model did not work with linear material properties and could not be used for this comparison. The results are summarized in table 8. The models exhibit expected behavior, the displacements of the FE models are greater than the ones from the force-beam element based ME models. This is due to the fact that the shear lagging is not accounted for in the force-beam element at this stage. The difference due to shear deformation decreases with increased slenderness ratio[6] as expected. This also serves to demonstrate how important it is to know the limitations of the macro elements when using them to represent a structural member, even with simple linear analysis the force-beam element shows three times less the displacement than the FE model of the 5x3 wall while a wall with high slenderness ratio could be represented accurately with that element.

Table 8: Linear displacement of the walls subjected to 1MN load.

Wall	3x3	3x4	3x5	4x3	4x4	4x5	5x3	5x4	5x5
Slenderness ratio	1,00	1,33	1,67	0,75	1,00	1,25	0,60	0,80	1,00
FE model	1,4E-3	2,6E-3	4,6E-3	7,7E-4	1,4E-3	2,2E-3	5,2E-4	8,6E-4	1,4E-3
ME model	7,8E-4	1,8E-3	3,6E-3	3,3E-4	7,8E-4	1,5E-3	1,7E-4	4,0E-4	7,8E-4
Difference	175%	142%	127%	234%	175%	148%	311%	218%	175%

---

[6]Based on the load is constant the difference in displacement is also a tangent difference of the stiffness.

5.1.2 Non-linear results

Results of the non-linear tests are shown in figures 32 through 45. For the FE results the wall response falls into two categories, the one who exhibit one jump in the displacement curve due to an initial tear at the bottom of the model and then undergo failure and secondly walls that exhibit two jumps, one due to the initial tear and then a big portion of the wall cracking before it fails. More in depth look at the FE models is in chapter 5.2.3 The models who have a two jump displacement curve 3x3, 3x4, 3x5, 4x4 and 4x5 are shown with the full FE results as well as truncated results to better exhibit the correlation between the FE and the ME models.

The non-linear results show quite good relation in the ultimate force for both the ME and the FE model. Displacement wise the force-beam element yields results that are closer to the FE model than the flexure-beam element, this is not surprising considering that the shear spring was attuned to follow the displacements provided by the FE model. Two other tests were done using a 5.0 m by 10.0 m wall and 5.0 m by 15.0 m wall to examine the effects of increasing the height. The results are shown in figures 46 and 47. The slenderness ratio does not seem to have effect on the correlation between the models.

To get a better overview of the differences table 9 shows displacements are measured at 80% of the ultimate load of the flexure member for each wall and the percental differnces between the force-beam and flexure-beam elements based on the FE model displacements.

The results show that the flexure-beam element assumes greater stiffness than the FE model and the shear-spring aggregated force-beam model. It therefore exhibits less deformations while the wall is still linear. On the other hand the flexure-beam element shows more non-linear behavior than the force-beam element. For the 3x4 and 3x5 wall the non-linear curvature of the flexure-beam element is quite close to the one of the FE model so there might be some correlation between slenderness ratio and non-linear displacement curvature.

Table 9: Displacements of the non-linear models at 80% ultimate load of the flexure-beam element (displacements are in meters).

Wall	Load (kN)	FE model	Force-Beam	%	Flexure-Beam	%
3x3	398.4	$1.09E-03$	$9.10E-04$	84	$4.79E-04$	44
3x4	304.8	$1.53E-03$	$1.20E-03$	79	$7.34.E-04$	48
3x5	247.2	$2.01E-03$	$1.56E-03$	77	$1.06E-03$	53
4x3	686.4	$9.89E-04$	$9.80E-04$	99	$4.39E-04$	44
4x4	533.6	$1.87E-03$	$1.21E-03$	65	$6.35E-04$	34
4x5	435.2	$2.15E-03$	$1.50E-03$	70	$8.84E-04$	41
5x3	1028.8	$9.79E-04$	$1.18E-03$	121	$4.27E-04$	44
5x4	813.6	$1.68E-03$	$1.28E-03$	76	$5.92E-04$	35
5x5	669.6	$2.12E-03$	$1.52E-03$	72	$7.94E-04$	37
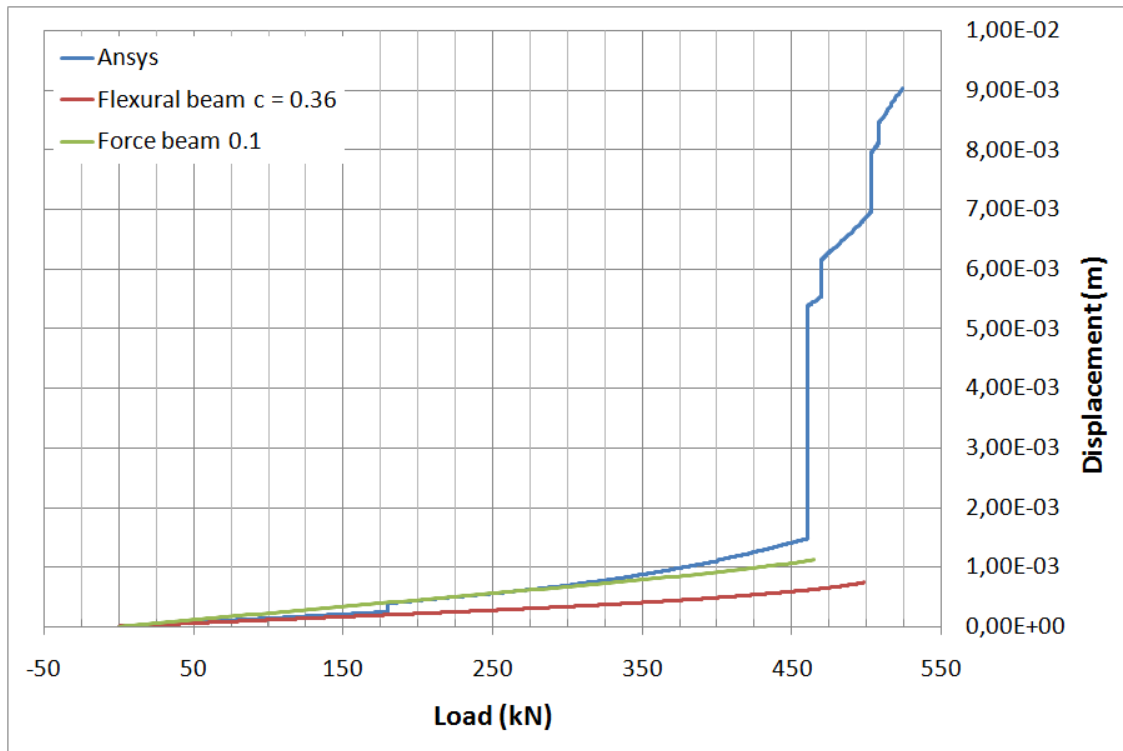
Figure 32: The full results of the 3.0 m by 3.0 m wall.
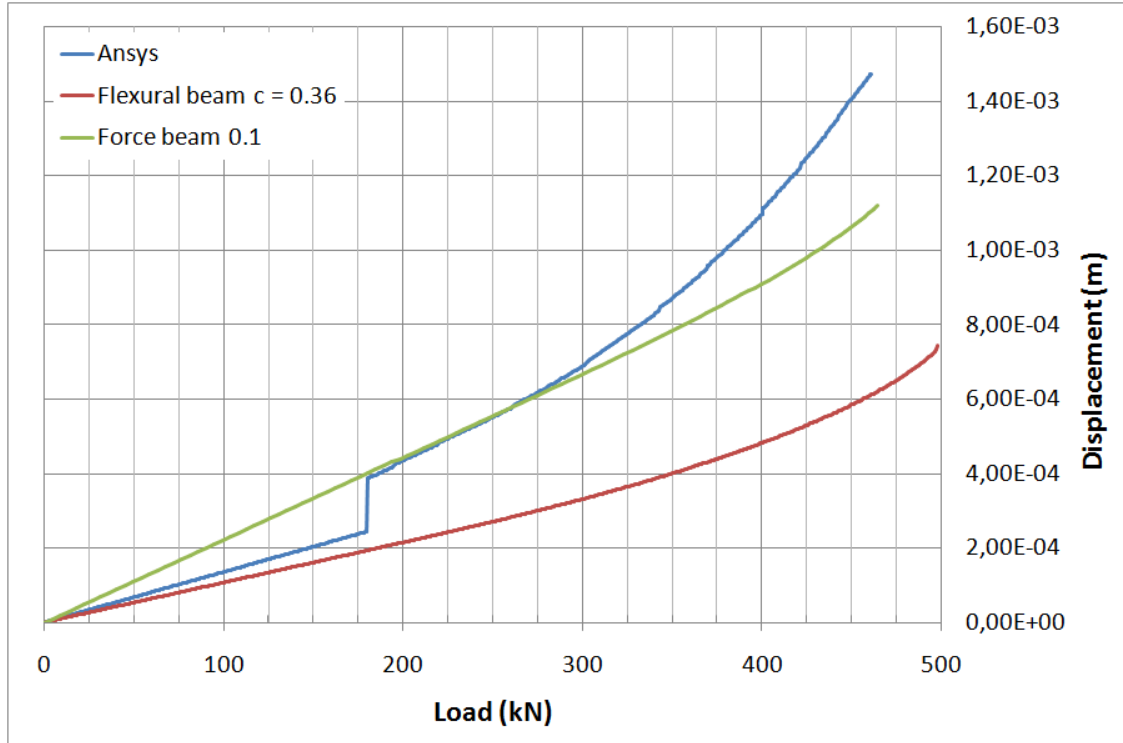
Figure 33: The truncated results of the 3.0 m by 3.0 m wall.

45
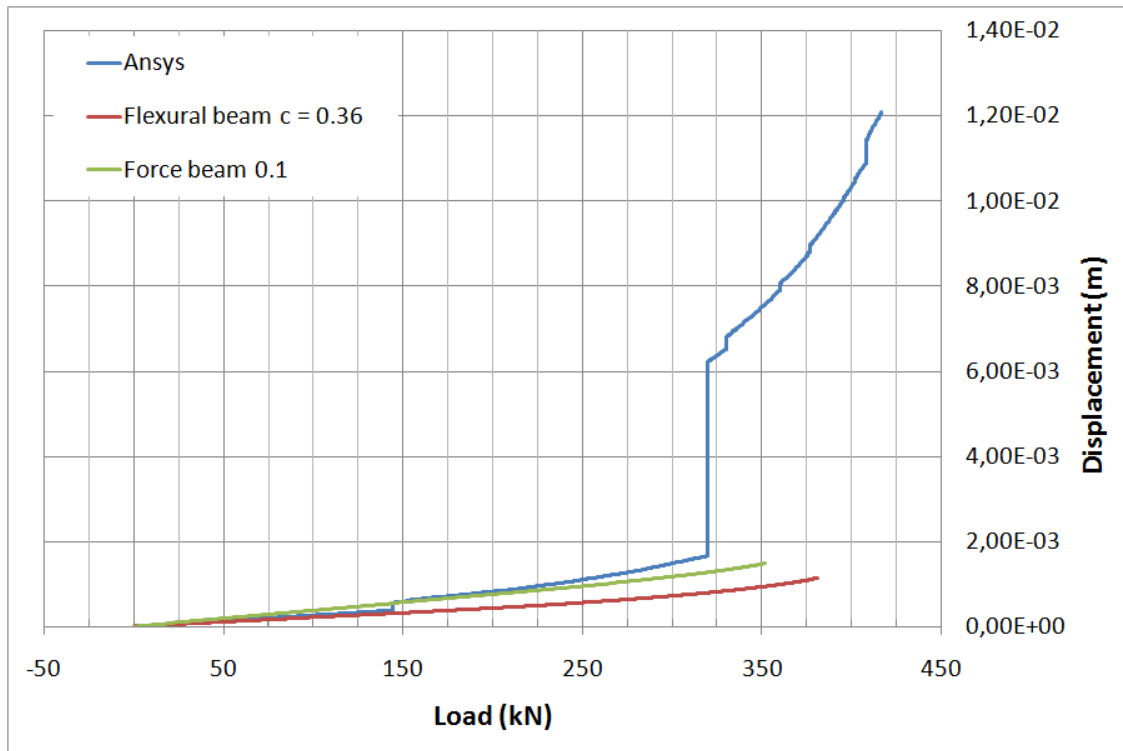
Figure 34: The full results of the 3.0 m by 4.0 m wall.
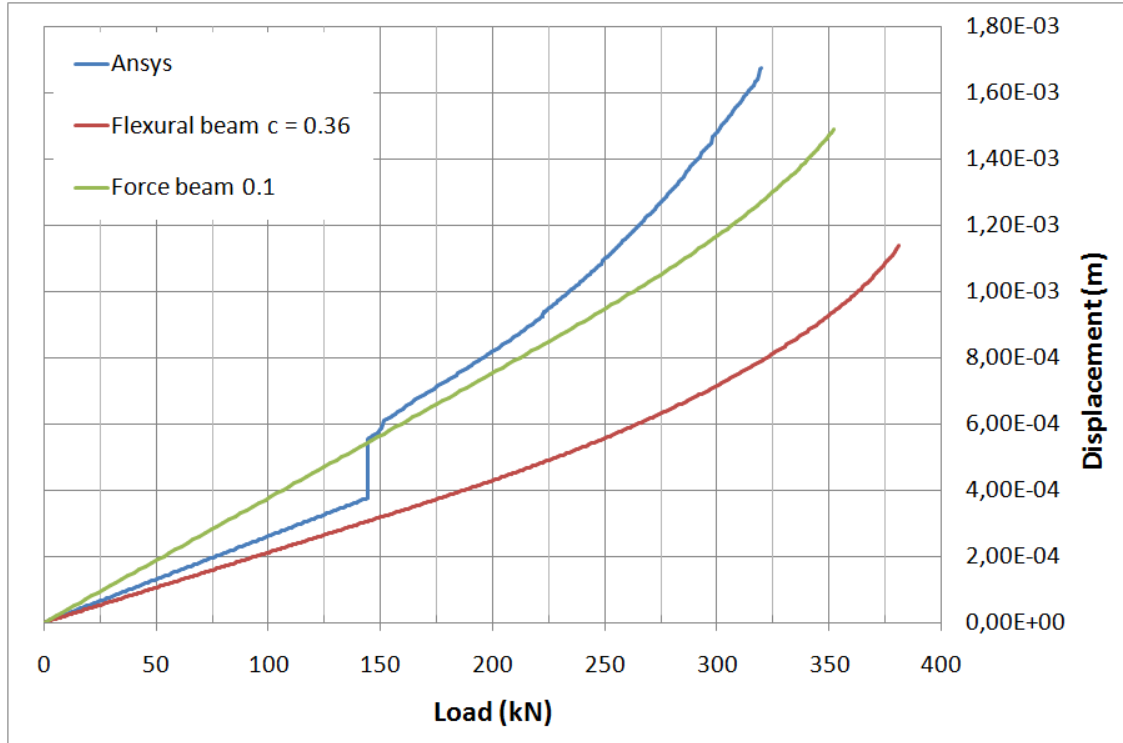
Figure 35: The truncated results of the 3.0 m by 4.0 m wall.

46
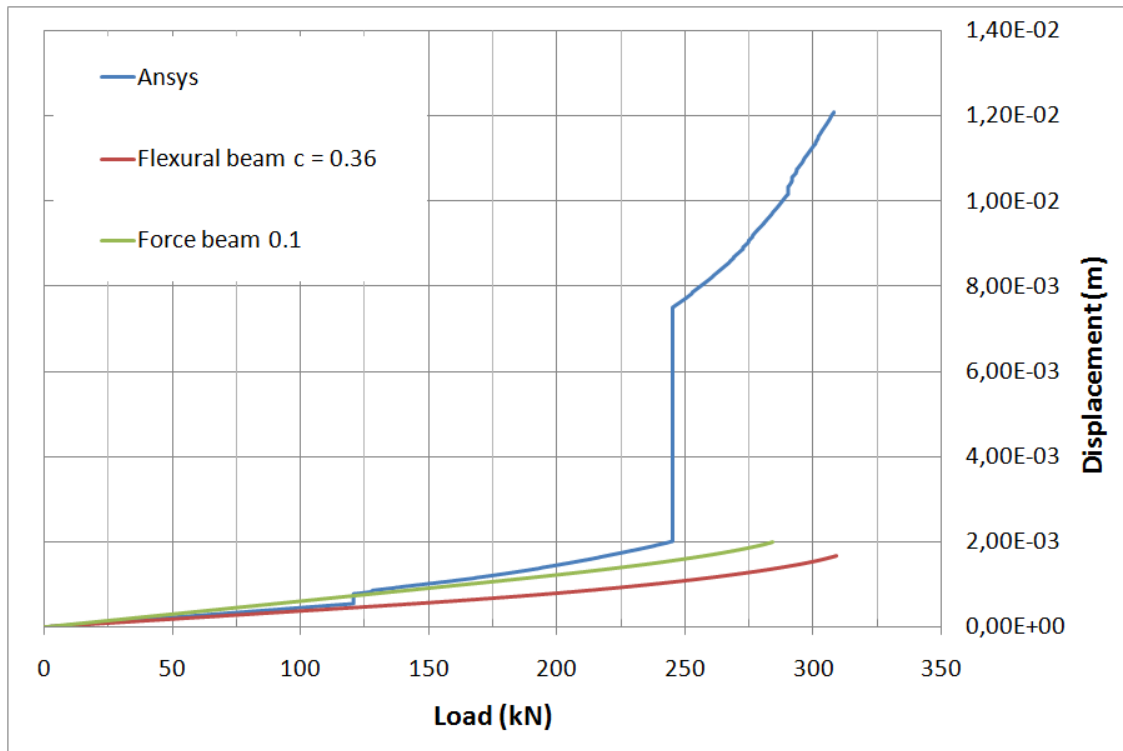
Figure 36: The full results of the 3.0 m by 5.0 m wall.
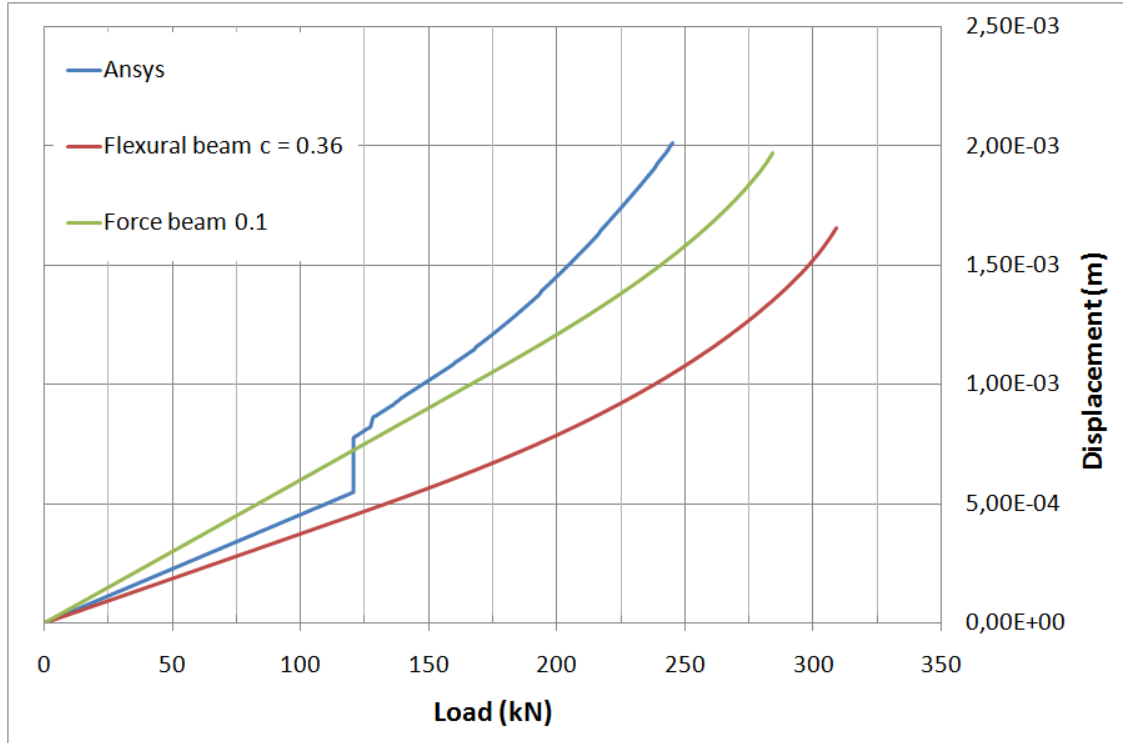
Figure 37: The truncated results of the 3.0 m by 5.0 m wall.
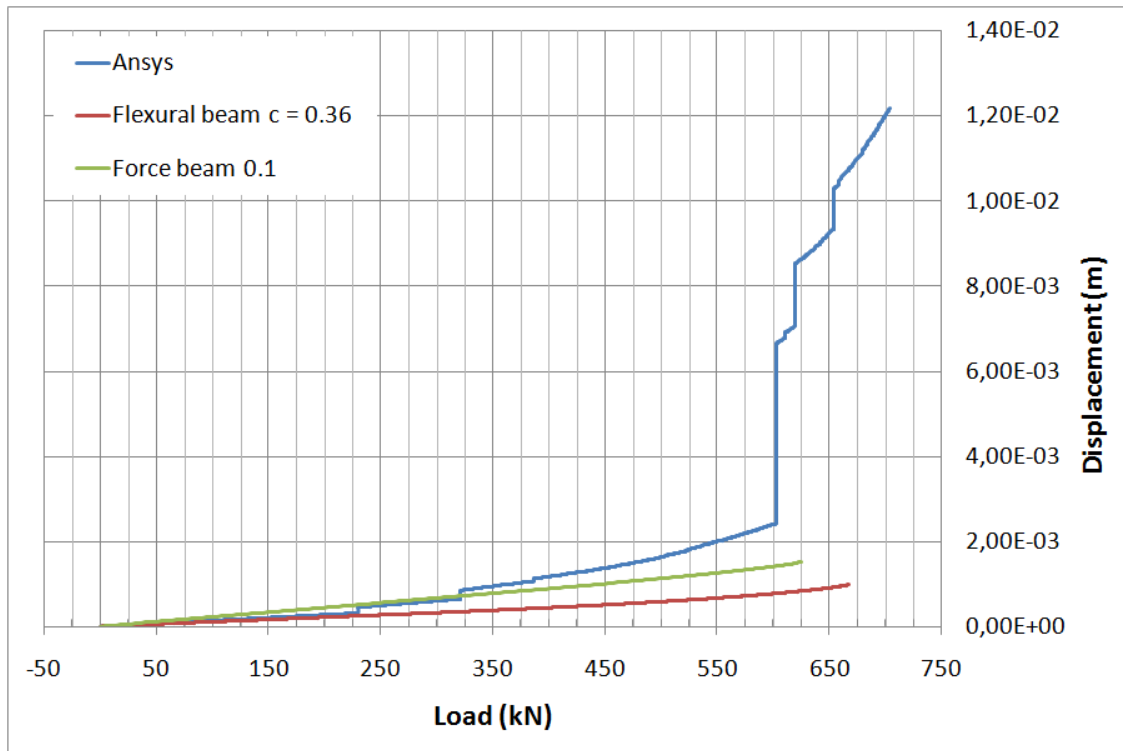
Figure 38: The full results of the 4.0 m by 4.0 m wall.
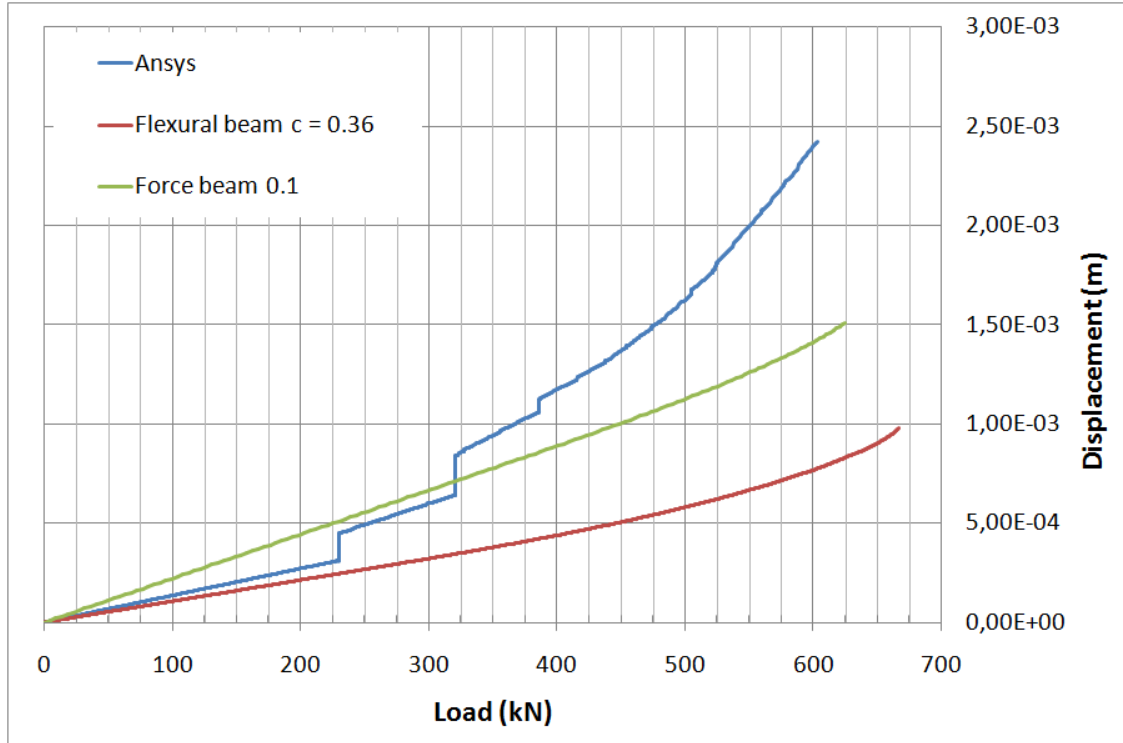
Figure 39: The truncated results of the 4.0 m by 4.0 m wall.

48
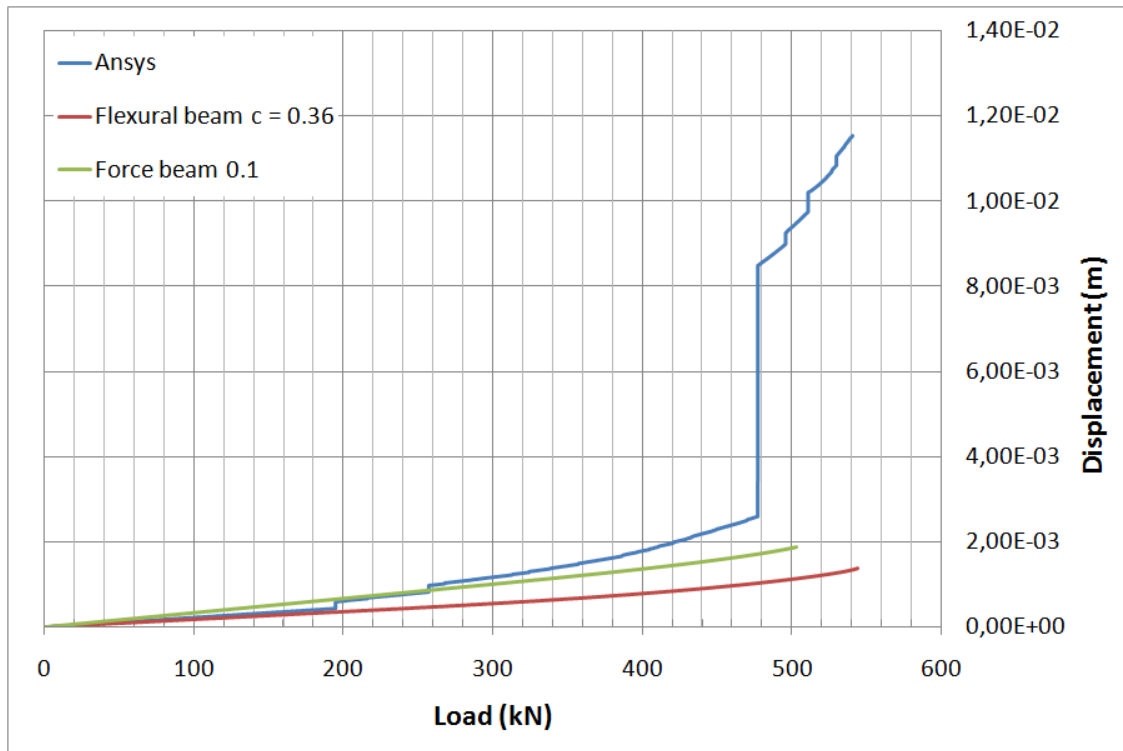
Figure 40: The full results of the 4.0 m by 5.0 m wall.
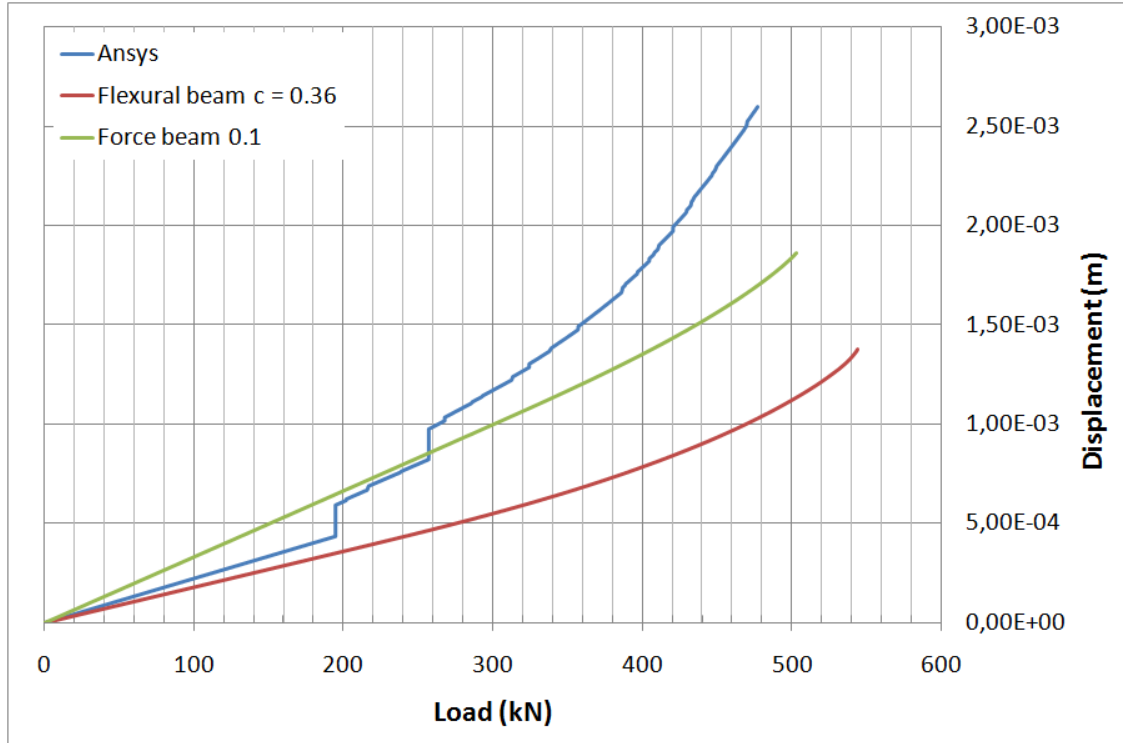
Figure 41: The truncated results of the 4.0 m by 5.0 m wall.

49
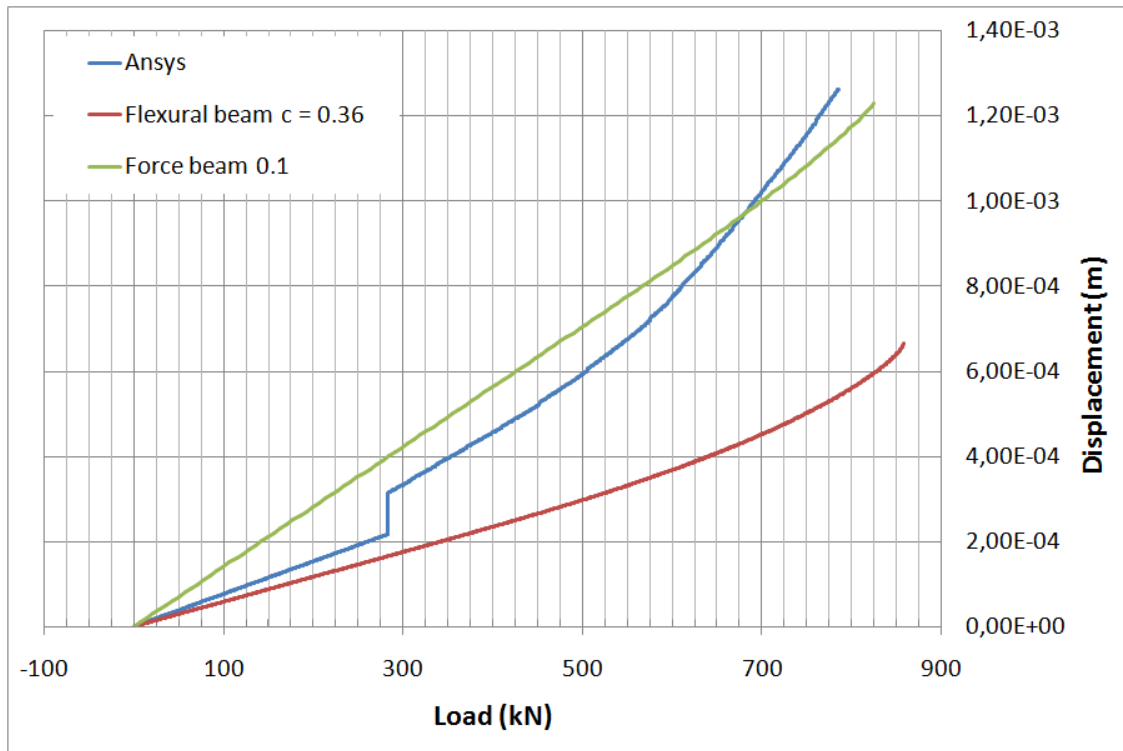
Figure 42: The full results of the 4.0 m by 3.0 m wall.
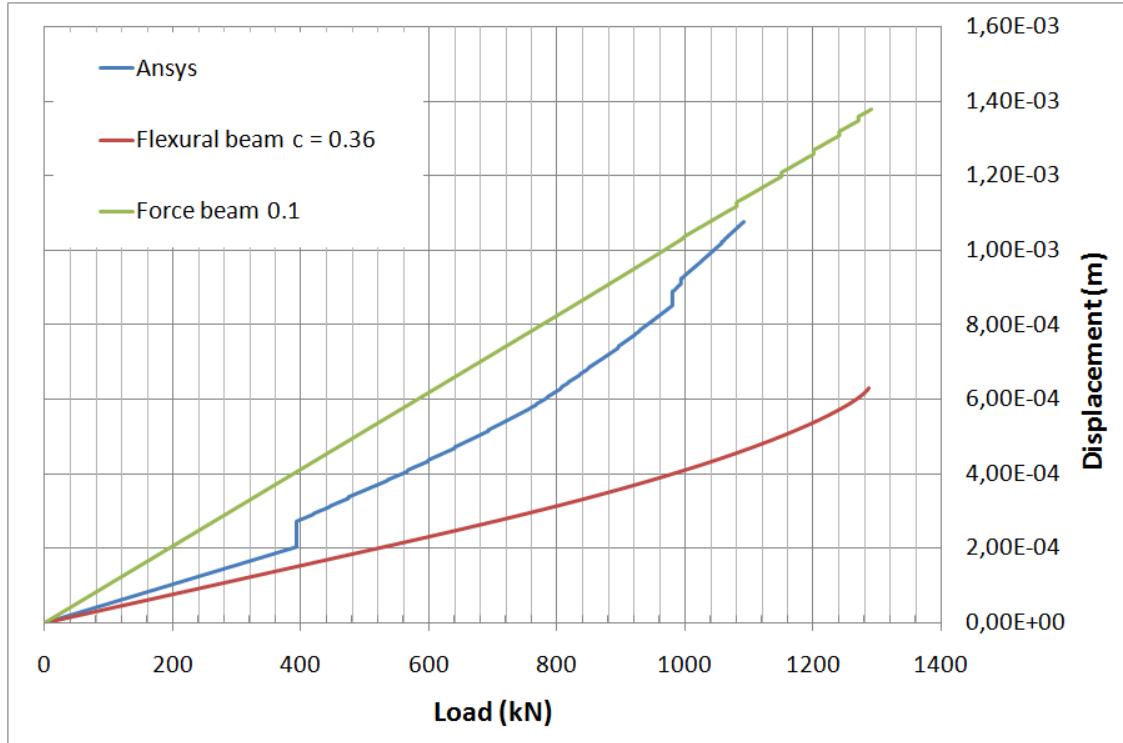
Figure 43: The full results of the 5.0 m by 3.0 m wall.

50
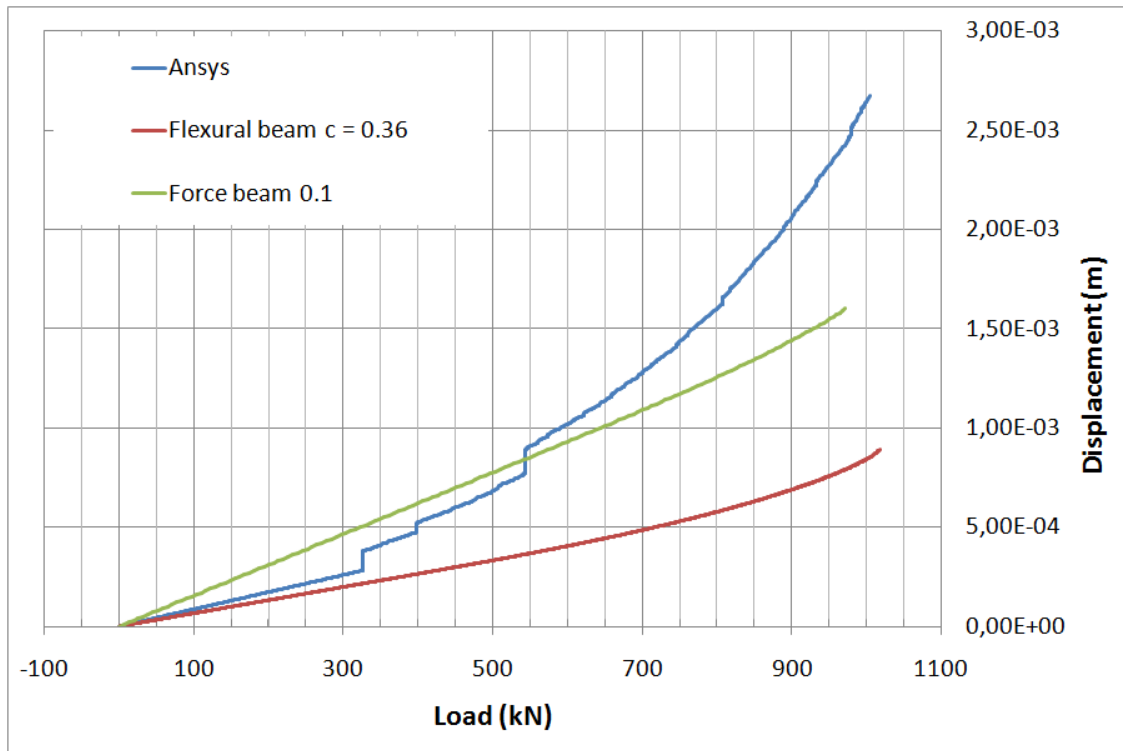
Figure 44: The full results of the 5.0 m by 4.0 m wall.
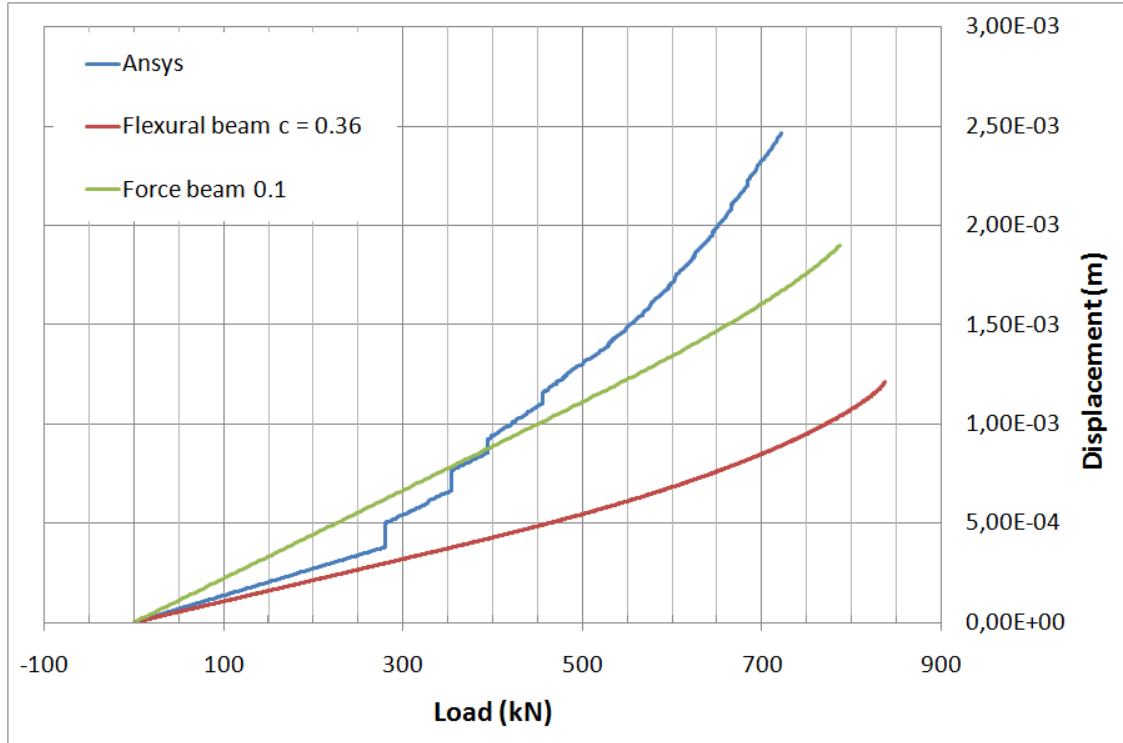
Figure 45: The full results of the 5.0 m by 5.0 m wall.

51
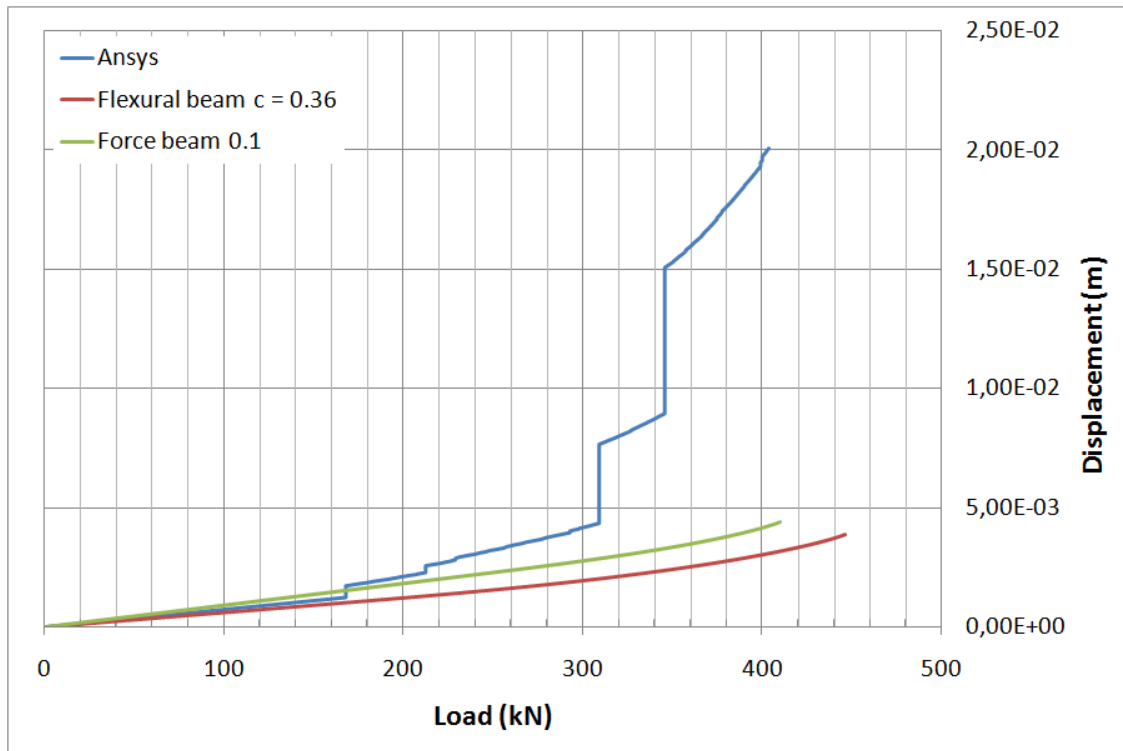
Figure 46: The full results of the 5.0 m by 10.0 m wall.
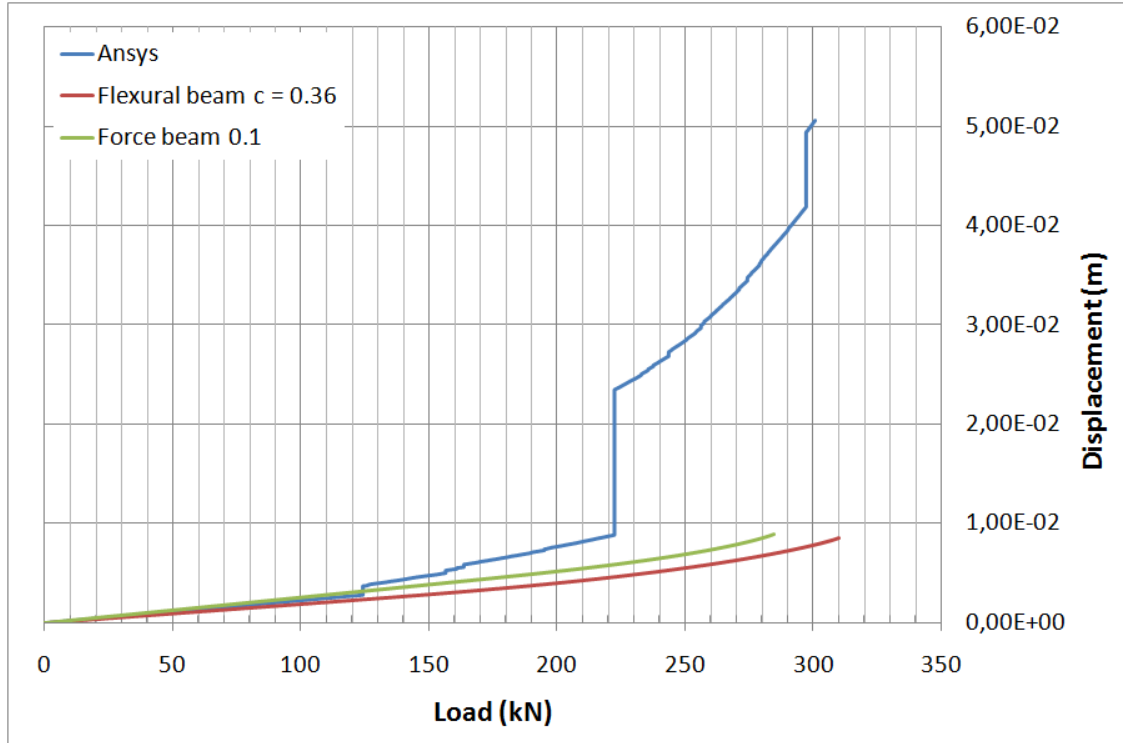
Figure 47: The full results of the 5.0 m by 15.0 m wall.

5.1.3 More in depth look at the FE model results

If the FE models are examined with greater care there is always a first jump, an initial tear at the bottom of the model where the wall starts to behave non-linear. This is not the case with the 4x3, 5x3, 5x4 and 5x5 models where failure happens at the top elements of the wall. Figures 48 through 61 show the crack formation before and after each jump as well as the stresses in Z direction, XZ shear stresses, plastic strains in X and Z direction as well as plastic strain intensity.

It seems that another loading scheme is needed for shear wall models with low aspect ratio to capture failure at the bottom of the wall, however as seen in figures 48 and 61 the stresses in Z direction and shear in XZ plane predicts how the next cracking form will be so.

It is interesting to note how the stresses vary non-linearly as well as how the cracks are strained in the X and Z direction. The strain intensity is identical to the crack formations. Figure 62 compares the 3x3 wall meshed with 0.05 m edge length elements versus the model with 0.1 edge length.The crack pattern is more subtle in the more finely meshed wall.

(a) Crack Pattern of a 3x3 wall.

(b) Stresses in Z direction in a 3x3 wall.

(c) XZ shear stresses in a 3x3 wall.

(d) Strains in X direction in a 3x3 wall.

(e) Strains in Z direction in a 3x3 wall.

(f) Strain intensity in a 3x3 wall.

Figure 48: Figures showing crack pattern, stresses and strains in a 3x3 before first crack formation @ substep 182.

(a) Crack Pattern of a 3x3 wall.

(b) Stresses in Z direction in a 3x3 wall.

(c) XZ shear stresses in a 3x3 wall.

(d) Strains in X direction in a 3x3 wall.

(e) Strains in Z direction in a 3x3 wall.

(f) Strain intensity in a 3x3 wall.

Figure 49: Figures showing crack pattern, stresses and strains in a 3x3 after first crack formation @ substep 183.

(a) Crack Pattern of a 3x3 wall.

(b) Stresses in Z direction in a 3x3 wall.

(c) XZ shear stresses in a 3x3 wall.

(d) Strains in X direction in a 3x3 wall.

(e) Strains in Z direction in a 3x3 wall.

(f) Strain intensity in a 3x3 wall.

Figure 50: Figures showing crack pattern, stresses and strains in a 3x3 before second crack formation @ substep 496.
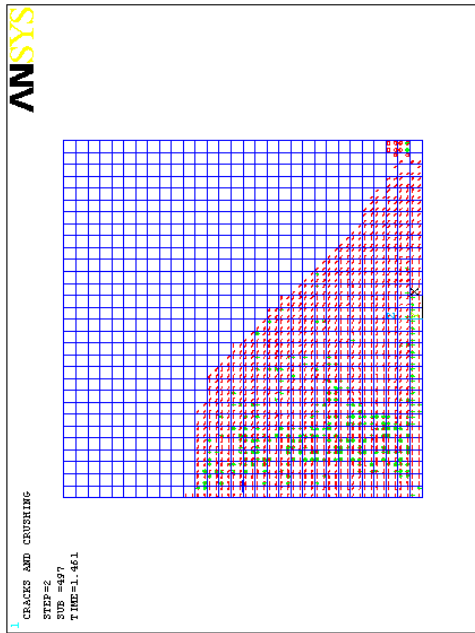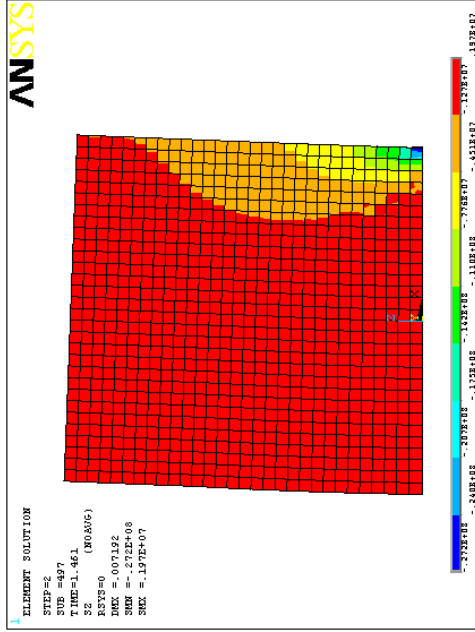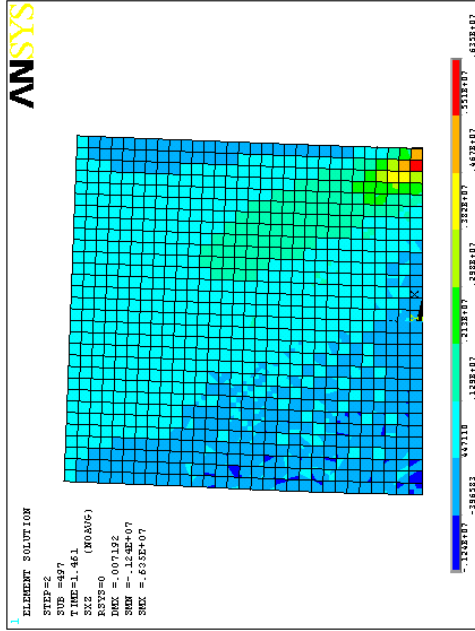
(c) XZ shear stresses in a 3x3 wall.

(b) Stresses in Z direction in a 3x3 wall.

(a) Crack Pattern of a 3x3 wall.
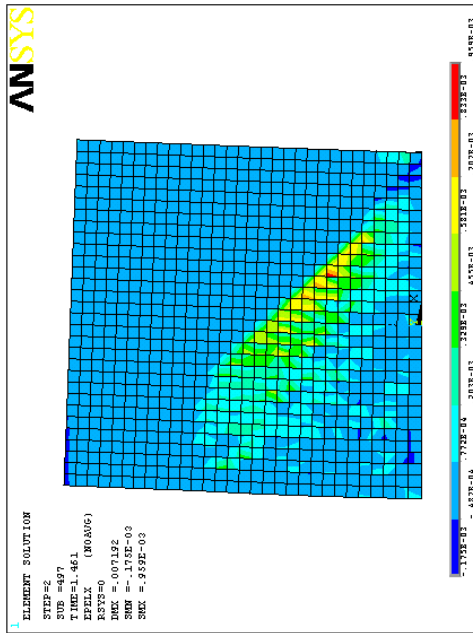
(f) Strain intensity in a 3x3 wall.
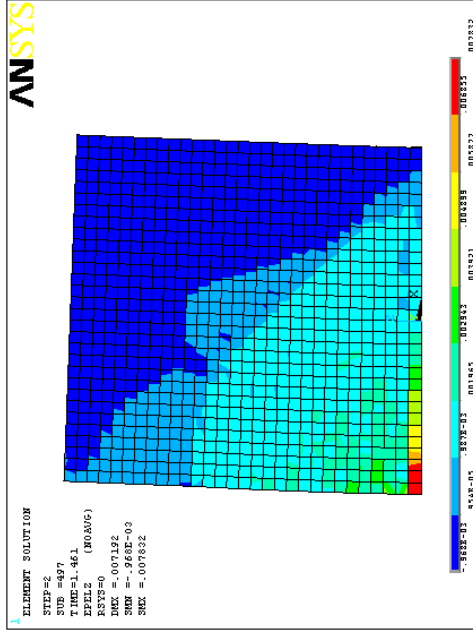
(e) Strains in Z direction in a 3x3 wall.
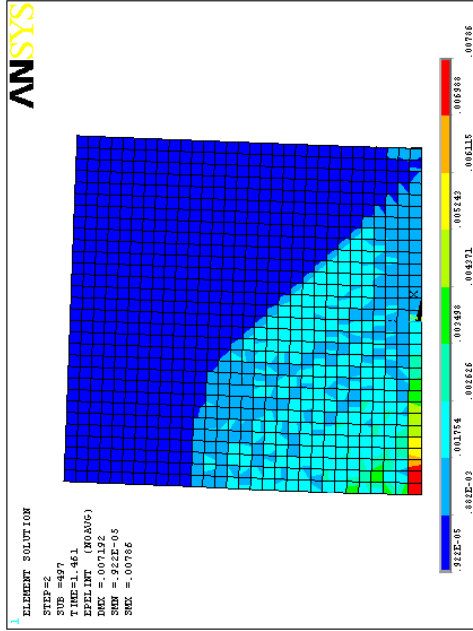
(d) Strains in X direction in a 3x3 wall.

Figure 51: Figures showing crack pattern, stresses and strains in a 3x3 after second crack formation @ substep 497.
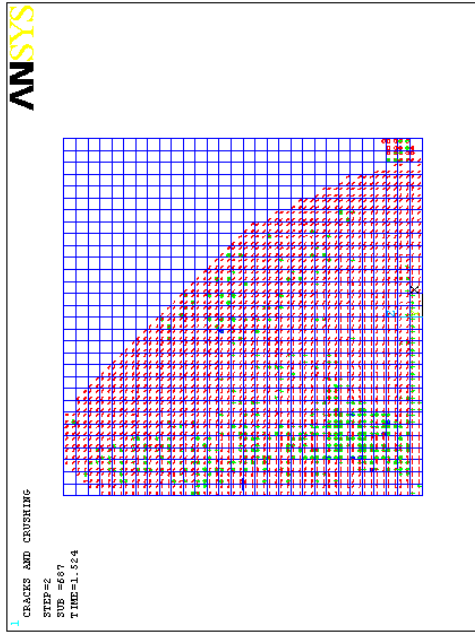
(a) Crack Pattern of a 3x3 wall.
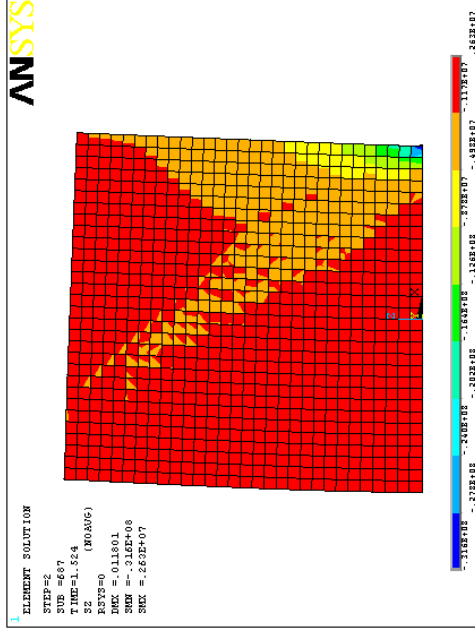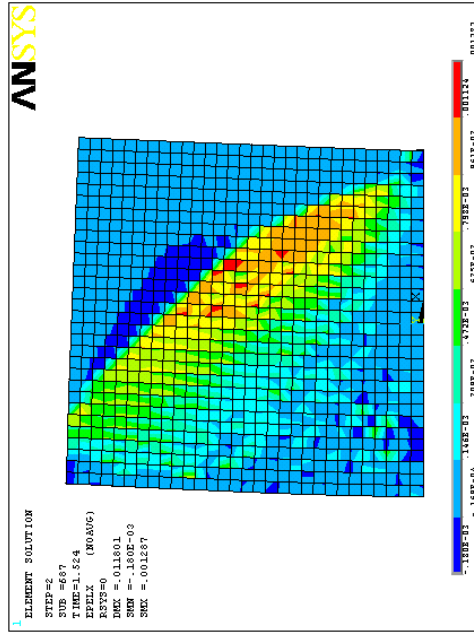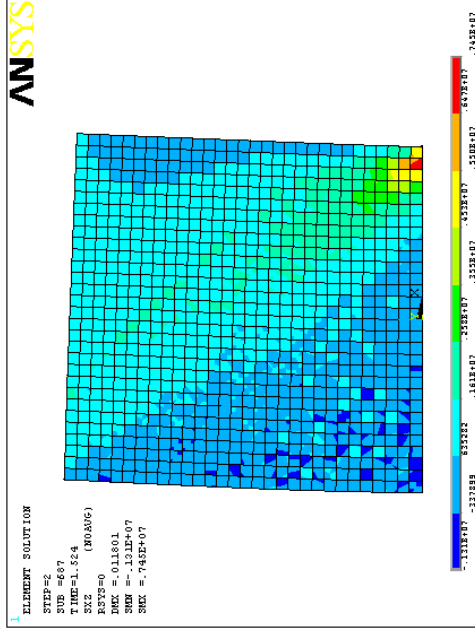
(b) Stresses in Z direction in a 3x3 wall.

(c) XZ shear stresses in a 3x3 wall.

(d) Strains in X direction in a 3x3 wall.
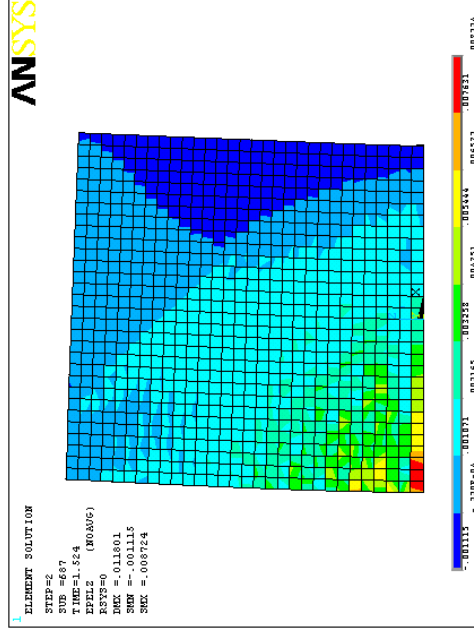
(e) Strains in Z direction in a 3x3 wall.
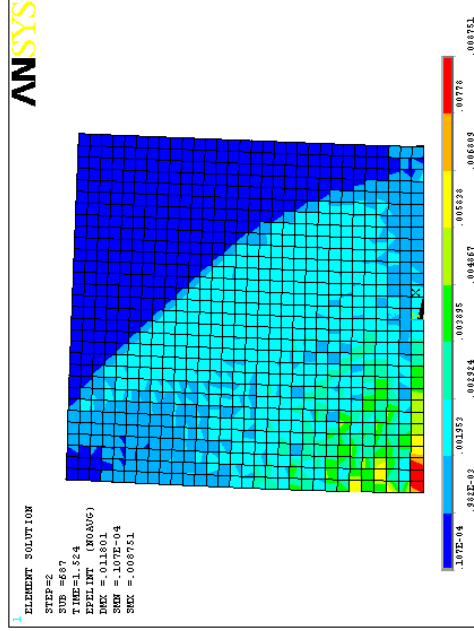
(f) Strain intensity in a 3x3 wall.

Figure 52: Figures showing crack pattern, stresses and strains in a 3x3 before failure @ formation 687.
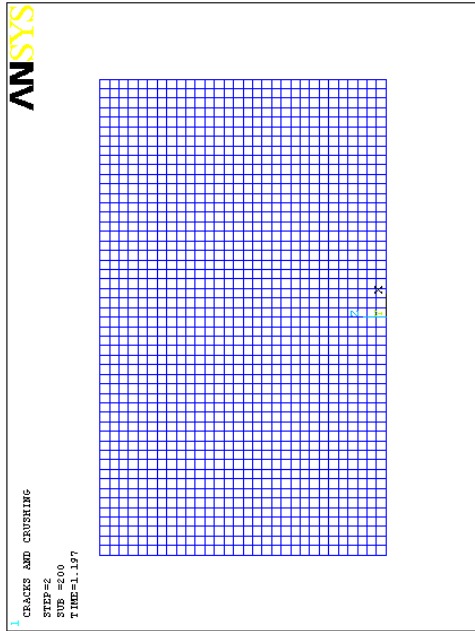
(a) Crack Pattern of a 5x3 wall.
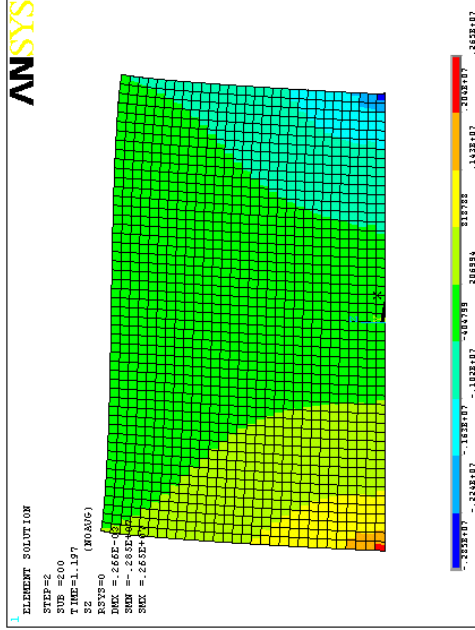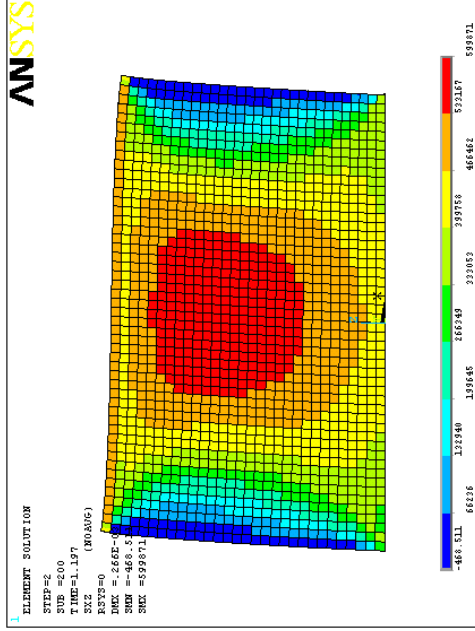
(b) Stresses in Z direction in a 5x3 wall.

(c) XZ shear stresses in a 5x3 wall.
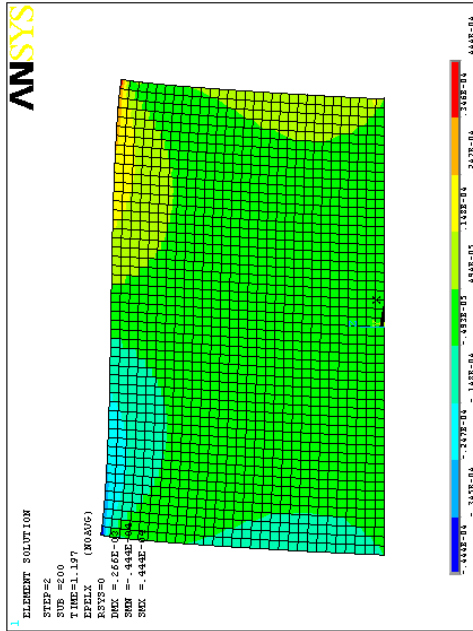
(d) Strains in X direction in a 5x3 wall.
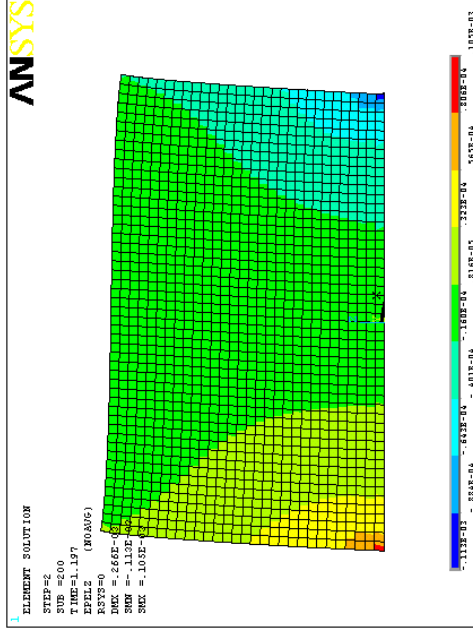
(e) Strains in Z direction in a 5x3 wall.
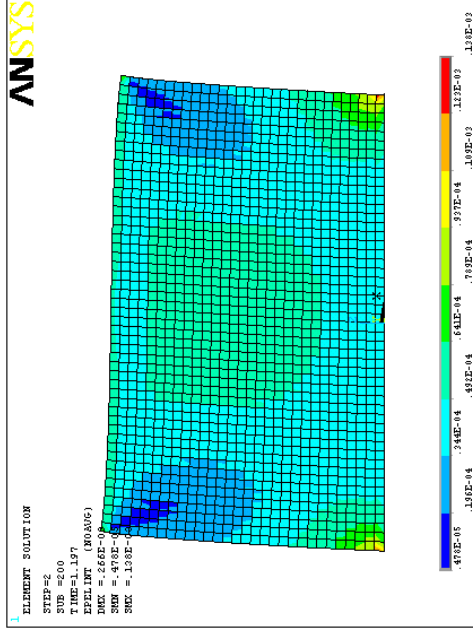
(f) Strain intensity in a 5x3 wall.

Figure 53: Figures showing crack pattern, stresses and strains in a 5x3 before first crack formation @ substep 200.
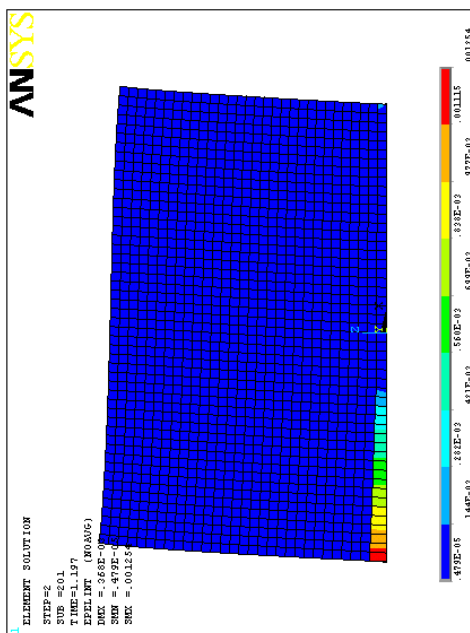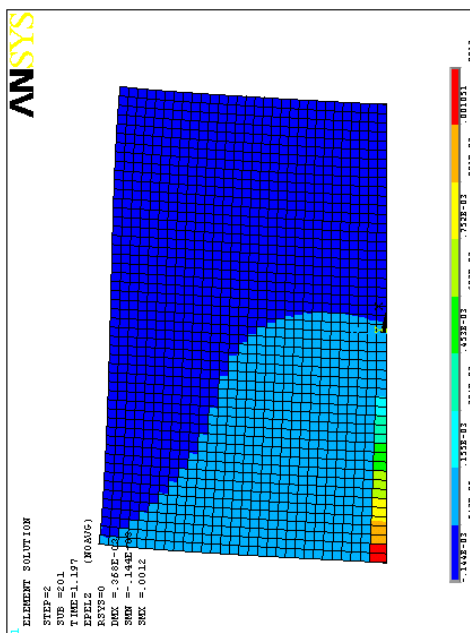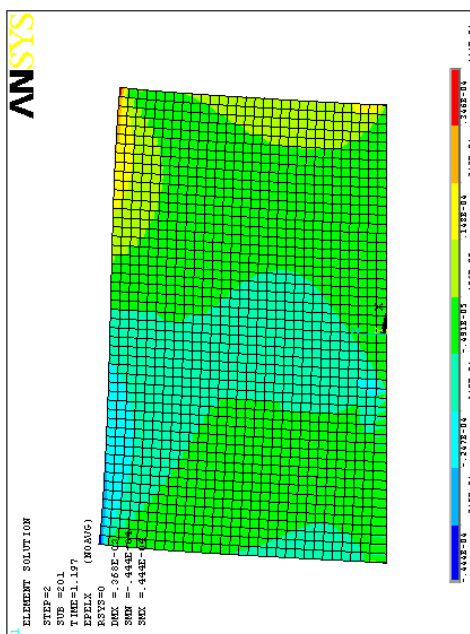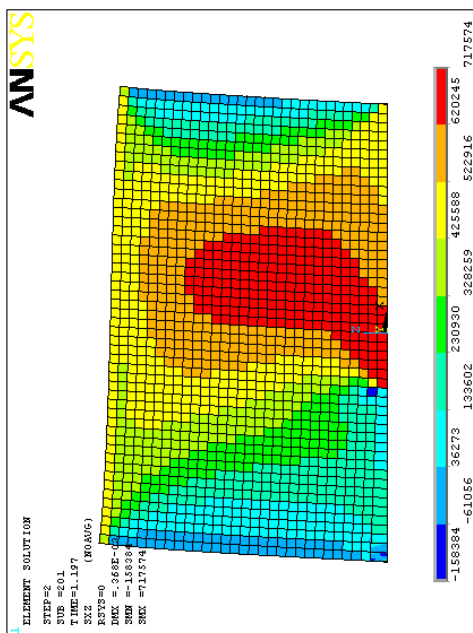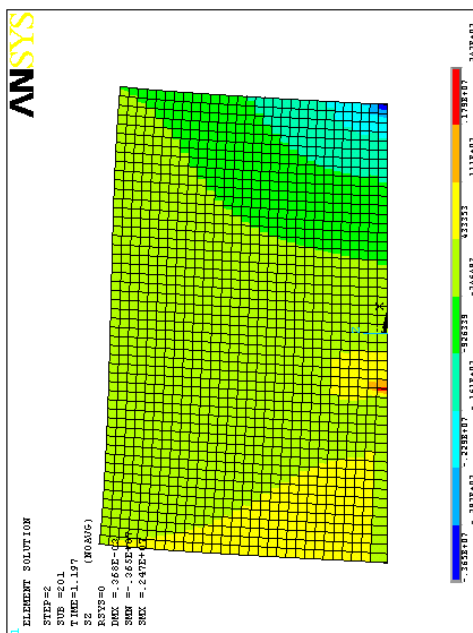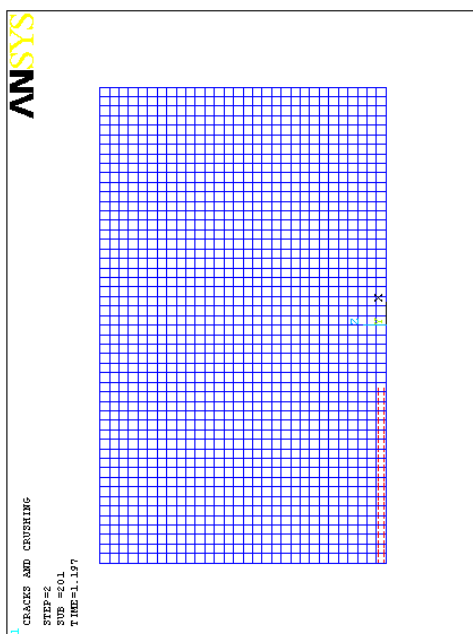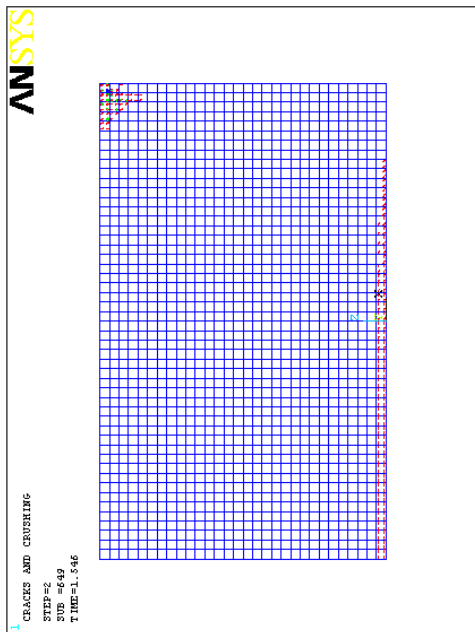
(a) Crack Pattern of a 5x3 wall.
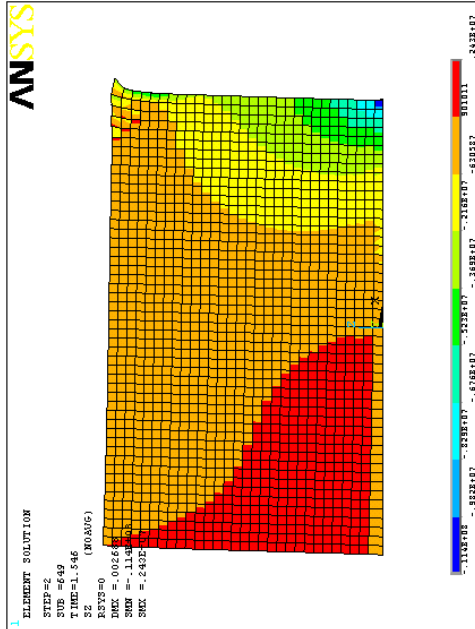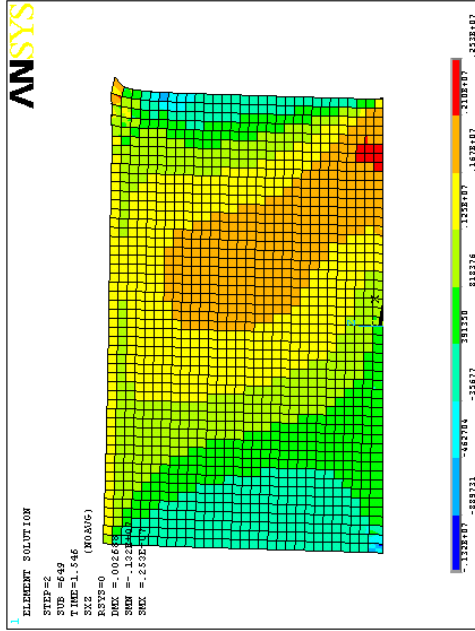
(b) Stresses in Z direction in a 5x3 wall.

(c) XZ shear stresses in a 5x3 wall.

(d) Strains in X direction in a 5x3 wall.

(e) Strains in Z direction in a 5x3 wall.

(f) Strain intensity in a 5x3 wall.

Figure 54: Figures showing crack pattern, stresses and strains in a 5x3 after first crack formation @ substep 201.

(a) Crack Pattern of a 5x3 wall.

(b) Stresses in Z direction in a 5x3 wall.

(c) XZ shear stresses in a 5x3 wall.
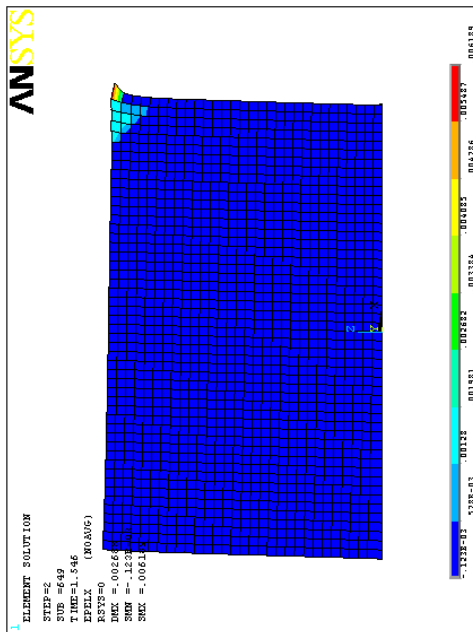
(d) Strains in X direction in a 5x3 wall.
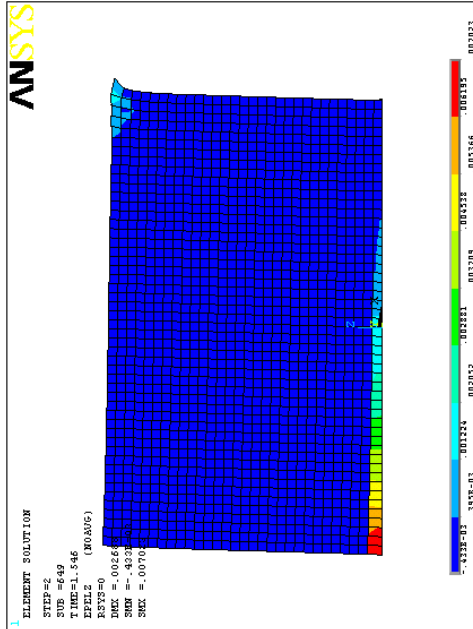
(e) Strains in Z direction in a 5x3 wall.
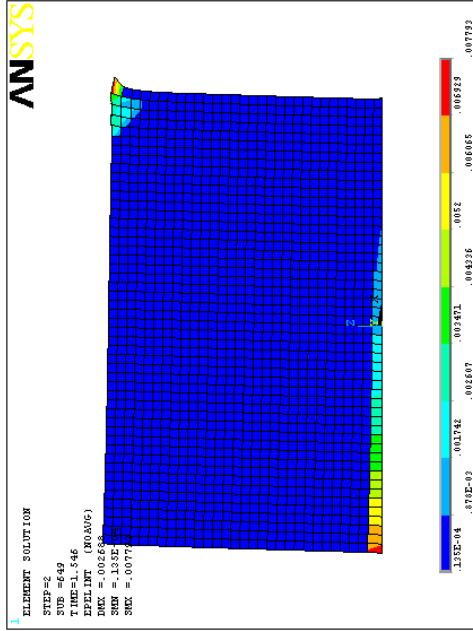
(f) Strain intensity in a 5x3 wall.

Figure 55: Figures showing crack pattern, stresses and strains in a 5x3 before failure @ substep 649.
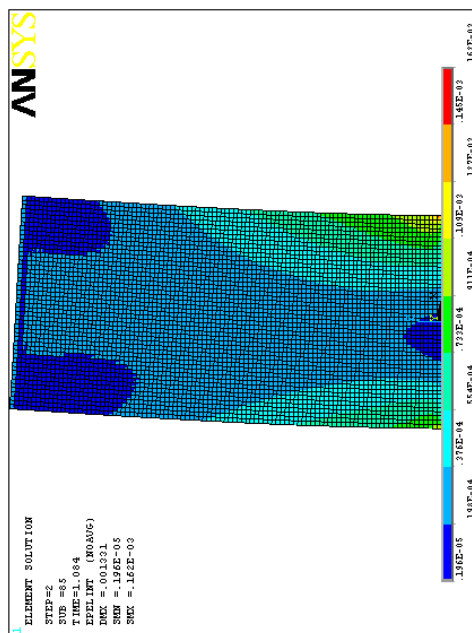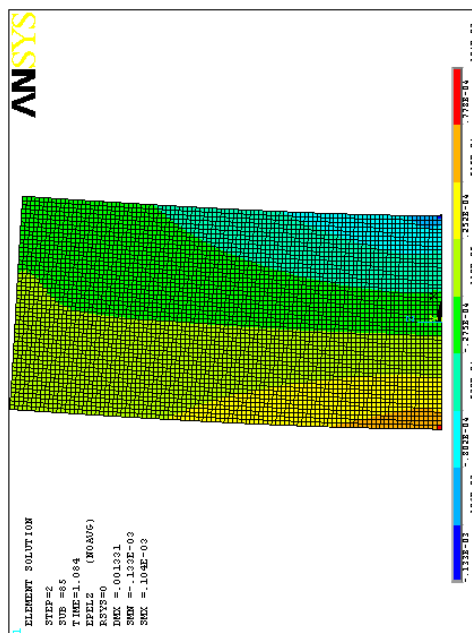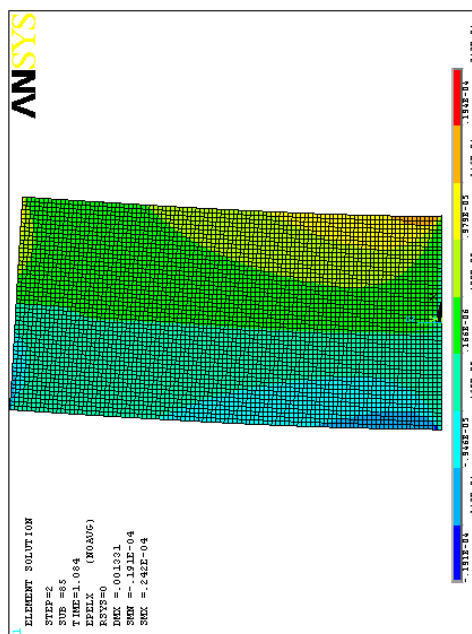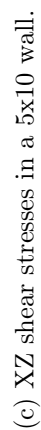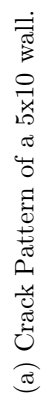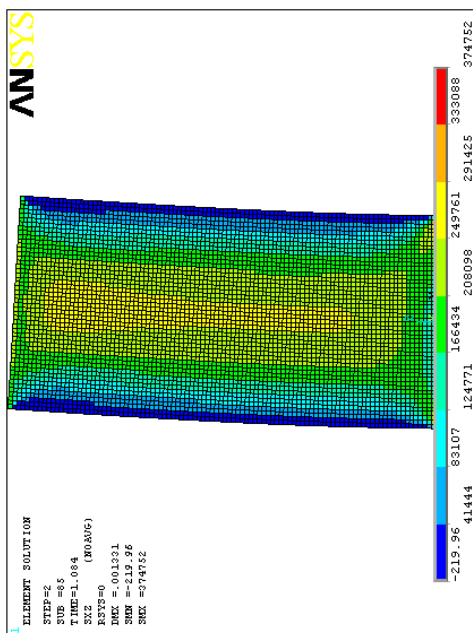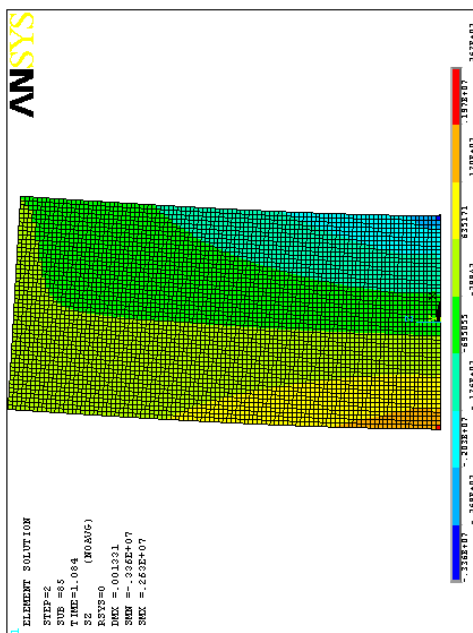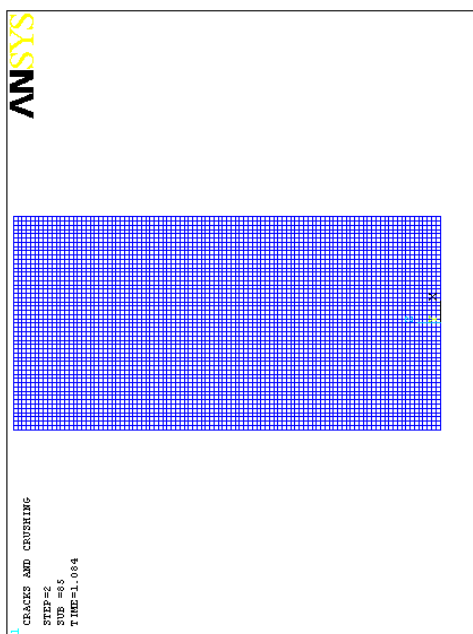
(a) Crack Pattern of a 5x10 wall.

(b) Stresses in Z direction in a 5x10 wall.

(c) XZ shear stresses in a 5x10 wall.

(d) Strains in X direction in a 5x10 wall.

(e) Strains in Z direction in a 5x10 wall.

(f) Strain intensity in a 5x10 wall.

Figure 56: Figures showing crack pattern, stresses and strains in a 5x10 before first crack formation @ substep 85.
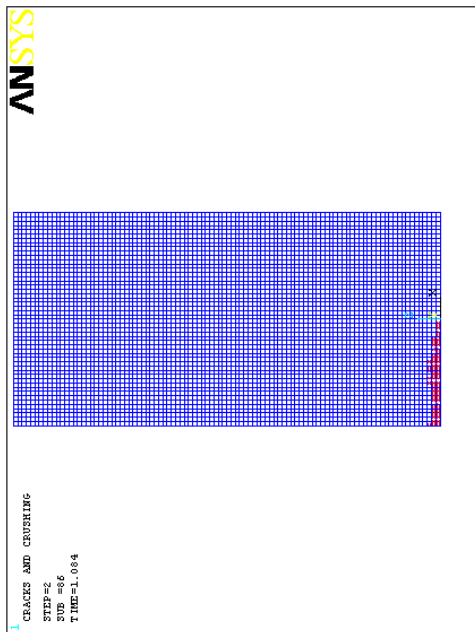
(a) Crack Pattern of a 5x10 wall.
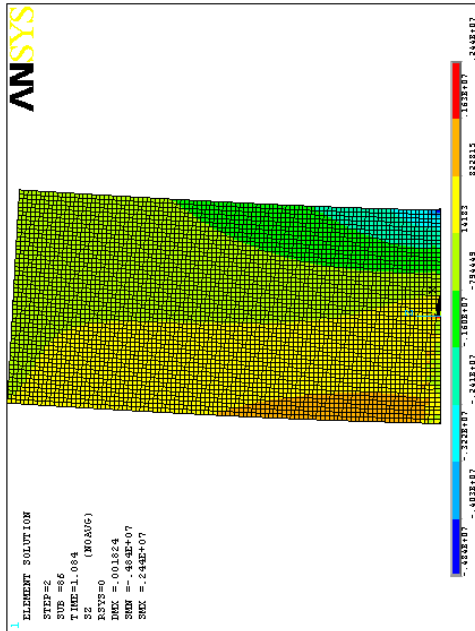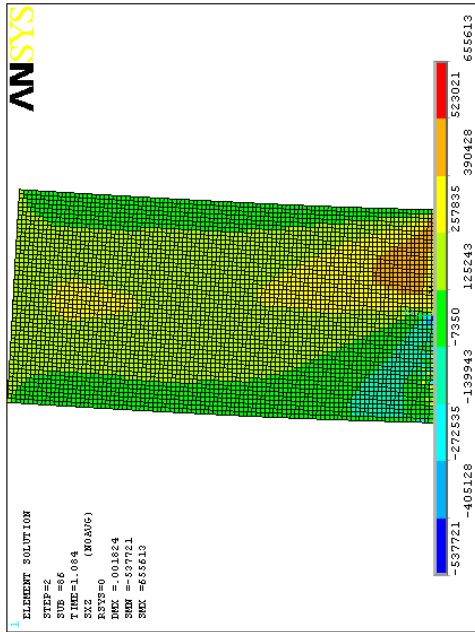
(b) Stresses in Z direction in a 5x10 wall.

(c) XZ shear stresses in a 5x10 wall.
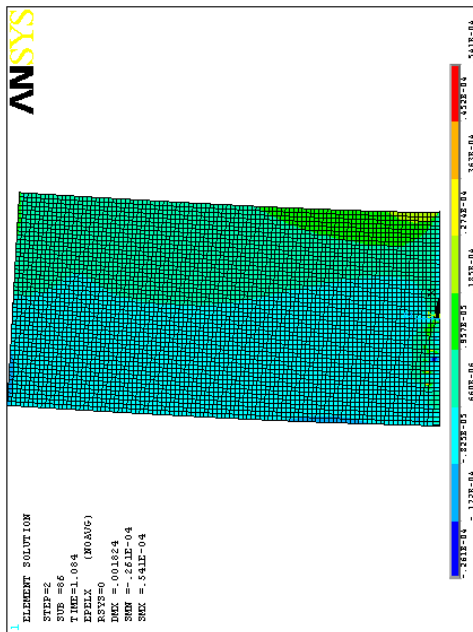
(d) Strains in X direction in a 5x10 wall.
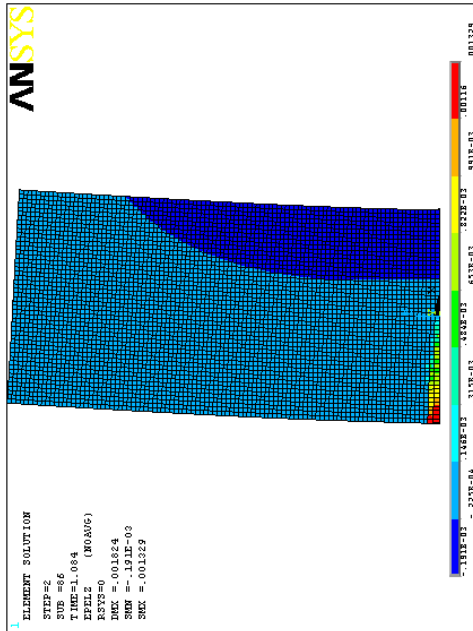
(e) Strains in Z direction in a 5x10 wall.
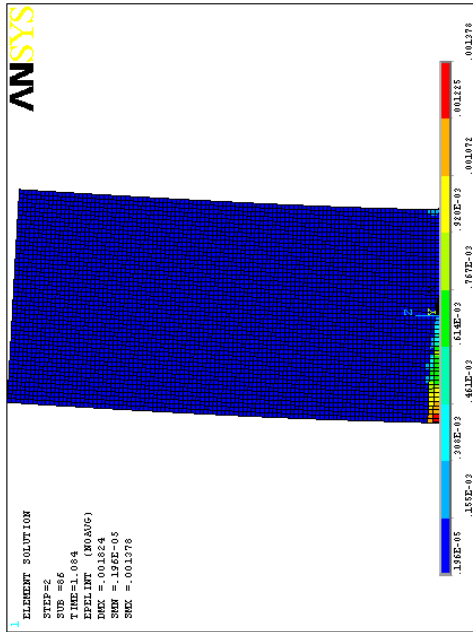
(f) Strain intensity in a 5x10 wall.

Figure 57: Figures showing crack pattern, stresses and strains in a 5x10 after first crack formation @ substep 86.
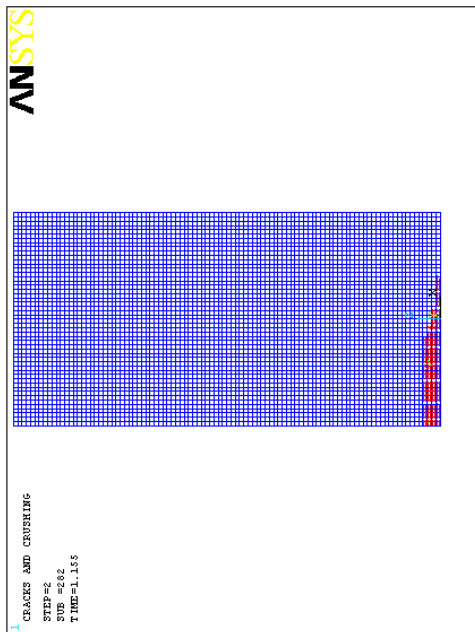
(a) Crack Pattern of a 5x10 wall.
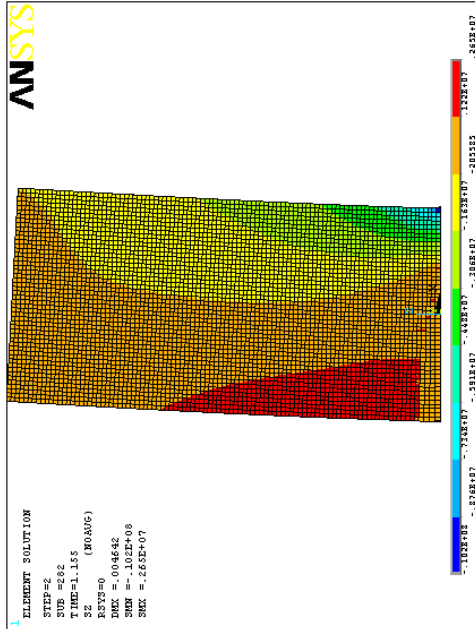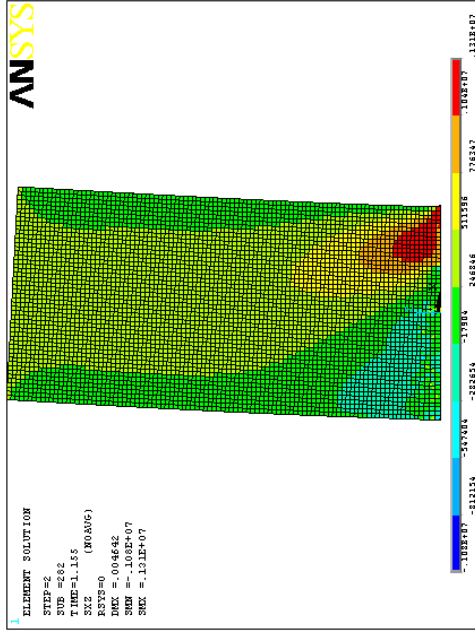
(b) Stresses in Z direction in a 5x10 wall.

(c) XZ shear stresses in a 5x10 wall.
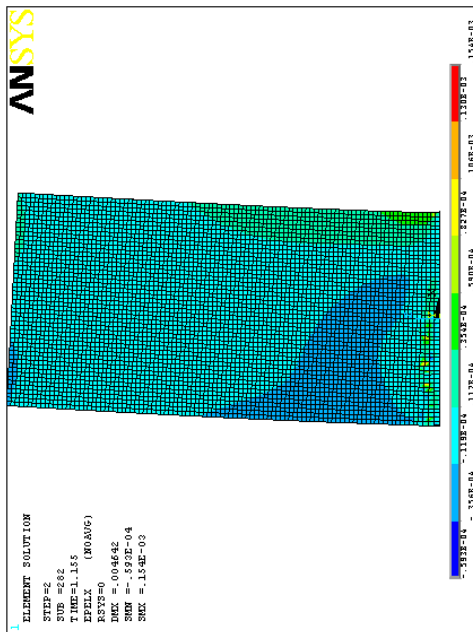
(d) Strains in X direction in a 5x10 wall.
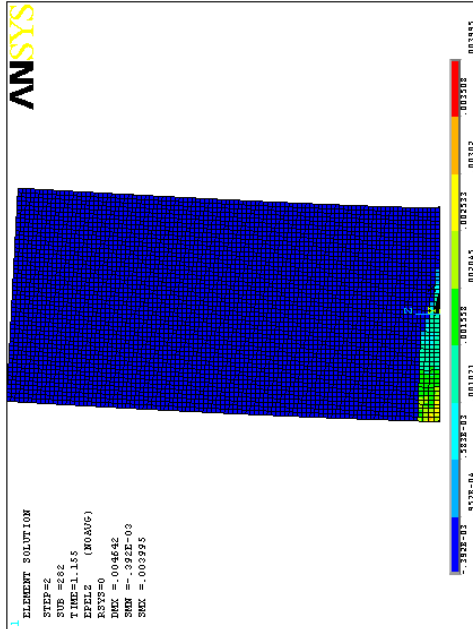
(e) Strains in Z direction in a 5x10 wall.
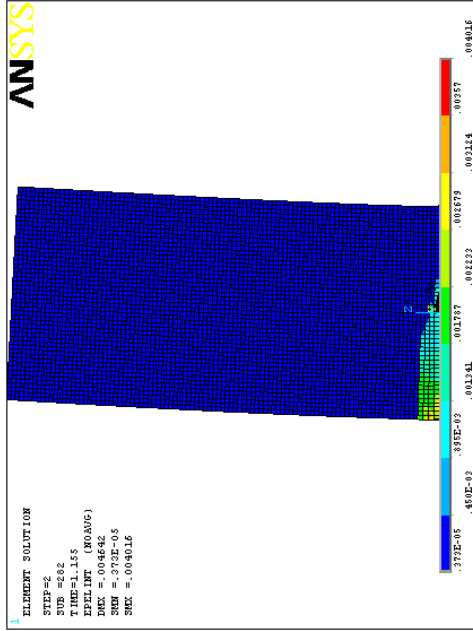
(f) Strain intensity in a 5x10 wall.

Figure 58: Figures showing crack pattern, stresses and strains in a 5x10 before second crack formation @ substep 282.
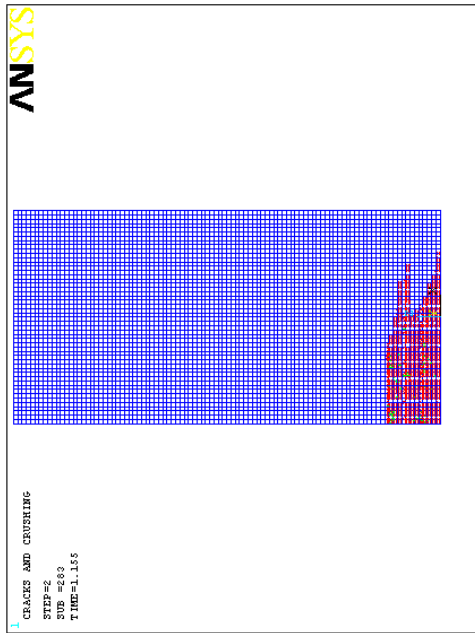
(a) Crack Pattern of a 5x10 wall.
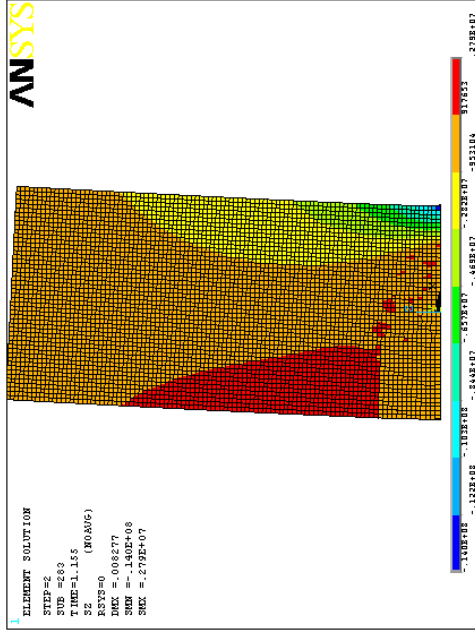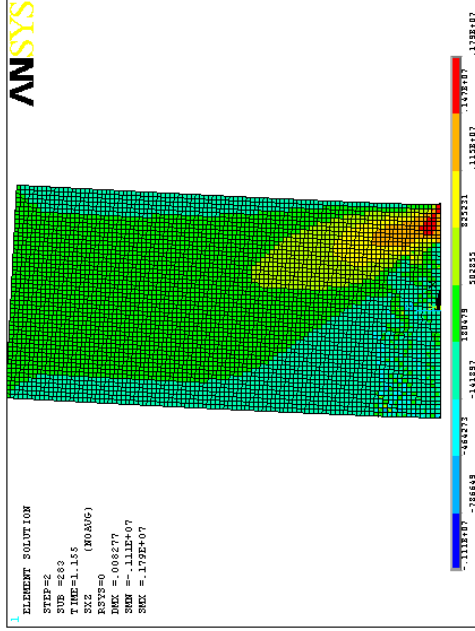
(b) Stresses in Z direction in a 5x10 wall.

(c) XZ shear stresses in a 5x10 wall.
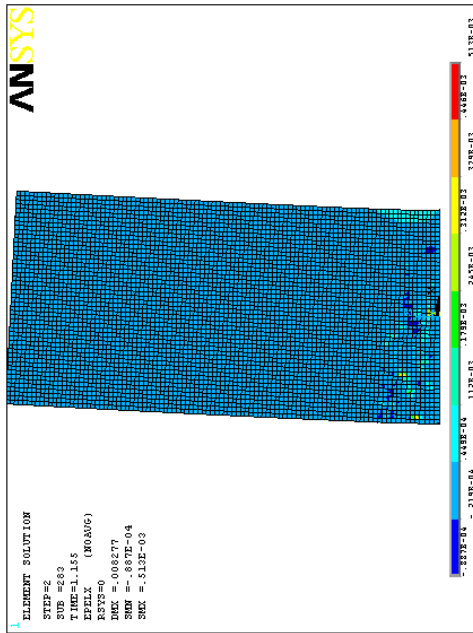
(d) Strains in X direction in a 5x10 wall.
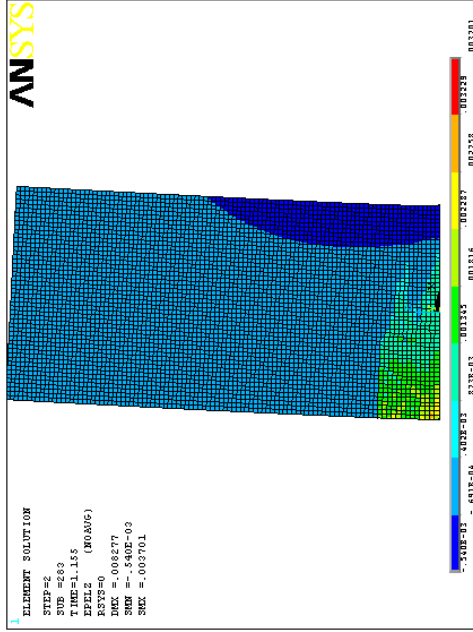
(e) Strains in Z direction in a 5x10 wall.
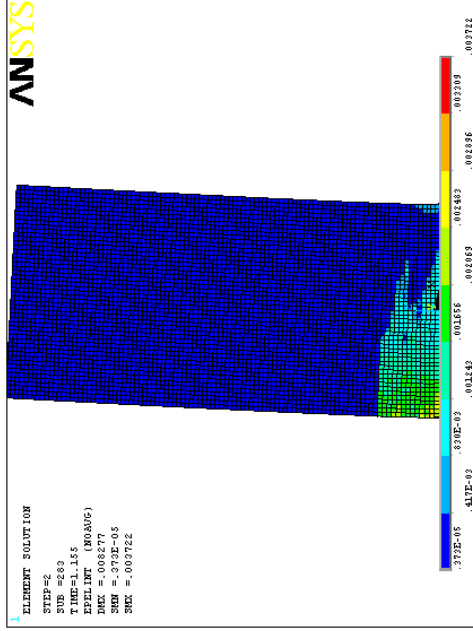
(f) Strain intensity in a 5x10 wall.

Figure 59: Figures showing crack pattern, stresses and strains in a 5x10 after second crack formation @ substep 283.
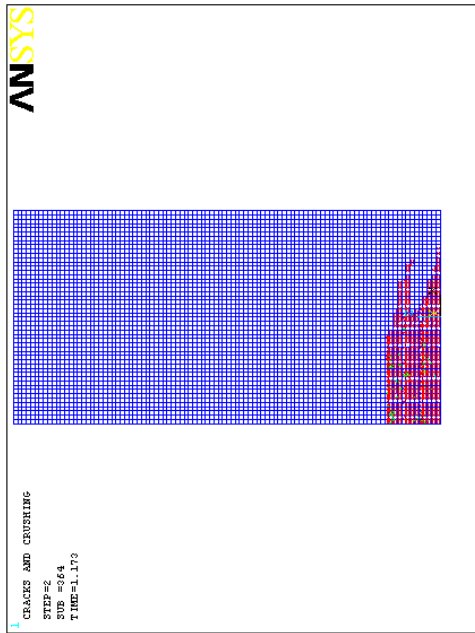
(a) Crack Pattern of a 5x10 wall.
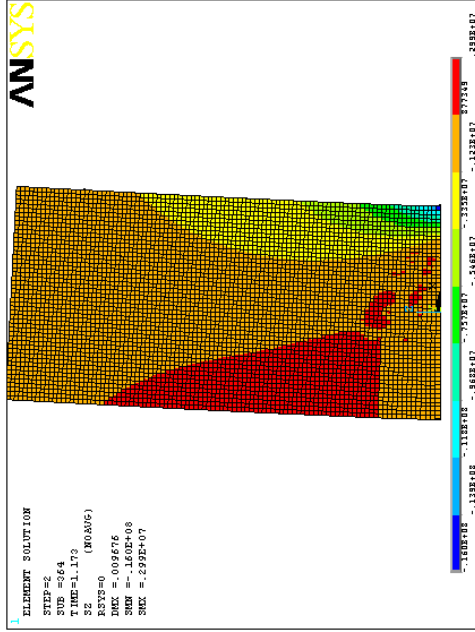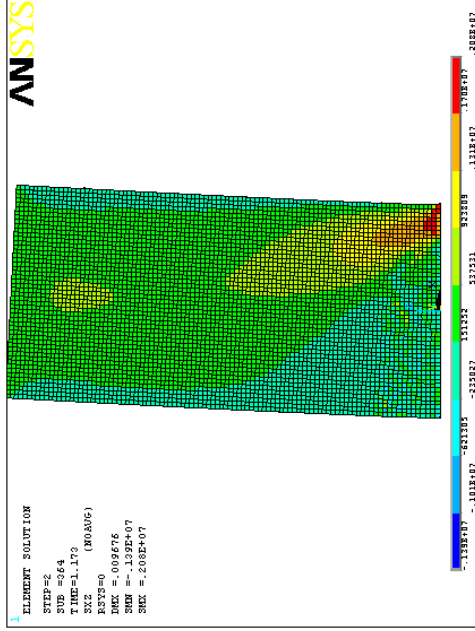
(b) Stresses in Z direction in a 5x10 wall.

(c) XZ shear stresses in a 5x10 wall.
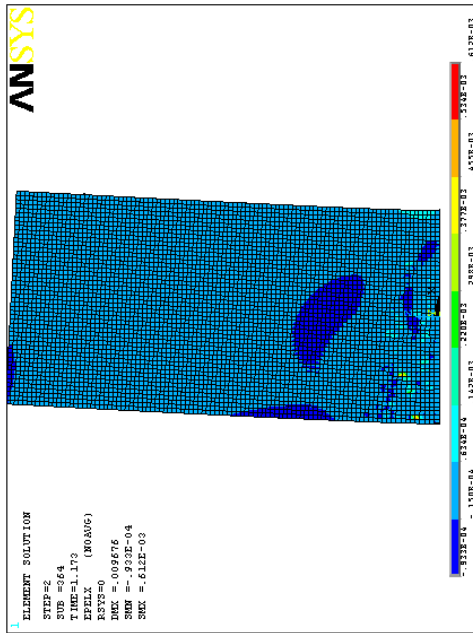
(d) Strains in X direction in a 5x10 wall.
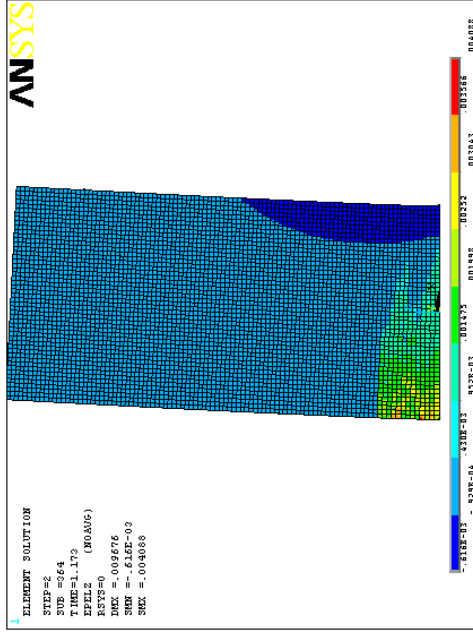
(e) Strains in Z direction in a 5x10 wall.
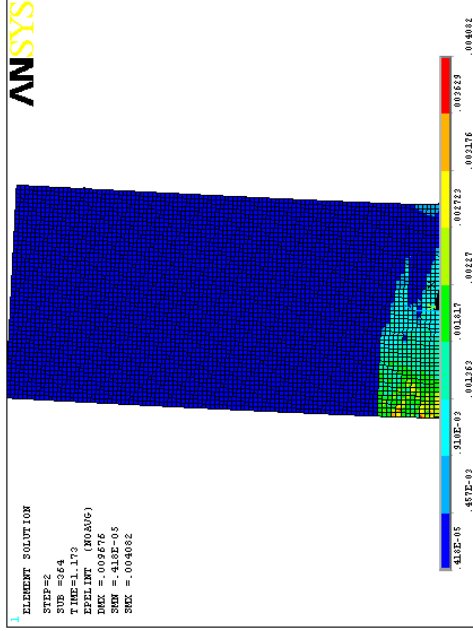
(f) Strain intensity in a 5x10 wall.

Figure 60: Figures showing crack pattern, stresses and strains in a 5x10 before third crack formation @ substep 364.
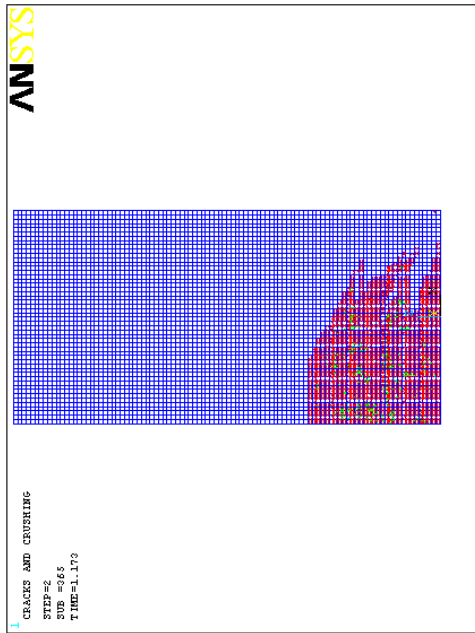
(a) Crack Pattern of a 5x10 wall.
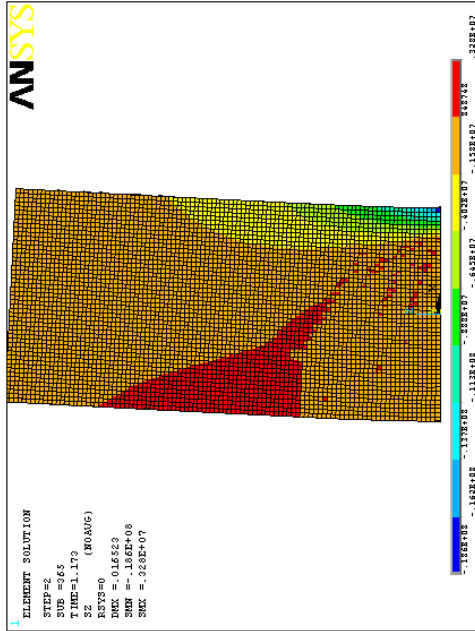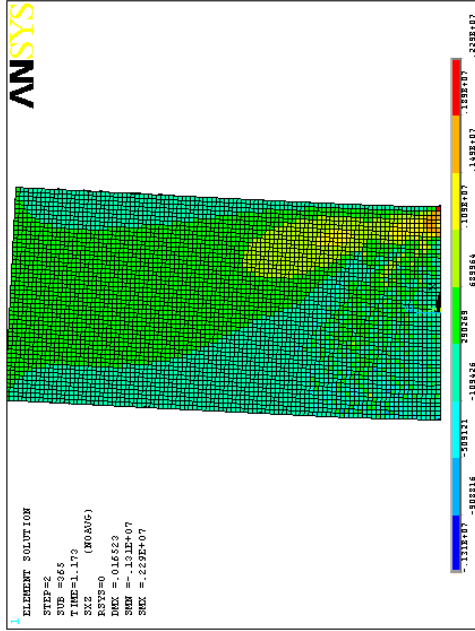
(b) Stresses in Z direction in a 5x10 wall.

(c) XZ shear stresses in a 5x10 wall.
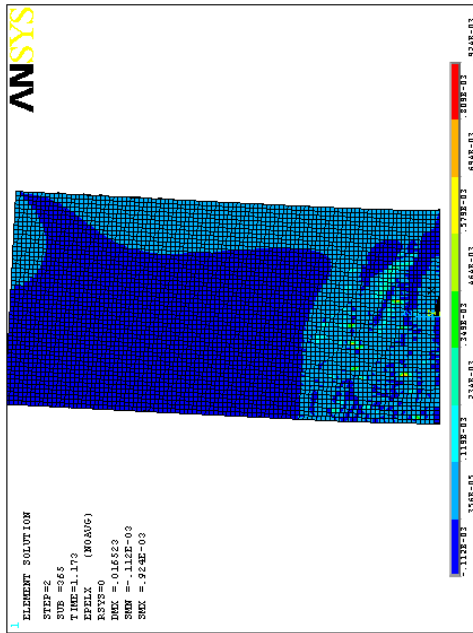
(d) Strains in X direction in a 5x10 wall.
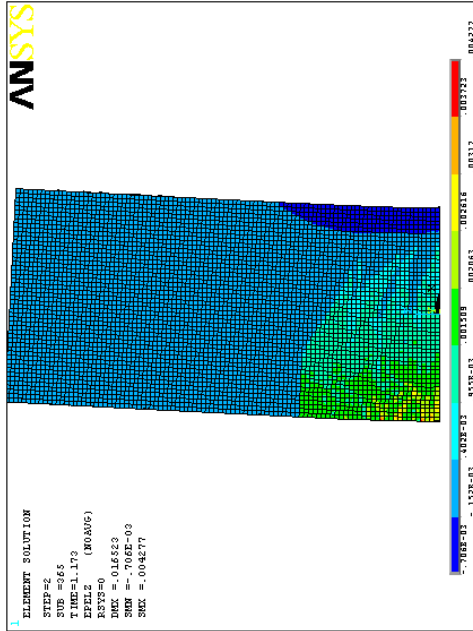
(e) Strains in Z direction in a 5x10 wall.
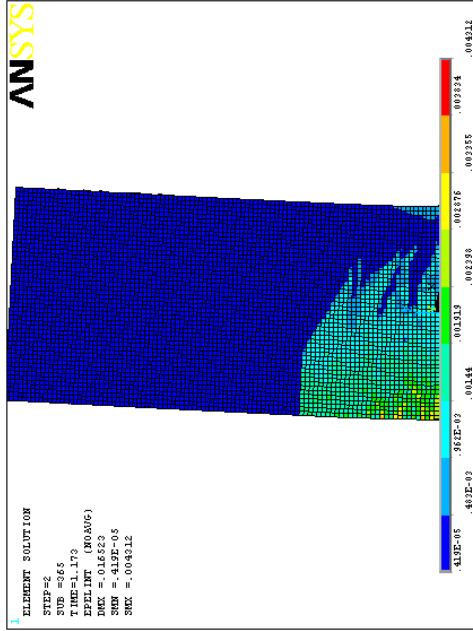
(f) Strain intensity in a 5x10 wall.

Figure 61: Figures showing crack pattern, stresses and strains in a 5x10 after third crack formation @ substep 365.
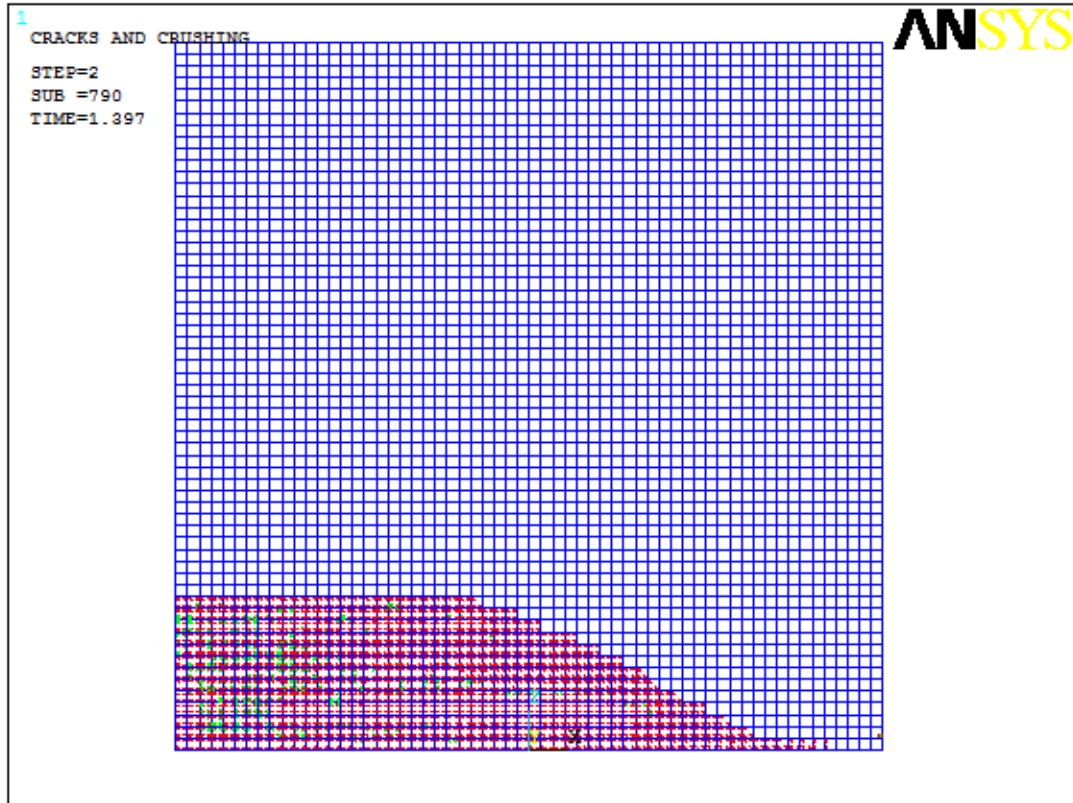
(a) Mesh with 0.05 m edge length elements.
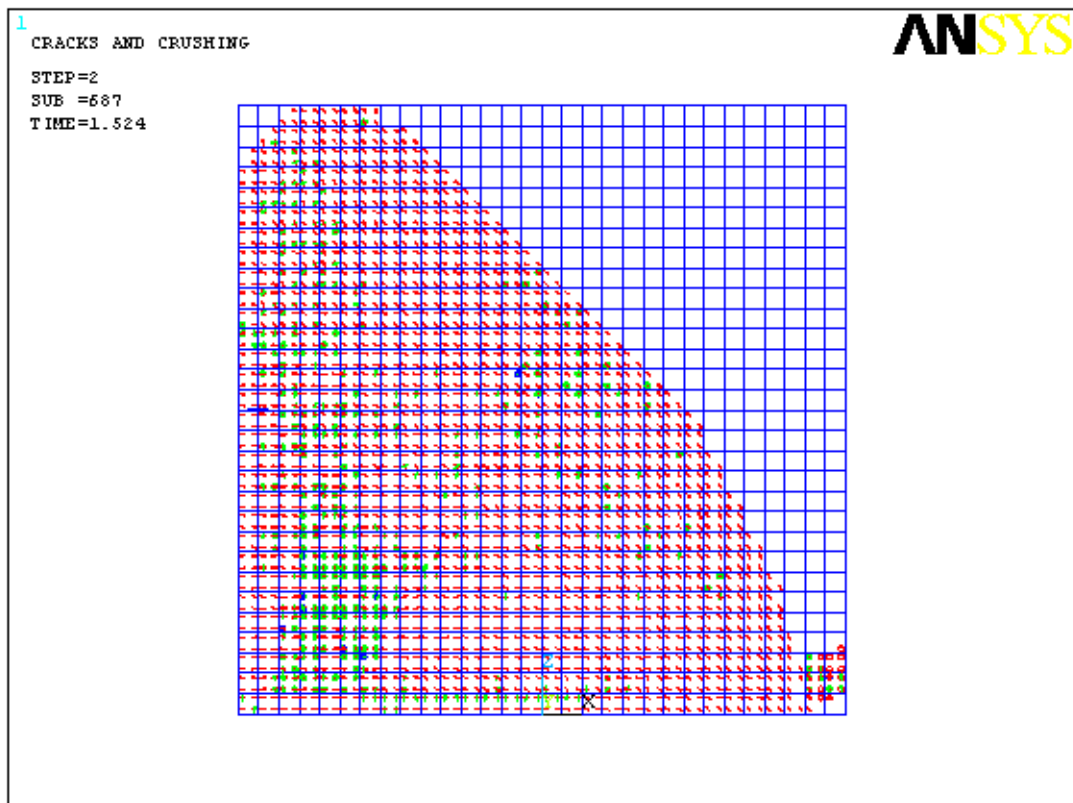
(b) Mesh with 0.1 m edge length elements.

Figure 62: Crack Pattern comparison of a 3x3 wall in failure using different size elements in the model.

5.2   A coupled soil- and wall with footing system

In this section the response of a linear wall resting on a sand soil layer is examined. The wall used is 3.0 m x 5.0 m x 0.2 m with a 3.0 m x 0.25 m x 0.6 m footing. The wall is given linear attributes for faster analysis since the soil response is of main interest. The response of the soil is calculated for the gravity loading of the wall and cyclic loading of 100 kN with frequency 1 Hz and 5 Hz to compare the dynamic stiffness.

5.2.1   Soil response due to gravity loading of a wall

As previously stated the footing and the soil in the ME models is represented by a Beam on non-linear Winkler foundation. The BNWF model already accounts for gapping between the footing and the soil. To simulate gapping behavior the interface between the footing and the soil in the FE model is created by using special contact elements, these contact elements are given friction coefficient of 0.6 between the concrete and soil [30]. To simulate granular soil behavior Drucker-Prager model is supplemented to the soil properties in the FE model.

   The BNWF model also needs some further information than just the soil properties. It places stiffer springs at the ends of the footing. The extra stiffness value R_k and the length of the portion of the footing with extra stiffness R_e are calculated using recommendations based on ATC-40[7] [5] where:

$$R_k = \frac{k_{end}}{k_{mid}} \tag{43}$$

where

$$k_{end} = \frac{6.8G}{(1-\upsilon)B} \tag{44}$$

$$k_{mid} = \frac{0.78G}{(1-\upsilon)B} \tag{45}$$

$$R_e = \frac{L_{end}}{L} \tag{46}$$

$$L_{end} = \frac{B_f}{6} \tag{47}$$

B_f is the breadth of the footing. The last parameter is the spacing between springs l_e/L, it is taken as 2% as recomended in Raychowdhury [35]. The values can be found in table 10.

   The output of the analysis is somewhat different between the FE and ME model. The FE model provides pressure results while the spring output is force based so displacements are used as a measurement of the soil response. The displacement is monitored at the center and ends of the footing.

---

[7]A report made by the Applied Technology Council and California seismic safety commission. The values within are used for comparison in Raychowdhury's research [35]. More suitable parameters can be found and used given time.

The results for gravity loading are listed in table 11. It is noticeable that the end displacements are very different between the models, the ATC-40 values for end region stiffness and length don't agree very well with the FE results.

Table 10: Mesh information for the BNWF model.

R_k	R_e	l_e/L
9.3	0.033	0.02

The FE model is set up with soil domain of 9 by 6 by 5 meters in the x, y and z direction respectively, the soil domain size is larger than the model to reduce the effect the side boundaries have on the soil[8]. The material parameters used for the soil are the ones given in table 6.

Figures 63 and 64 shows the stresses in the Z direction of the FE model using linear and DP material models respectively. The section cuts are at the center of the wall in XZ and YZ plane. The grey regions are sections that are outside the specified contour range. This happens where tension is present in the soil and in the wall where pressure due to self weight has exceeded the pressure range chosen to display the distribution in the soil. Figure 65 shows the hydrostatic pressure in the soil, the bulging at the sides of the domain does not conflict with the stress distribution so the soil domain is sufficiently large.

Table 11: Displacements of the center and end of the wall due to gravity loads.

	Center disp. (m)	End disp. (m)
ME model	$-4.4399E-04$	$5.99682E-05$
FE model w. DP	$-4.6221E-04$	$-4.6152E-04$
FE model wo. DP	$-3.9351E-04$	$-3.9116E-04$

---

[8]A larger soil domain is recommended but the number of elements quickly increases and slows down the calculation time.

(a) Linear stresses in the XZ plane of the wall.

(b) Linear stresses in the YZ plane in the center of the wall.
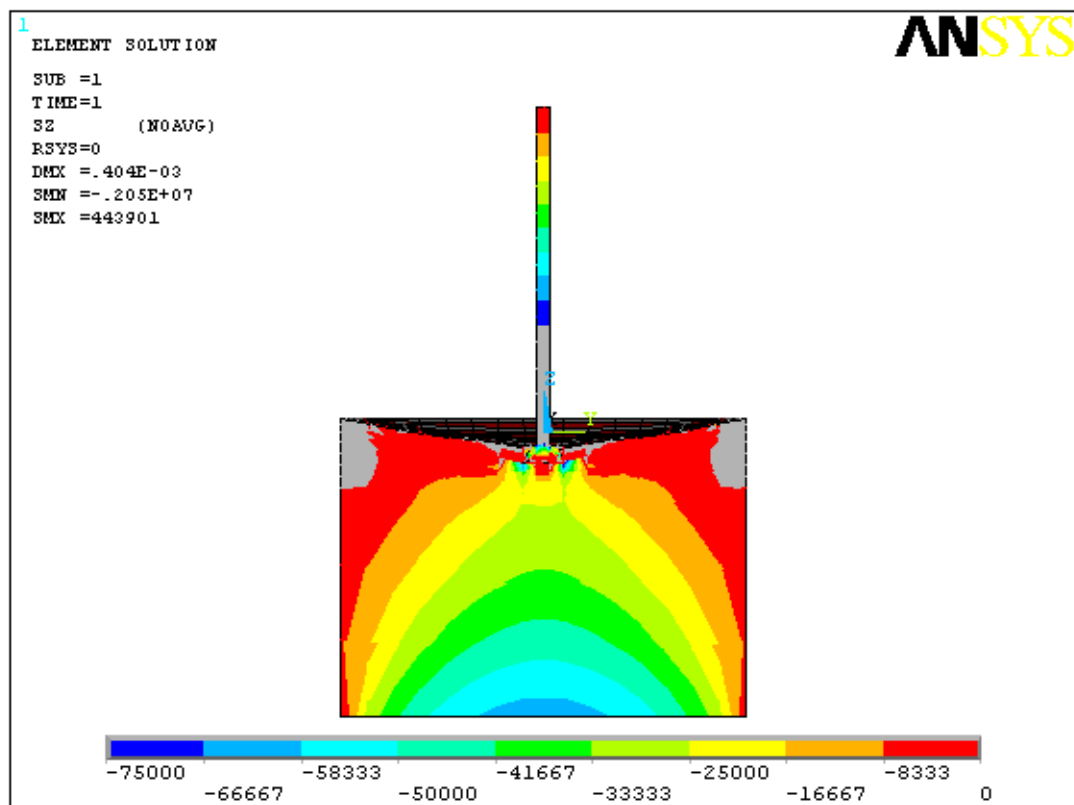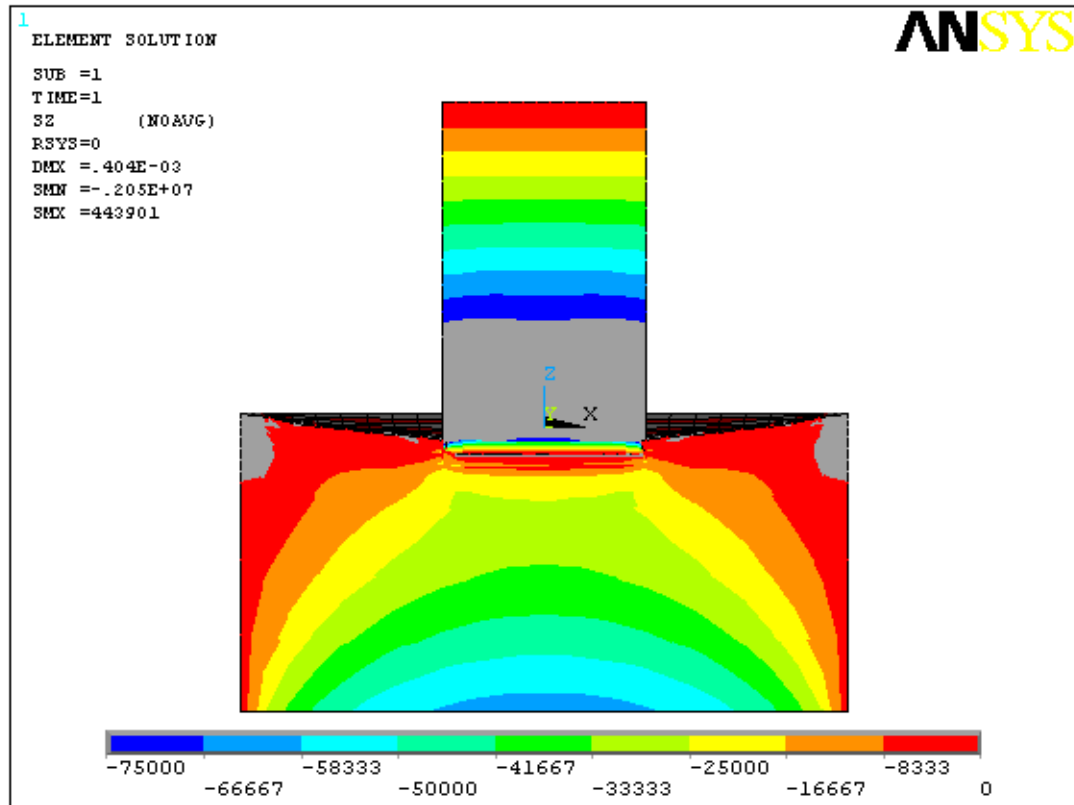
Figure 63: Stress distributions in Z direction in the soil below a 3x5 wall using linear soil material model.
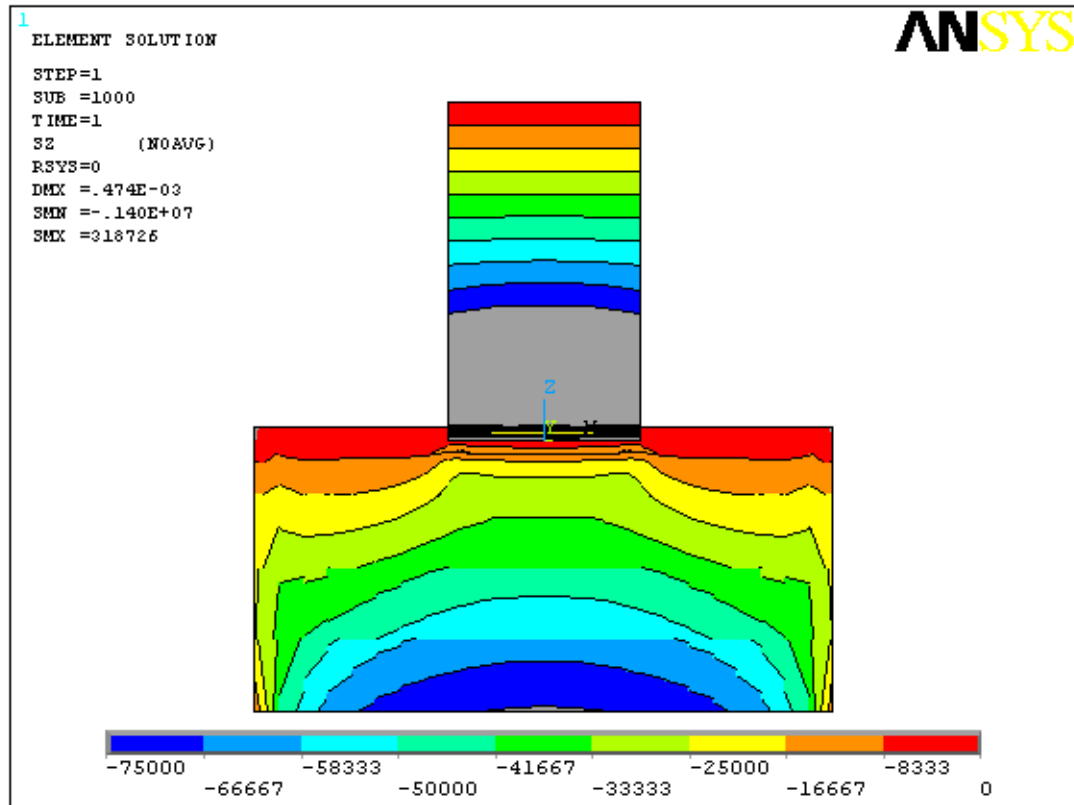
(a) Stresses using Drucker-Prager model in the XZ plane of the wall.
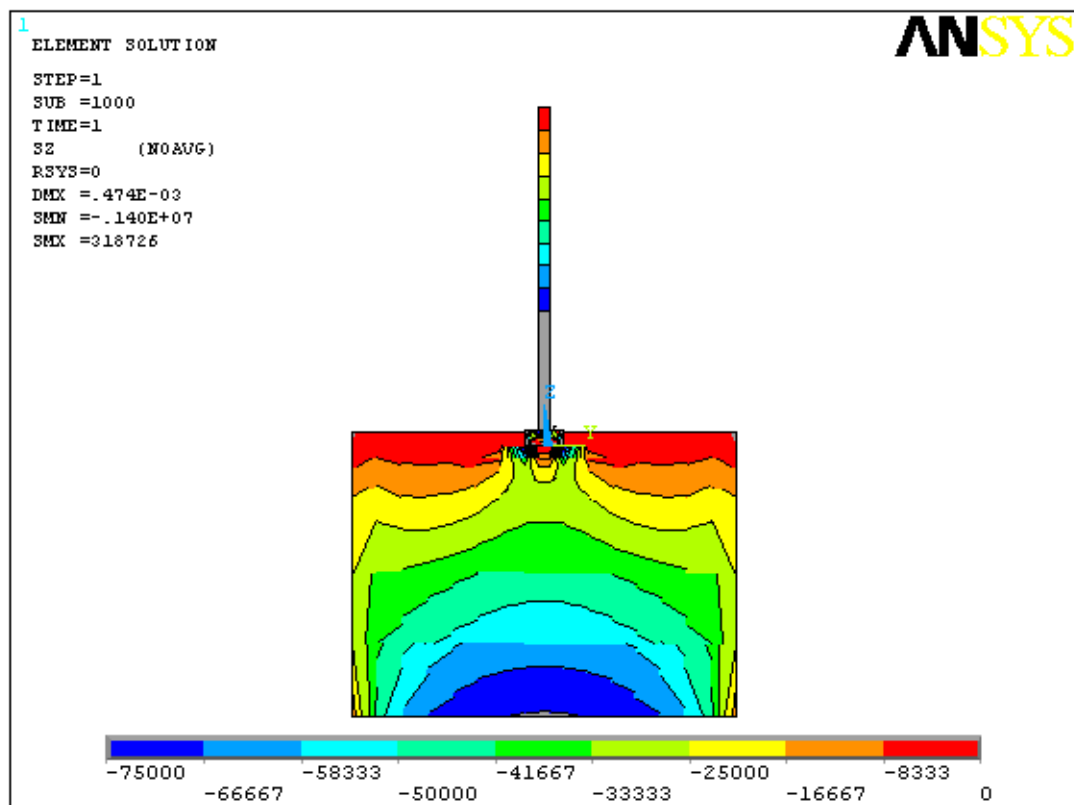
(b) Stresses using Drucker-Prager model in the YZ plane in the center of the wall.

Figure 64: Stress distributions in Z direction in the soil below a 3x5 wall using Drucker-Prager soil material model.
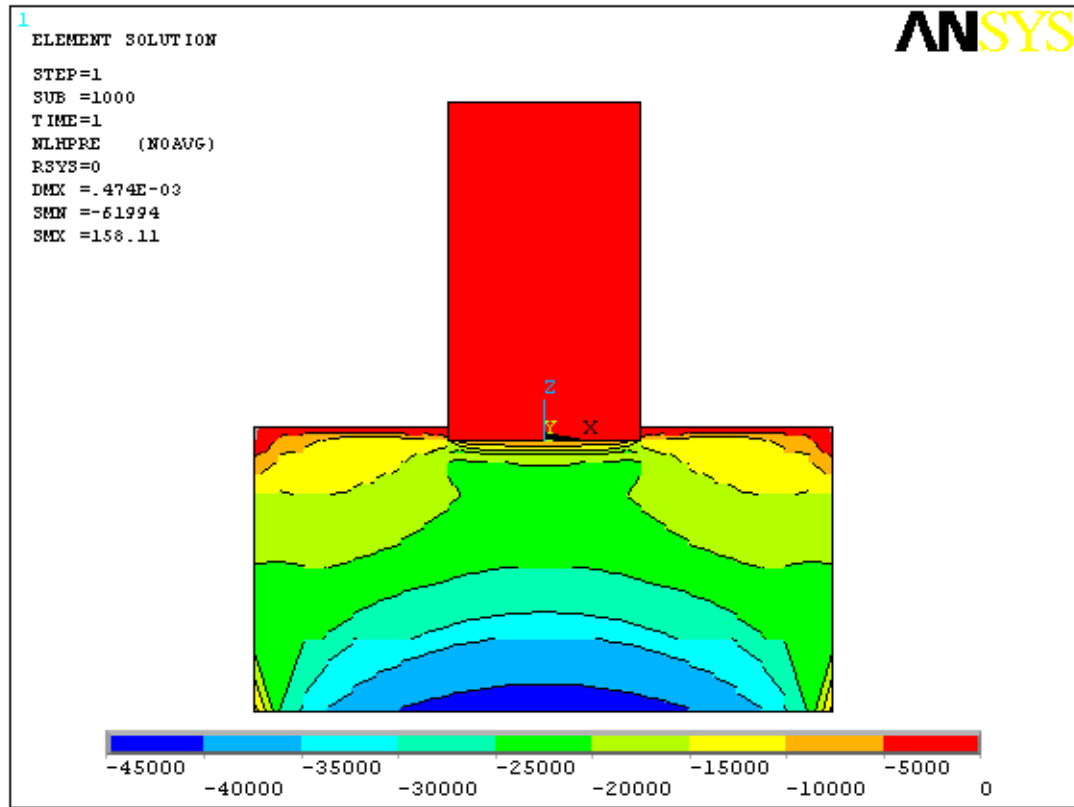
Figure 65: Hydrostatic stresses using Drucker-Prager model in the XZ plane of the wall.

5.2.2 Soil response due to cyclic loading of varying frequency on the wall

Once the gravity case has been solved the models are subjected to 1 hz and 5 hz 100 kN load at the top of the wall for 5 seconds. Timestep is chosen 0.005 for the ME models based on attuning of timesteps between $0.001 - 0.01$. The results for the ME center and end displacements are shown in figures 66 and 67. To better display the differences between the frequencies the first period of both the loading schemes are plotted against each other in figure 68. It is clear that loading frequency of 1 hz causes greater displacements. The soil model exhibits settling of the soil between each cycle for both loading schemes.

The FE model with given DP material model since the analysis was terminated by the program at the first timestep of the solution, reducing the timestep was not successful. The DP properties were removed from the soil properties and 5% damping added to account for the damping c_{rad} already built in the BNWF model. The only non-linear component of the FE model is the contact element between the footing and the soil. The results for the center[9] displacements in the FE model due to frequency load of 100 kN is shown in figure 69. The behavior is linear and in line with the loading scheme. There is no settlement of the soil but there is agreement between the FE and the ME model that the 1 hz frequency load causes greater displacement and is closer to the natural frequency of the soil-structure system.

---

[9]End displacements were not noticably different.
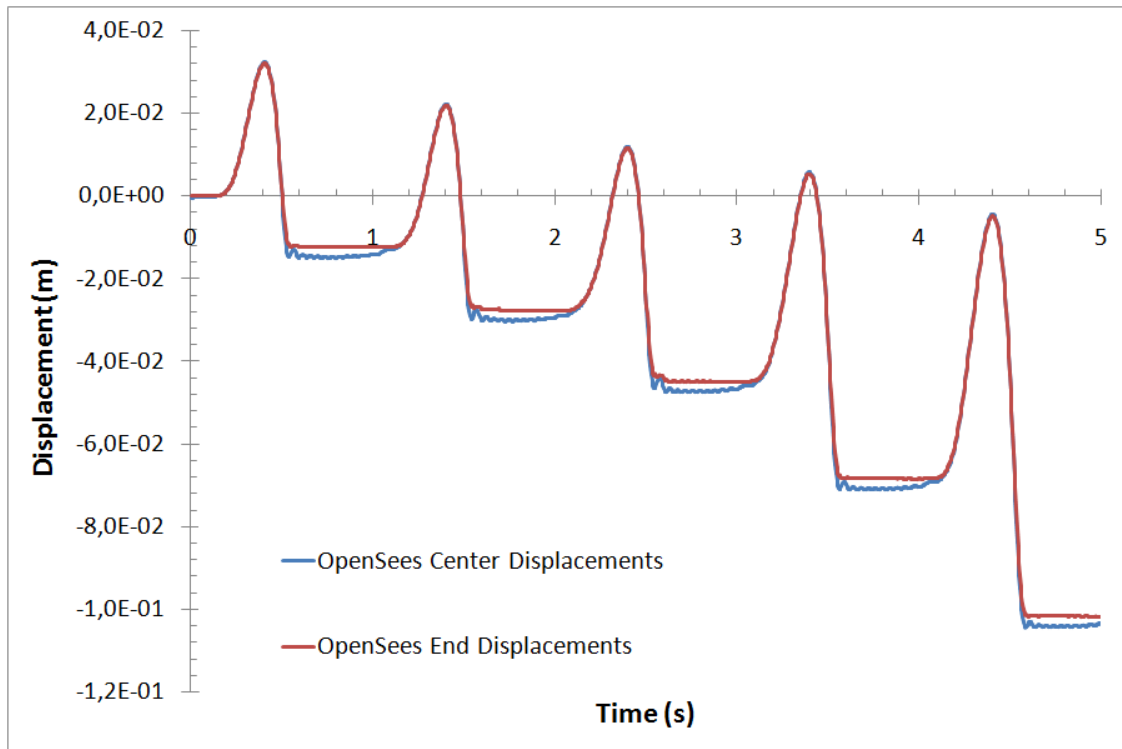
Figure 66: Displacement of the BNWF when subjected to 1 hz 100 kN load for 5 seconds.
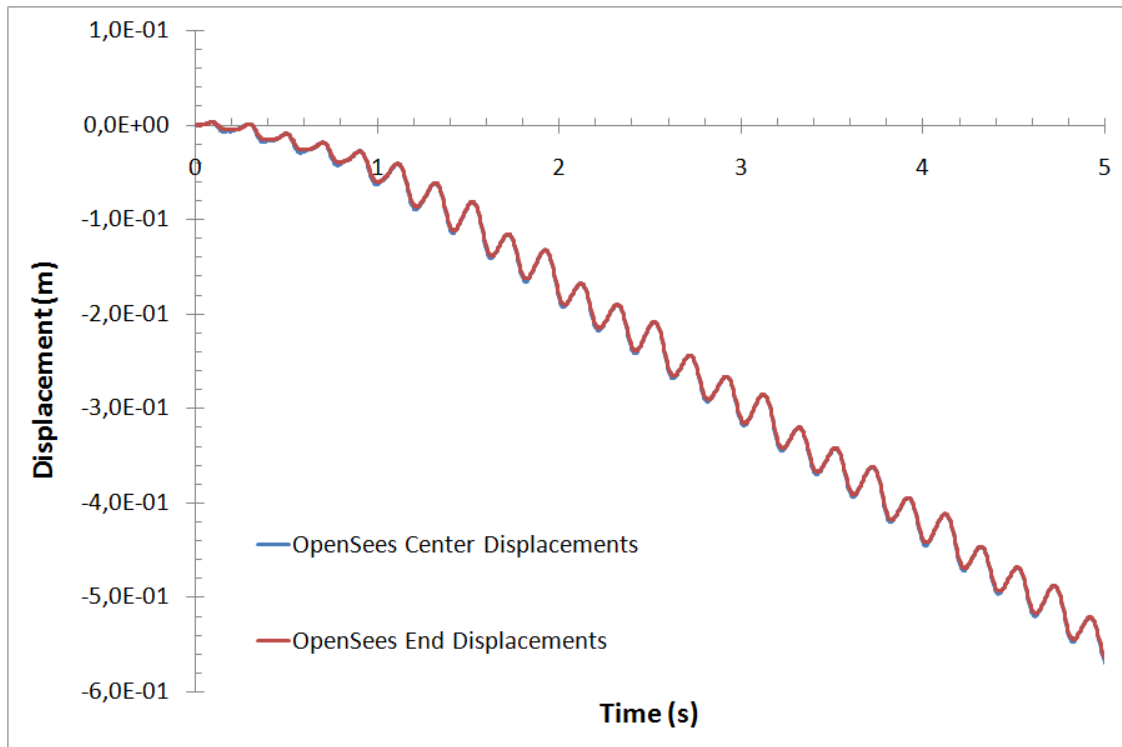
Figure 67: Displacement of the BNWF when subjected to 5 hz 100 kN load for 5 seconds.
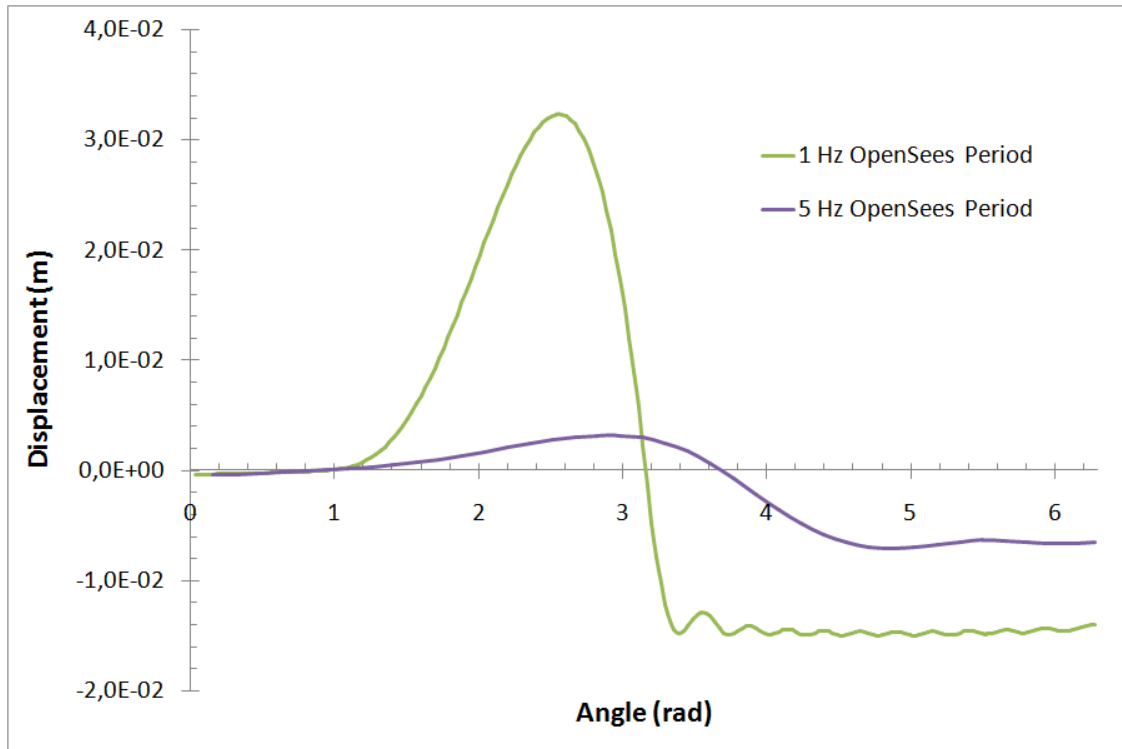
Figure 68: Comparison between displacements in a 1 hz period and 5 hz period of the BNWF model subjected to 100 kN load.
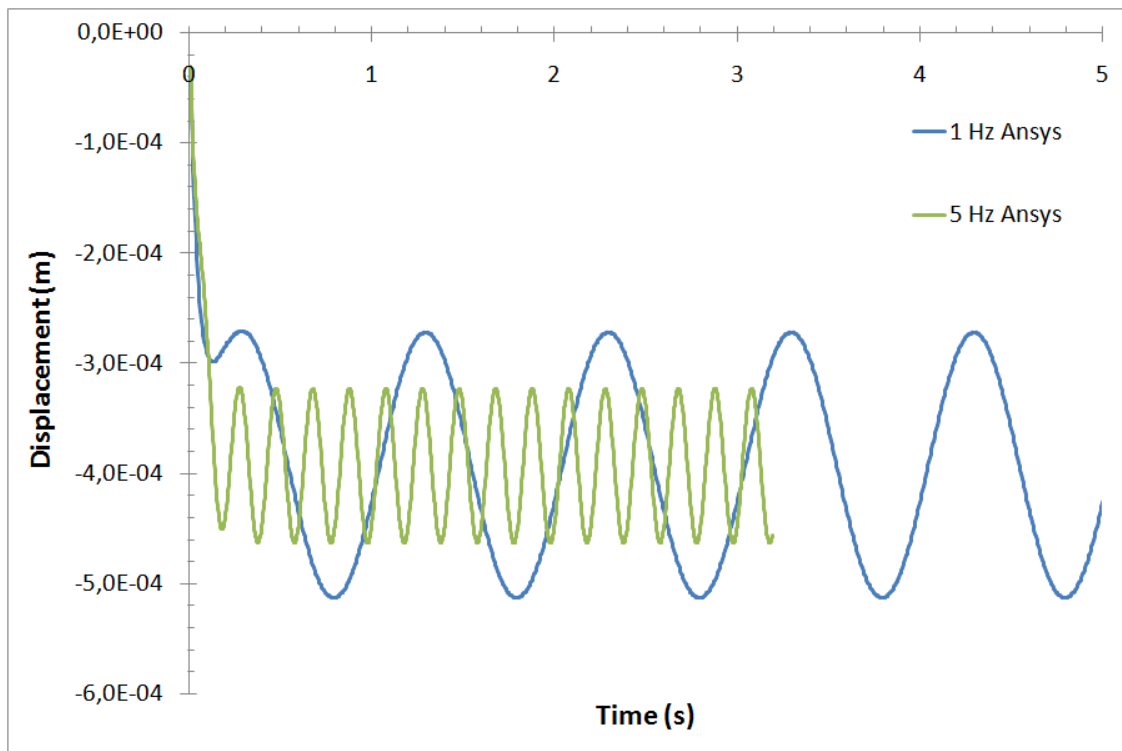
Figure 69: Displacements of the FE model when subjected to a 1 and 5 hz 100 kN load.

6 Conclusions

Based on the results from the lateral pushover tests all the models seem to agree on ultimate force capacity while displacement comparison varies. The displacement comparison is quite good before second crack generation takes place in the FE models. It is perhaps not expected that the macro elements are able to capture such crack patterns as that occur there. However, if figures 24 and 62 are considered it can be seen that a finer 0.05 m mesh results in a more subtle crack pattern in the FE model than the standard 0.1 m mesh. Alas the agreement between the ME models and the FE model can be considered to be fairly good up to a point where cracks occur and the force transmittance is through the reinforcement. Unfortunately, there is no real data to validate the results and they, therefore, must be regarded only as a comparison between the two methods used.

The force-beam element provides better displacement results than the flexure-beam element when the FE model is used as a baseline, but that is because the shear spring was attuned to fit the FE model results to begin with. Without real displacement data to calibrate the shear spring, the flexure-beam element using a center of rotation parameter of around 0.36 provides a reasonable estimation of the initial stiffness but is lacking in non-linear capabilities as well as the force-beam elements. It is not known if the poor non-linear performance is because of wrong input parameters, thought much care was taken in the setup of the models, or because of the element formulation.

The time difference in solving problems involving a lateral pushover load on a reinforced concrete wall is considerable. While the model using mesh size of 0.05 m took 9 hours to solve the models using a flexure-beam element to represent the wall took from 3 to 15 minutes to solve depending on the dimensions and for the models using the force-beam element the solution time was from 30 seconds to 6 minutes.

For the coupled soil- and wall system the differences are not directly comparable. That is due to the fact that a realistic FE soil model could not be solved with the desired parameters for cyclic loading. When using the Drucker-Prager material model in the FE model to simulate the soil, the gravity analysis alone took over 24 hours to calculate. The ME model utilizing the Beam on non-linear Winkler's foundation the gravity load case was calculated in few seconds. For the harmonic load cases, the FE model took several hours to solve when the only non-linear component was the contact element between the wall footing and the soil while the ME models were solved within minutes.

Based on the comparison of these case studies, a simulation trying to capture non-linear behavior of material and deformation of the wall is still somewhat lacking when using these macro elements, the setup of the BNWF is simple enough but the end stiffness needs to be attuned so as the both models would yield similar results. The benefit in reduced calculation time is however apparent and is a reason enough to continue the development of macro elements for earthquake response calculations.

6.1 Review of the current study and future research possibilities

The initial plan for this study was to use Ruaumoko [4] and wall elements designed by Taylor [41]. OpenSees was, however, the choice because of the non-linear foundation capabilities and the different MVLEM available. The OpenSees modeling had a steep learning curve, and slight input errors can be hard to notice. Also OpenSees is not used as such to discover the failure in members; it will only stop to converging. Therefore the convergence criteria need to be chosen carefully. Furthermore, the version 2.3.1 of OpenSees which was the latest version used for this study did not support BNWF elements, last version that supported the BNWF command was version 2.2.2. This might be fixed in the latest version 2.3.2 released while this study was performed. The concrete modeling in ANSYS is largely dependent upon the shear transfer coefficients that were chosen based on comparison with the OpenSees model without much certainty of the actual values. The Drucker-Prager model was chosen because of its relationship to the friction angle that is used as an input in OpenSees. The Drucker-Prager model caused convergence problems when using the SOLID 45 element that was initially used in the analysis, some models worked while other did not. It was only by chance that the convergence difficulties were observed to be in relation to the number of elements on the edge of the model, that is whether the number was even or odd. The models with an even number of elements failed thus the conclusion was to use elements with mid nodes between the corners to achieve convergence.

The logical continuation of this study would be to apply a true earthquake excitation and couple in the non-linear wall. It was the original plan to include that part within the framework of this theses, in the end, however, there was not sufficient time for an earthquake simulation to be executed as originally planned due to the various complications incurred in the initial phases of the numerical simulations. Such a study comparing a FE and ME model, requires a working soil model. A capped Drucker-Prager model that gives a hydrostatic stress cone with a smooth tip for easier convergence might be a possible solution or perhaps more computational resources are needed. The FE soil model should at least show some settlement between load cycles.

References

[1] N. Allotey and M. H. E. Naggar. Analytical moment-rotation curves for rigid foundations based on a winkler model. *Soil Dynamics and Earthquake Engineering*, 23(5):367 – 381, 2003.

[2] M. Apostolou, G. Gazetas, and E. Garini. Seismic response of slender rigid structures with foundation uplifting. *Soil Dynamics and Earthquake Engineering*, 27(7):642 – 654, 2007.

[3] M. Browne, A. J. Carr, and D. Bull. The analysis of reinforced concrete rocking wall behavior. In *2006 NZSEE Conference*, 2006.

[4] A. J. Carr. *Ruaumoko Manual Volume: 1 Theory.* University of Canterbury, 2007.

[5] C. D. Comartin, R. W. Niewiarowski, and C. Rojahn. ATC-40. Technical report, Applied Technology Council (ATC), 2006.

[6] K. Dasgupta. Seismic design of slender reinforced concrete structural walls. In *Directions*, volume 8(2), pages 129–134, 2007. Proceedings of First IITK REACH symposium at Parwanoo.

[7] E. Dimitrakopoulos, A. J. Kappos, and N. Makris. Dimensional analysis of yielding and pounding structures for records without distinct pulses. *Soil Dynamics and Earthquake Engineering*, 29(7):1170 – 1180, 2009.

[8] J. Domínguez. Dynamic stiffness of rectangular foundations. Technical report, Massachusetts Institute of Technology, 1978.

[9] J. Domínguez. Twenty five year of bounadry elements for dynamic soil-structure interaction. *Boundary Element Methods For Soil-Structure Interaction*, pages 1–60, 2003.

[10] S. C. Dutta, K. Bhattacharya, and R. Roy. Response of low-rise buildings under seismic ground excitation incorporating soil-structure interaction. *Soil Dynamics and Earthquake Engineering*, 24(12):893 – 914, 2004.

[11] S. Gajan, T. C. Hutchinson, B. L. Kutter, P. Raychowdhury, J. A. Ugalde, and J. P. Stewart. Numerical models for analysis and performance-based design of shallow foundations subjected to seismic loading. Technical report, Pacific Earthquake Engineering Research Center, 2008.

[12] S. Gajan, P. Raychowdhury, T. C. Hutchinson, B. L. Kutter, and J. P. Stewart. Application and validation of practical tools for nonlinear soil-foundation interaction analysis. *Earthquake Spectra*, 26(1):111–129, 2010.

[13] H. E. Ganainy and M. E. Naggar. Efficient 3D nonlinear Winkler model for shallow foundations. *Soil Dynamics and Earthquake Engineering*, 29(8):1236 – 1248, 2009.

[14] G. Gazetas. Formulas and charts for impedances of surface and embedded foundations. *Journal of Geotechnical Engineering*, 117(9):1363–1381, 1991.

[15] A. M. Halabian and M. H. E. Naggar. Effect of non-linear soil-structure interaction on seismic response of tall slender structures. *Soil Dynamics and Earthquake Engineering*, 22(8):639 – 658, 2002.

[16] B. Halldórsson and R. Sigbjörnsson. The M_ω6.3 Ölfus earthquake at 15:45 UTC on 29 May 2008 in South Iceland: ICEARRAY strong-motion recordings. *Soil Dynamics and Earthquake Engineering*, 29(6):1073 – 1083, 2009.

[17] G. W. Housner. The behavior of inverted pendulum structures during earthquakes. *Bulletin of the Seismological Society of America*, 53(2):409–417, 1963.

[18] L. Jingbo and L. Yandong. A direct method for analysis of dynamic soil-structure interaction based on interface idea. *Dynamic Soil-Structure Interaction*, pages 261–276, 1998.

[19] E. Kausel. Early history of soil-structure interaction. *Soil Dynamics and Earthquake Engineering*, 30(9):822 – 832, 2010. Special Issue in honour of Prof. Anestis Veletsos.

[20] G. Lacey, G. Thenoux, and F. Rodriguez-Roa. Three-dimensional finite element model for flexible pavement analyses based on field modulus measurements. *The Arabian Journal for Science and Engineering*, 33(1B):65 – 76, 2008.

[21] P. Li, X. Lu, B. Chen, and Y. Chen. Computer simulation on dynamic soil-structure interaction system. *13th World Conference on Earthquake Engineering*, 2004. Paper No. 3233.

[22] G. R. Liu and S. S. Quek. *The finite element a practical course.* Butterworth-Heinemann, 2003.

[23] R. Livaoglu and A. Dogangun. Effect of foundation embedment on seismic behavior of elevated tanks considering fluid-structure-soil interaction. *Soil Dynamics and Earthquake Engineering*, 27(9):855 – 863, 2007.

[24] L. M. Massone. *RC Wall Shear - Flexure Interaction: Analytical and Experimental Responses.* PhD thesis, University of California, 2006.

[25] F. McKenna. OpenSeesWiki. http://opensees.berkeley.edu/wiki/index.php/Main_Page. Accessed: 10/01/2012.

[26] B. Méndez, E. Botero, and M. Romo. A new friction law for sliding rigid blocks under cyclic loading. *Soil Dynamics and Earthquake Engineering*, 29(5):874 – 882, 2009.

[27] M. Mohammadi and D. L. Karabalis. 3-d soil-structure interaction analysis by BEM: Comparison studies and computational aspects. *Soil Dynamics and Earthquake Engineering*, 9(2):96 – 108, 1990.

[28] T. Nogami, K. Konagai, and A. Mikami. Simple formulations of ground impedance functions for rigid surface foundations. *Soil Dynamics and Earthquake Engineering*, 21(6):475 – 484, 2001.

[29] T. Nogami, A. Mahbub, and S. Chen. A new method for formulation of dynamic responses of shallow foundations in simple general form. *Soil Dynamics and Earthquake Engineering*, 25(7-10):679 – 688, 2005. 11th International Conference on Soil Dynamics and Earthquake Engineering (ICSDEE): Part 1.

[30] H. S. Olafsson. Concrete walls founded on earthquake areas. Master's thesis, Reykjavik University, 2010.

[31] K. Orakcal, L. M. Massone, and J. W. Wallace. Analytical modeling of reinforced concrete walls for predicting flexural and coupled-shear-flexural responses. Technical report, Pacific Earthquake Engineering Research Center, 2006.

[32] M. Petrangeli, P. E. Pinto, and V. Ciampi. Fiber element for cyclic bending and shear of RC structures. I: Theory. *Journal of engineering mechanics*, 125(9):994–1001, 1999.

[33] P. K. Pradhan, D. K. Baidya, and D. P. Ghosh. Dynamic response of foundations resting on layered soil by cone model. *Soil Dynamics and Earthquake Engineering*, 24(6):425 – 434, 2004.

[34] C. d. Prisco, A. Galli, and M. Vecchiotti. Cyclic and dynamic mechanical behaviour of shallow foundations on granular deposits. *Coupled Site and Soil-Structure Interaction Effects with Application to Seismic Risk Mitigation*, 26(1):139–150, 2009.

[35] P. Raychowdhury. *Nonlinear Winkler-based Shallow Foundation Model for Performance Assessment of Seismically Loaded Structures*. PhD thesis, University of California, 2008.

[36] P. D. Spanos and A.-S. Koh. Analysis of block random rocking. *Soil Dynamics and Earthquake Engineering*, 5(3):178–183, 1986.

[37] C. Spyrakos, I. Koutromanos, and C. Maniatakis. Seismic response of base-isolated buildings including soil-structure interaction. *Soil Dynamics and Earthquake Engineering*, 29(4):658 – 668, 2009.

[38] M. Srbulov. *Ground vibration engineering Simplified Analysis with Case studies and Examples*, volume 12(17) of *Geotechnical, Geological and Earthquake Engineering*. Springer, 1 edition, 2010.

[39] H. R. Tabatabaiefar and A. Massumi. A simplified method to determine seismic responses of reinforced concrete moment resisting building frames under influence of soil-structure interaction. *Soil Dynamics and Earthquake Engineering*, 30(11):1259 – 1267, 2010.

[40] Y. Tang and J. Zhang. Probabilistic seismic demand analysis of a slender RC shear wall considering soil-structure interaction effects. *Engineering Structures*, 33(1):218 – 229, 2011.

[41] R. G. Taylor. *The Nonlinear Seismic Response of Tall Shear Wall Structures*. PhD thesis, University of Canterbury, 1977.

[42] E. R. Thorhallsson, I. S. Rikhardsson, A. M. Olafsson, and H. M. Olafsson. Analysis of a squat concrete wall, difference in translation during seismic excitation due to foundation support. 2010.

[43] A. S. Veletsos and Y. T. Wei. Lateral and rocking vibration of footings. *Soil mechanics and foundations division*, 97(SM9):1227–1248, 1971.

[44] A. Vulcano, V. V. Bertero, and V. Colotti. Analytical modeling of r/c structural walls. pages 41–46.

[45] J. P. Wolf. Simple physical models for foundation dynamics. *Dynamic Soil-Structure Interaction*, pages 1–70, 1998.

[46] J. P. Wolf and G. R. Darbre. Dynamic-stiffness matrix of surface foundation on layered halfspace based on stiffness-matrix approach. In *IAEA speacialists' meeting on "Gas-cooled reactor seismic design problems and solutions "*, pages 183–206, 1983. GA-A17034 IAEA No. IWGGCR/6 UC-77.

[47] W.-H. Wu. Equivalent fixed-base models for soil-structure interaction systems. *Soil Dynamics and Earthquake Engineering*, 16(5):323 – 336, 1997.

[48] W. H. Wu and C. Y. Chen. An effective fixed-base model with classical normal modes for soil-structure interaction systems. *Soil Dynamics and Earthquake Engineering*, 21(8):689 – 698, 2001.

[49] J. Yang, J. Li, and G. Lin. A simple approach to integration of acceleration data for dynamic soil-structure interaction analysis. *Soil Dynamics and Earthquake Engineering*, 26(8):725 – 734, 2006.

[50] M. Yazdchi, N. Khalili, and S. Valliappan. Dynamic soil-structure interaction analysis via coupled finite-element-boundary-element method. *Soil Dynamics and Earthquake Engineering*, 18(7):499 – 517, 1999.

[51] J. Zhang and Y. Tang. Dimensional analysis of structures with translating and rocking foundations under near-fault ground motions. *Soil Dynamics and Earthquake Engineering*, 29(10):1330 – 1346, 2009.

[52] C. Zhao. Applications of infinite elements to dynamic soil-structure interaction problems. In Z. Chuhan and J. P. Wolf, editors, *Dynamic Soil-Structure Interaction Current Research in China and Switzerland*, volume 83 of *Developments in Geotechnical Engineering*, pages 153 – 160. Elsevier, 1998.

Appendices

A Setup of the model in ANSYS

For ANSYS the method of input was rather straightforward. The wall is represented by a BLOCK command and dimensions. The material data is added and the required real constant for reinforcement. The meshing was carried out by choosing a global size for the elements using mapped hex meshing. The different models and material values were changed in an input file used to create the model and the analysis case.

A.1 Input file for ANSYS wall and lateral pushover

```
!—————————————————————————————————————————————————


/PREP7                          ! Starts the model building interface
 ET,1 ,SOLID65                   ! Define element to use. solid65 is special
                                 ! concrete element


*ask , LENGTH, How long is the wall?
*ask , HEIGHT, How tall is the wall?
*ask , THICK, How thick is the wall?,0.2

x_1 = −LENGTH/2
x_2 = −x_1

y_1 = −THICK/2
y_2 = −y_1

z_1 = 0
z_2 = HEIGHT

BLOCK,x_1,x_2,y_1,y_2,z_1,z_2,! Define geometry as a rectangular block

!—————————————————————————————————————————————————

! Material data

!—————————————————————————————————————————————————
! Concrete model 1 used for nonlinear concrete

MPTEMP, , , , , , , ,
MPTEMP,1 ,0
MPDATA,DENS,1 , ,2400                       ! Density of the concrete
```

```
MPTEMP, , , , , , , ,
MPTEMP, 1 , 0
MPDATA, EX, 1 , , 25000000000              ! Young's modulus for concrete
MPDATA, PRXY, 1 , , 0.2                    ! Poisson's ratio


TB, KINH, 1 , 1 , 6 , 0                    ! States that the model has kinematic
                                          ! hardening with 6 points

TBTEMP, 0
TBPT, , 0.0002 , 5000000
TBPT, , 0.0004 , 9000000
TBPT, , 0.0008 , 16000000
TBPT, , 0.0012 , 21000000
TBPT, , 0.0016 , 24000000
TBPT, , 0.002 , 25000000


TB, CONC, 1 , 1 , 9 ,                      ! William−Warnke attributes
TBTEMP, 0
TBDATA, , 0.1 , 0.2 , 2500000 , 25000000 , ,  ! Open/Closed shear transfer and
                                          ! ultimate tensile/crushing strength

TBDATA, , , , , , ,


! Steel model

MPTEMP, , , , , , , ,
MPTEMP, 1 , 0
MPDATA, DENS, 2 , , 7800
MPTEMP, , , , , , , ,
MPTEMP, 1 , 0
MPDATA, EX, 2 , , 210000000000
MPDATA, PRXY, 2 , , 0.3


TB, BISO, 2 , 1 , 2 ,                      ! Bilinear attributes for steel
TBTEMP, 0
TBDATA, , 410000000 , 21000000000 , , , ,  ! The bilinear properties, yield
                                          ! strength and Yong's modulus after
                                          ! Yielding



R,  1 , 2 , 0.003927 , 0 , 90 , 2 , 0.003927 ,  ! Real constants for element 1
                                          ! concrete65 defining the ratio of
                                          ! reinforcement
```

!——

! This part is the attribute allocation part for the volumes for meshing.

!——

*ask, MESH, Edge length of elements (m)?,0.1

! Selection of the volume that represents the wall where elements, materials
! real constants, mesh size is attributes and the execution of the mesh.

```
CM,_Y,VOLU
VSEL, , , ,        1
CM,_Y1,VOLU
CMSEL,S,_Y
CMSEL,S,_Y1
VATT,        1,        1,   1,        0
CMSEL,S,_Y

CMDELE,_Y
CMDELE,_Y1
ESIZE,MESH,0,
MSHAPE,0,3D
MSHKEY,1

CM,_Y,VOLU
VSEL, , , ,        1
CM,_Y1,VOLU
CHKMSH, 'VOLU'
CMSEL,S,_Y
VMESH,_Y1
CMDELE,_Y
CMDELE,_Y1
CMDELE,_Y2
```

!——

!——

```
FLST,2,1,5,ORDE,1              ! Selection of area to apply dof boundary
FITEM,2,1                      ! The application of rigid boundary
/GO
DA,P51X,ALL,0
ACEL,0,0,9.81,                 ! Application of inertial acceleration i.e.
                               ! gravity


FINISH
/SOL
```

III

```
DELTIM,0.1,0,0.1                    ! The time step control for gravity analysis
OUTRES,ERASE
OUTRES,ALL,ALL
AUTOTS,1
TIME,1
SOLVE




DELTIM,0.001,0,0.001               ! The time step control for lateral analysis
NEQIT,10000                        ! Number of allowed iterations

PSTRES,1                           ! The prestress is kept the gravity
                                   ! analysis is carried on to the lateral
                                   ! analysis
```

!——

! Calculation for the number of nodes at the top of the wall and application
! of loads to each node.

!——

```
DivX = LENGTH/MESH+1
DivY = THICK/MESH+1
NrNodes = DivX*DivY
RefLoad = 1000000                  ! The reference load applied on the top of
                                   ! the wall.
NodeLoad = RefLoad/NrNodes



FLST,2,NrNodes,1,ORDE,2            ! Selection of nodes at the top of the wall
```

! The model is so that the area at the bottom of the wall is first to be
! meshed and given node numbers. The top area of the wall is the second.

```
StartNode = NrNodes+1
EndNode = NrNodes*2

FITEM,2,StartNode
FITEM,2,-EndNode
/GO
F,P51X,FX,NodeLoad                 ! Load applied to each node based on 1MN load.
SOLVE
```

!——

```
!————————————————————————————————————————————
/post26                        ! Places ansys in the post processing package
nsel ,s ,node , ,StartNode ,EndNode  ! Select nodes that are to be examined

cm,EQP_DISPS, node             ! Save these nodes in a component
alls


cmsel ,s ,EQP_DISPS            ! Select a displacement component for output

*get ,num_n,NODE,0 ,COUNT      ! Get number of nodes
*get ,n_min ,NODE,0 ,NUM,MIN   ! Get min node number

*do ,i ,1 ,num_n,1             ! Output to ascii by looping over nodes
curr_n=n_min
nsol ,10 ,curr_n ,u,x          ! Output is UX


*dim ,N%curr_n%_output ,array ,1000 ,2    ! How long should the output be

vget ,N%curr_n%_output (1 ,1) ,1          ! Put time in array
vget ,N%curr_n%_output (1 ,2) ,10         ! Put UX in array


*cfopen ,"Your Path where to store results "\N%curr_n%,dat
*vwrite ,N%curr_n%_output (1 ,1) ,N%curr_n%_output (1 ,2)
(4(E15.6))
*cfopen

*get ,n_min ,NODE, curr_n ,NXTH
*enddo


!————————————————————————————————————————————
```

A.2 Input file for Ansys wall and soil model

For a case with soil the input is slightly different. The wall footing is divided into three volumes, one below the wall and one to each side of that volume. The reason for this was that the mesh tool did not recognize the volumes, created and joined together by a boolean, that could be meshed with bricks. The soil is arranged so that bodies adjacent to the wall footing and below could be given finer mesh while trying to keep a large soil domain to minimize reflection effects of waves from boundaries. The volumes are created by denoting the keypoints that define it, this also minimizes the creation of areas that are made if the block command is used. The keypoints are arranged in layers. Since the setup is always the same lines are for each model always have the same number, this is used to hardcode mesh edge length/divisions of those lines. The reason why embedment cannot be zero or equal and greater than the footing height is related to the fact that the contact interface is only coded to handle one case. Other boundaries can be set up manually if the user wishes to do so. The boundaries of the model are put in manually by adding 0 DOF displacement around and below the soil box. Gravity is solved separately and load cases then applied.

The application of frequency loads is done manually since the node numbering varies, the load pattern is also created with the graphical user interface in the parameters section. The created function is then saved and loaded into the program as a table. The nodal forces are created using the existing table, analysis is changed to a transient analysis. Time step is chosen and end time is specified as 5 seconds. Prestresses are kept to account for initial state of the wall and soil.

!——

```
finish
/clear
/VIEW,1,1,1,1
/VUP,1,Z
/REPLOT
/PREP7
*ask,LENGTH,How long is the wall (x-dir)?
*ask,HEIGHT,How tall is the wall (z-dir)?
*ask,THICK,How thick is the wall (y-dir)?
*ask,FHEIGHT,How thick is the footing (z-dir)?
*ask,FWIDTH,How wide is the footing (y-dir)?
*ask,LENGTHG,How long is the soil domain (x-dir)?
*ask,HEIGHTG,How high is the soil domain (z-dir)?
*ask,WIDTHG,How wide is the soil domain (y-dir)?
*ask,EMBEDMENT, What is the embedment of the wall (d> embedment > 0)?
*ask,RATIOSOIL, What is the ratio between the soil height and the first layer?
*ask,DILATION, What is the dilation of the soil (psi)?
```

!——

```
!――――――――――――――――――――――            K,120, -x1,  y2,  z1,


! Parameters controlling keypoint
! creation.                           K,201, -x1, -y1,  z2,
                                      K,202,  x1, -y1,  z2,
                                      K,203,  x1,  y1,  z2,
x1 = LENGTH/2                         K,204, -x1,  y1,  z2,
x2 = LENGTHG/2

y1 = FWIDTH/2                         K,217, -x1, -y2,  z2,
y2 = THICK/2                          K,218,  x1, -y2,  z2,
y3 = WIDTHG/2                         K,219,  x1,  y2,  z2,
                                      K,220, -x1,  y2,  z2,
z1 = 0.0
z2 = FHEIGHT
z3 = HEIGHT+FHEIGHT                   K,317, -x1, -y2,  z3,
z4 = EMBEDMENT                        K,318,  x1, -y2,  z3,
z6 = -(EMBEDMENT+HEIGHTG)             K,319,  x1,  y2,  z3,
z5 = z6*RATIOSOIL                     K,320, -x1,  y2,  z3,



! Keypoint creation, numbering is     K,401, -x1, -y1,  z4,
! clockwise.                          K,402,  x1, -y1,  z4,
                                      K,403,  x1,  y1,  z4,
! The 100's describe in what height   K,404, -x1,  y1,  z4,
! the point is
                                      K,405, -x2, -y3,  z4,
K,101, -x1, -y1,  z1,                 K,406, -x1, -y3,  z4,
K,102,  x1, -y1,  z1,                 K,407,  x1, -y3,  z4,
K,103,  x1,  y1,  z1,                 K,408,  x2, -y3,  z4,
K,104, -x1,  y1,  z1,                 K,409,  x2, -y1,  z4,
                                      K,410,  x2,  y1,  z4,
K,105, -x2, -y3,  z1,                 K,411,  x2,  y3,  z4,
K,106, -x1, -y3,  z1,                 K,412,  x1,  y3,  z4,
K,107,  x1, -y3,  z1,                 K,413, -x1,  y3,  z4,
K,108,  x2, -y3,  z1,                 K,414, -x2,  y3,  z4,
K,109,  x2, -y1,  z1,                 K,415, -x2,  y1,  z4,
K,110,  x2,  y1,  z1,                 K,416, -x2, -y1,  z4,
K,111,  x2,  y3,  z1,
K,112,  x1,  y3,  z1,
K,113, -x1,  y3,  z1,                 K,501, -x1, -y1,  z5,
K,114, -x2,  y3,  z1,                 K,502,  x1, -y1,  z5,
K,115, -x2,  y1,  z1,                 K,503,  x1,  y1,  z5,
K,116, -x2, -y1,  z1,                 K,504, -x1,  y1,  z5,

K,117, -x1, -y2,  z1,                 K,505, -x2, -y3,  z5,
K,118,  x1, -y2,  z1,                 K,506, -x1, -y3,  z5,
K,119,  x1,  y2,  z1,                 K,507,  x1, -y3,  z5,
```

VIII

```
K,508,   x2,  −y3,   z5,
K,509,   x2,  −y1,   z5,
K,510,   x2,   y1,   z5,
K,511,   x2,   y3,   z5,
K,512,   x1,   y3,   z5,
K,513,  −x1,   y3,   z5,
K,514,  −x2,   y3,   z5,
K,515,  −x2,   y1,   z5,
K,516,  −x2,  −y1,   z5,


K,601,  −x1,  −y1,   z6,
K,602,   x1,  −y1,   z6,
K,603,   x1,   y1,   z6,
K,604,  −x1,   y1,   z6,

K,605,  −x2,  −y3,   z6,
K,606,  −x1,  −y3,   z6,
K,607,   x1,  −y3,   z6,
K,608,   x2,  −y3,   z6,
K,609,   x2,  −y1,   z6,
K,610,   x2,   y1,   z6,
K,611,   x2,   y3,   z6,
K,612,   x1,   y3,   z6,
K,613,  −x1,   y3,   z6,
K,614,  −x2,   y3,   z6,
K,615,  −x2,   y1,   z6,
K,616,  −x2,  −y1,   z6,


!————————————————————————————

! Wall volumes, first 2 the sides of
! the footing then middle of the
! footing and the wall last.

V,101,102,118,117,201,202,218,217
V,120,119,103,104,220,219,203,204
V,117,118,119,120,217,218,219,220
V,217,218,219,220,317,318,319,320

! Volumes of the soil embedment.

V,105,106,101,116,405,406,401,416
V,106,107,102,101,406,407,402,401
V,107,108,109,102,407,408,409,402
V,102,109,110,103,402,409,410,403
V,103,110,111,112,403,410,411,412
```

```
V,104,103,112,113,404,403,412,413
V,115,104,113,114,415,404,413,414
V,116,101,104,115,416,401,404,415


! Volumes for soil refinement
! (in z−dir) directly under the
! footing.

V,505,506,501,516,105,106,101,116
V,506,507,502,501,106,107,102,101
V,507,508,509,502,107,108,109,102
V,502,509,510,503,102,109,110,103
V,503,510,511,512,103,110,111,112
V,504,503,512,513,104,103,112,113
V,515,504,513,514,115,104,113,114
V,516,501,504,515,116,101,104,115


V,501,502,503,504,101,102,103,104

! Soil volumes coarse mesh in (z−dir)


V,605,606,601,616,505,506,501,516
V,606,607,602,601,506,507,502,501
V,607,608,609,602,507,508,509,502
V,602,609,610,603,502,509,510,503
V,603,610,611,612,503,510,511,512
V,604,603,612,613,504,503,512,513
V,615,604,613,614,515,504,513,514
V,616,601,604,615,516,501,504,515


V,601,602,603,604,501,502,503,504


!————————————————————————————————


! Element type used.

ET,1,SOLID95

! Linear concrete properties

MPTEMP,,,,,,,,
MPTEMP,1,0
MPDATA,DENS,1,,2400
MPTEMP,,,,,,,,
MPTEMP,1,0
```

```
MPDATA, EX, 1 , , 25000000000
MPDATA, PRXY, 1 , , 0 . 2


! Soil with Drucker−Prager failure.


MPTEMP, , , , , , , ,
MPTEMP, 1 , 0
MPDATA, DENS, 2 , , 1 9 2 1 . 4 4
MPTEMP, , , , , , , ,
MPTEMP, 1 , 0
MPDATA, EX, 2 , , 389898525
MPDATA, PRXY, 2 , , 0 . 2 5
TB, DP, 2
TBDATA, 1 , 0 , 2 9 , DILATION


! Volume attributes of footing and
! wall.


FLST, 5 , 4 , 6 , ORDE, 2
FITEM, 5 , 1
FITEM, 5 , −4
CM, _Y, VOLU
VSEL, , , , P51X
CM, _Y1, VOLU
CMSEL, S , _Y

CMSEL, S , _Y1
VATT,         1 , ,    1 ,         0
CMSEL, S , _Y
CMDELE, _Y
CMDELE, _Y1


! Volume attributes of the soil


FLST, 5 , 26 , 6 , ORDE, 2
FITEM, 5 , 5
FITEM, 5 , −30
CM, _Y, VOLU
VSEL, , , , P51X
CM, _Y1, VOLU
CMSEL, S , _Y

CMSEL, S , _Y1
VATT,         2 , ,    1 ,         0
CMSEL, S , _Y
CMDELE, _Y
```

```
CMDELE, _Y1


!——————————————————————————


! Size control of the mesh of the
! wall.


! The mesh in the x−dir of the wall
! /footing and adjacent soil to the
! wall edges.


Mesh_x_wall = 0.2          ! Edge length


FLST, 5 , 6 , 4 , ORDE, 6
FITEM, 5 , 1
FITEM, 5 , 10
FITEM, 5 , 15
FITEM, 5 , 18
FITEM, 5 , 109
FITEM, 5 , 127
CM, _Y, LINE
LSEL, , , , P51X
CM, _Y1, LINE
CMSEL, , _Y
LESIZE, _Y1, Mesh_x_wall , , , , , , , 1


! The mesh in the x−dir of the wall
! /footing and adjacent soil to the
! wall edges.


Mesh_y_wall = 0.2          ! Edge length


FLST, 5 , 7 , 4 , ORDE, 7
FITEM, 5 , 2
FITEM, 5 , 14
FITEM, 5 , 27
FITEM, 5 , 66
FITEM, 5 , 97
FITEM, 5 , 119
FITEM, 5 , 137

CM, _Y, LINE
LSEL, , , , P51X
CM, _Y1, LINE
CMSEL, , _Y
LESIZE, _Y1, Mesh_y_wall , , , , , , , 1
```

X

! The mesh in the z−dir of the wall,
! footing and soil

! Footing

Mesh_z_footing = 1   ! Divisions
FLST,5,2,4,ORDE,2
FITEM,5,9
FITEM,5,19
CM,_Y,LINE
LSEL, , , ,P51X
CM,_Y1,LINE
CMSEL, ,_Y
LESIZE,_Y1,,,Mesh_z_footing,,,,,1

! Wall meshing

Mesh_z_wall = 0.4   ! Edge length

FLST,5,1,4,ORDE,1
FITEM,5,31

CM,_Y,LINE
LSEL, , , ,P51X
CM,_Y1,LINE
CMSEL, ,_Y
LESIZE,_Y1,Mesh_z_wall,,,,,,,1

! Soil embedment

Mesh_z_embed = 1   ! Divisions

FLST,5,4,4,ORDE,4
FITEM,5,45
FITEM,5,54
FITEM,5,70
FITEM,5,83
CM,_Y,LINE
LSEL, , , ,P51X
CM,_Y1,LINE
CMSEL, ,_Y
LESIZE,_Y1,,,Mesh_z_embed,,,,,1

! Mesh of the soil

! Coarse division in the x and y
! direction.

Soil_coarse_x = 1.5   ! Edge length

FLST,5,12,4,ORDE,12
FITEM,5,39
FITEM,5,58
FITEM,5,65
FITEM,5,87
FITEM,5,99
FITEM,5,101
FITEM,5,112
FITEM,5,114
FITEM,5,118
FITEM,5,123
FITEM,5,132
FITEM,5,133
CM,_Y,LINE
LSEL, , , ,P51X
CM,_Y1,LINE
CMSEL, ,_Y
LESIZE,_Y1,Soil_coarse_x,,,,,,,1

Soil_coarse_y = 2   ! Edge length

FLST,5,16,4,ORDE,16
FITEM,5,38
FITEM,5,50
FITEM,5,74
FITEM,5,81
FITEM,5,100
FITEM,5,102
FITEM,5,108
FITEM,5,113
FITEM,5,122
FITEM,5,124
FITEM,5,129
FITEM,5,134
FITEM,5,142
FITEM,5,153
FITEM,5,162
FITEM,5,174
CM,_Y,LINE
LSEL, , , ,P51X
CM,_Y1,LINE
CMSEL, ,_Y

```
LESIZE,_Y1,Soil_coarse_y,,,,,,,,1

Soil_fine_z = 5          ! Divisions


FLST,5,4,4,ORDE,4
FITEM,5,105
FITEM,5,111
FITEM,5,121
FITEM,5,130
CM,_Y,LINE
LSEL, , , ,P51X
CM,_Y1,LINE
CMSEL,,_Y
LESIZE,_Y1,,,Soil_fine_z,,,,,1

Soil_coarse_z = 1.5      ! Edge length


FLST,5,4,4,ORDE,4
FITEM,5,145
FITEM,5,151
FITEM,5,161
FITEM,5,170
CM,_Y,LINE
LSEL, , , ,P51X
CM,_Y1,LINE
CMSEL,,_Y
LESIZE,_Y1,Soil_coarse_z,,,,,,,1


!————————————————————————————————


! The meshing

FLST,5,30,6,ORDE,2
FITEM,5,1
FITEM,5,-30
CM,_Y,VOLU
VSEL, , , ,P51X
CM,_Y1,VOLU
CHKMSH,'VOLU'
CMSEL,S,_Y
VMESH,_Y1
CMDELE,_Y
CMDELE,_Y1
CMDELE,_Y2


!————————————————————————————————
```

```
! Boundary creation between soil and
! wall. Contact!

! Side contact

/COM, CONTACT PAIR CREATION - START
CM,_NODECM,NODE
CM,_ELEMCM,ELEM
CM,_KPCM,KP
CM,_LINECM,LINE
CM,_AREACM,AREA
CM,_VOLUCM,VOLU
/GSAV,cwz,gsav,,temp
MP,MU,2,0.6
MAT,2
R,3
REAL,3
ET,2,170
ET,3,174
KEYOPT,3,9,0
KEYOPT,3,10,2
R,3,
RMORE,
RMORE,,0
RMORE,0
! Generate the target surface
ASEL,S,,,2
ASEL,A,,,3
ASEL,A,,,5
ASEL,A,,,9
ASEL,A,,,10
ASEL,A,,,11
ASEL,A,,,14
ASEL,A,,,15
CM,_TARGET,AREA
TYPE,2
NSLA,S,1
ESLN,S,0
ESLL,U
ESEL,U,ENAME,,188,189
NSLE,A,CT2
! CZMESH patch (fsk qt-40109 8/2008)
ESURF
CMSEL,S,_ELEMCM
! Generate the contact surface
ASEL,S,,,31
```

XII

```
ASEL,A, , ,41
ASEL,A, , ,49
ASEL,A, , ,59
CM,_CONTACT,AREA
TYPE,3
NSLA,S,1
ESLN,S,0
NSLE,A,CT2
! CZMESH patch (fsk qt-40109 8/2008)
ESURF
ALLSEL
ESEL,ALL
ESEL,S,TYPE, ,2
ESEL,A,TYPE, ,3
ESEL,R,REAL, ,3
/PSYMB,ESYS,1
/PNUM,TYPE,1
/NUM,1
EPLOT
ESEL,ALL
ESEL,S,TYPE, ,2
ESEL,A,TYPE, ,3
ESEL,R,REAL, ,3
CMSEL,A,_NODECM
CMDEL,_NODECM
CMSEL,A,_ELEMCM
CMDEL,_ELEMCM
CMSEL,S,_KPCM
CMDEL,_KPCM
CMSEL,S,_LINECM
CMDEL,_LINECM
CMSEL,S,_AREACM
CMDEL,_AREACM
CMSEL,S,_VOLUCM
CMDEL,_VOLUCM
/GRES,cwz,gsav
CMDEL,_TARGET
CMDEL,_CONTACT
/COM, CONTACT PAIR CREATION - END


! Bottom contact


/COM, CONTACT PAIR CREATION - START
CM,_NODECM,NODE
CM,_ELEMCM,ELEM
CM,_KPCM,KP
CM,_LINECM,LINE

CM,_AREACM,AREA
CM,_VOLUCM,VOLU
/GSAV,cwz,gsav, ,temp
MP,MU,2 ,0.6
MAT,2
R,4
REAL,4
ET,5 ,170
ET,6 ,174
KEYOPT,6 ,9 ,0
KEYOPT,6 ,10 ,2
R,4 ,
RMORE,
RMORE, ,0
RMORE,0
! Generate the target surface
ASEL,S, , ,1
ASEL,A, , ,7
ASEL,A, , ,13
CM,_TARGET,AREA
TYPE,5
NSLA,S,1
ESLN,S,0
ESLL,U
ESEL,U,ENAME, ,188 ,189
NSLE,A,CT2
! CZMESH patch (fsk qt-40109 8/2008)
ESURF
CMSEL,S,_ELEMCM
! Generate the contact surface
ASEL,S, , ,95
CM,_CONTACT,AREA
TYPE,6
NSLA,S,1
ESLN,S,0
NSLE,A,CT2
! CZMESH patch (fsk qt-40109 8/2008)
ESURF
ALLSEL
ESEL,ALL
ESEL,S,TYPE, ,5
ESEL,A,TYPE, ,6
ESEL,R,REAL, ,4
/PSYMB,ESYS,1
/PNUM,TYPE,1
/NUM,1
EPLOT
```

```
ESEL , ALL
ESEL , S , TYPE, , 5
ESEL , A , TYPE, , 6
ESEL , R , REAL, , 4
CMSEL , A , _NODECM
CMDEL , _NODECM
CMSEL , A , _ELEMCM
CMDEL , _ELEMCM
CMSEL , S , _KPCM
CMDEL , _KPCM
CMSEL , S , _LINECM
CMDEL , _LINECM
CMSEL , S , _AREACM
CMDEL , _AREACM
CMSEL , S , _VOLUCM
CMDEL , _VOLUCM
/GRES , cwz , gsav
CMDEL , _TARGET
CMDEL , _CONTACT
/COM,  CONTACT  PAIR  CREATION − END
!———————————————————————————
```

B Setup of the model in OpenSees

The OpenSees wiki [25] contains all the description of the commands used in the files below. These files are either read into OpenSees using the command *source filename.extension*. If the files are not in the same folder as the OpenSees executable program the path needs to be included. Alternative the commands can be copied from the text files and pasted into OpenSees.

B.1 Lateral pushover program

The files on the following pages are used to create lateral pushover tests of the force- and flexure-beam elements. When using the recorders a wipe command needs to be used to write the results into the recorder files.

```
###################################################################################
###################################################################################


# Filename: SourceFile.txt
# Function: A program to activate nessecary functions to perform lateral
# pushover test on a shear wall consisting of either Force−Beam elements
# or Flexural−Beam elements.


###################################################################################
###################################################################################


# How to use: The commands are already written in this file, there are two
# different element types proposed for the shear wall. A Flexural−Beam element
# or a Force−Beam element. To test each individual element use # to cancel out
# the source commands that are not beeing used at the time.

# A for loop is commented out in this file but can be activated by removing
# the # in front of them. To do sensitivity checks for changing number of
# elements and such the variables m and mm can be used within the subfiles
# that are sourced.


###################################################################################


#for {set m 0} {$m <= 2} {incr m} {
#for {set mm 0} {$mm <= 2} {incr mm} {
```

```
###############################################################################

# SI units [m, N, Pa, kg]

###############################################################################



#@@@@@@@@@@@@@@@@@@@@@@@@@@@@@@@@@@@@@@@@@@@@@@@@@@@@@@@@@@@@@@@@@@@@@@@@@@@@@@@@@

wipe; wipeAnalysis;                          # A wipe performed to reset OpenSees
model basic -ndm 2 -ndf 3;                   # A two dimensional model using 3
                                             # degrees of freedom


set height [expr 3.0];                       # Height of the wall
set length [expr 3.0];                       # Length of the wall
set width 0.2;                               # Width of the wall



set nrElements [expr $height*4];             # Numbers of elements
set elLength [expr $height/$nrElements];     # Length of each element

set nrFibers_Y [expr int($length*5)];        # Number of fibers in the Y local
                                             # direction of the section
set nrFibers_Z [expr 3];                     # Number of fibers in the Z local
                                             # direction of the section
set RSpacing 0.2;                            # Spacing of the reinforcement

set maxDisp 0.0035;                          # Value used for pushover failure
                                             # test of Force element

source MaterialProperties.txt;               # Information about material
                                             # properties
source NodeCreation.txt;                     # The commands to create structural
                                             # nodes for elements

#source FlexSection.txt;                      # Section creation for a flexural beam
#source FlexElement.txt;                      # Element defenition for flexural beam
                                             # with previously defined section.

source ForceSection.txt;                     # Section creation for a force beam

set AggregationOnOff 1;                      # Use 0 if aggregation spring is not
                                             # used, use 1 if it is in use.

source sectionAggregator.txt;                # Creation of aggregagated section
```

XVI

```
                                          # grouping previously defined uniaxial
                                          # materials into single force
                                          # −deformation model.

source ForceElement.txt;                  # Element defenition for force beam
                                          # with previously defined section.



 fix 1 1 1 1;                             # Makes a rigid connection @ node 1
                                          # for all DOF

source LoadCaseGravity.txt;               # Applies self weight of the wall
source GravitySolver.txt;                 # Solves the self weight analysis of
                                          # the wall

#source LateralLoad.txt;                  # Applies lateral load to the top
                                          # node of the wall

source LateralDisplacement.txt;           # Applies a reference lateral
                                          # reference load of 1N

source LateralRecorders.txt;              # Recorders to monitor results for
                                          # each load step of the analysis



#source LateralForceSolver.txt;           # Solves the displacements for the
                                          # top node till the analysis fails
                                          # to converge

#source LateralDisplacementSolver.txt;    # Solves the force needed for a
                                          # displacement driven case

#}
#}
puts Done

#@@@@@@@@@@@@@@@@@@@@@@@@@@@@@@@@@@@@@@@@@@@@@@@@@@@@@@@@@@@@@@@@@@@@@@@@@@@@@@@@@@@
```

```
################################################################################
################################################################################

# Name of file: MaterialProperties.txt
# Function: Defines the material properties for Concrete and steel.

################################################################################
################################################################################

#@@@@@@@@@@@@@@@@@@@@@@@@@@@@@@@@@@@@@@@@@@@@@@@@@@@@@@@@@@@@@@@@@@@@@@@@@@@@@@@@@@@

#Material properties: Compression is negative, tensile positive. Parameters
are chosen to be used with Concrete02 and Steel01 in OpenSees.

#Concrete

set f_c [expr -25*pow(10,6)];          # Concrete compressive strength
set eps_0 -0.002;                      # Concrete strain at maximum strength
set E_c [expr 2*$f_c/$eps_0];          # Young's modulus
set dens_c 2400;                       # Density of concrete used for
                                       # gravity analysis
set f_t [expr -0.1*$f_c];               # Tensile capacity taken as 10%
set eps_20 -0.005;                     # Concrete strain at crushing
                                       # strength
set f_u [expr -5*pow(10,6)];           # Concrete crushing strength
set lambda 0.1;
set E_t [expr $E_c*$lambda];           # Tension softening stiffness

set Poisson 0.2;                       # Used for the section aggregator


#Steel

set dens_s 7800.0;
set E_s [expr 210*pow(10,9)];          # Young's modulus
set f_y [expr 410*pow(10,6)];          # Yield strength
set lambda_s 0.1;                      # Strain-hardening ratio (b)

# uniaxialMaterial Concrete02 $matTag $fpc $epsc0 $fpcu $epsU $lambda $ft $Ets
uniaxialMaterial Concrete02 1 $f_c $eps_0 $f_u $eps_20 $lambda $f_t $E_t

# uniaxialMaterial Steel01 $matTag $Fy $E0 $b <$a1 $a2 $a3 $a4>
uniaxialMaterial Steel01 1001 $f_y $E_s $lambda_s;

#@@@@@@@@@@@@@@@@@@@@@@@@@@@@@@@@@@@@@@@@@@@@@@@@@@@@@@@@@@@@@@@@@@@@@@@@@@@@@@@@@@@
```

```
###############################################################################
###############################################################################

# Name of file: NodeCreation.txt
# Function: Creates nodes along the height of the wall specified by the
# number of elements. The bottom of the wall is numbered as node 1 and the
# numbering from the bottom to the top.

###############################################################################
###############################################################################

#@@@@@@@@@@@@@@@@@@@@@@@@@@@@@@@@@@@@@@@@@@@@@@@@@@@@@@@@@@@@@@@@@@@@@@@@@@@@@@@

set nrNodes [expr $nrElements+1]

# node $nodeTag (ndm $coords) <-mass (ndf $massValues)>
node 1 0 0.0;

for {set i 1} {$i < $nrNodes} {incr i} {

node [expr $i+1] 0 [expr $i*$elLength]

}

# Identifiers for sections to make it easier to identify them in the code.

set FlexSecID 1
set ForceSecID 2
set AggrSecID 3
set shearEleID 4

#@@@@@@@@@@@@@@@@@@@@@@@@@@@@@@@@@@@@@@@@@@@@@@@@@@@@@@@@@@@@@@@@@@@@@@@@@@@@@@@
```

```
################################################################################
################################################################################


# Name of file: FlexSection.txt
# Function: The setup of a section to be used with the Flexure-Beam.


################################################################################
################################################################################

#@@@@@@@@@@@@@@@@@@@@@@@@@@@@@@@@@@@@@@@@@@@@@@@@@@@@@@@@@@@@@@@@@@@@@@@@@@@@@@@@@@@


# Definition of fibers and fiber discretization.
#        _____
#        |  fiber1.1  |   fiber2.1  |              |         |
#  ^     | A_c & A_s  |             |              |         |
#  |     |———————————————————————————————————————————————|
#  |     |  fiber1.2  |   fiber2.2  |              |         |
#  z     |_____|
#
#                              y---->
#
# The OpenSees model allows 3 strips with different width to model T-shape/
# barbell walls, two end sections and a middle one. Each section can be made
# from numerous fibers that need to be put in successive order, the change
# in y-coordinate will notify the prorgram a new fiber is activated. For
# this particular wall the end sections are not needed and the cross section
# is made using only the middle strip.


################################################################################


set rRadius 0.005;                   # Radius of reinforcement bars
set pi 3.14
set totReinforcement [expr $length/$RSpacing*2*$pi*pow($rRadius,2)]
set ratio [expr $totReinforcement/($length*$width)]
# The 2x multiplier in totReinforcement denotes a double layer



################################################################################


# Section definition

set FiberLength_y [expr $length/$nrFibers_Y]
set FiberLength_z [expr $width/$nrFibers_Z]
set A_c [expr $FiberLength_y*$FiberLength_z]
set A_s [expr $A_c*$ratio]
set horizontalReinforcement [expr $ratio*$width*$height/$nrElements]
```

XX

```
section FiberInt $FlexSecID −NStrip 0 0.0 $nrFibers_Y $width 0 0.0 {

# Vertical fibers

for {set i 0} {$i < $nrFibers_Y} {incr i} {
        for {set ii 0} {$ii < $nrFibers_Z} {incr ii} {

# fiber $yLoc $zLoc $A $matTag
fiber [expr −$length/2.0+$FiberLength_y*($i+0.5)]
[expr −$width/2.0+$FiberLength_z*($ii+0.5)] $A_c 1;
fiber [expr −$length/2.0+$FiberLength_y*($i+0.5)]
[expr −$width/2.0+$FiberLength_z*($ii+0.5)] $A_s 1 1001;


        }
}

# Horizontal reinforcement

    Hfiber 0 0 $horizontalReinforcement 1001;

}

#@@@@@@@@@@@@@@@@@@@@@@@@@@@@@@@@@@@@@@@@@@@@@@@@@@@@@@@@@@@@@@@@@@@@@@@@@@@@@@@@@@@
```

```
################################################################################
################################################################################

# Name of file: FlexElement.txt
# Function: Creation of the Flexure−Shear Interaction Displacement−Based
# Beam−Column Element between respective nodes using the previously defined
# cross section.

################################################################################
################################################################################

#@@@@@@@@@@@@@@@@@@@@@@@@@@@@@@@@@@@@@@@@@@@@@@@@@@@@@@@@@@@@@@@@@@@@@@@@@@@@@@@@


set np 5;                        # Number of integration points along an
                                 # element
set C 0.36;                      # Center of rotation
geomTransf LinearInt 1;          # Transformation tag treating the element as
                                 # a column/wall

# Element definition

# element dispBeamColumnInt $eleTag $iNode $jNode $numIntgrPts $secTag
# $transfTag $cRot

for {set i 1} {$i < $nrNodes} {incr i} {

element dispBeamColumnInt $i $i [expr $i+1] $np $FlexSecID 1 $C;

}

#@@@@@@@@@@@@@@@@@@@@@@@@@@@@@@@@@@@@@@@@@@@@@@@@@@@@@@@@@@@@@@@@@@@@@@@@@@@@@@@@
```

```
#################################################################################################
#################################################################################################

# Name of file: ForceSection.txt
# Function: Creation of the section used for the Force−Beam based element.


#################################################################################################
#################################################################################################

#@@@@@@@@@@@@@@@@@@@@@@@@@@@@@@@@@@@@@@@@@@@@@@@@@@@@@@@@@@@@@@@@@@@@@@@@@@@@@@@@@@@@@@@@@@@@@@@@@@@@

# Geometry of the wall and reinforcement plan


#################################################################################################


#   /   _____               _____        /
# 2cm  |                         \         /                              |     |
#  /   |  x   x   x   x     x      /       x    x    x   x     x  |     |
#  |   |                                <                                 |     |
#  16  |                                  \                               |   0.2m
#  cm  |                                   _>                             |     |
#  /   |  x   x   x   x     x      |        x    x    x   x     x  |     |
# 2cm  |_____/         _____|     |
#  /                                                                         /
#      /─────────────────────────length──────────────────────────/
#
#
#   ^
#   |
#  z|
#   |────>
#       y
#################################################################################################

set barDiameter 0.01;                              # Rebar diameter in meters

set pi 3.14

set A10 [expr pow(($barDiameter/2.0),2)*$pi];    # Area in m^2
set cover 0.02

#Coordinates for the wall

set y1 [expr −$length/2.0]
set y2 [expr −$y1]


                                    XXIII
```

```
set z1 [expr −$width/2.0]
set z2 [expr −$z1]

set y1Steel [expr $y1+$cover]
set y2Steel [expr $y2−$cover]

set z1Steel [expr $z1+$cover]
set z2Steel [expr $z2−$cover]


set nrReinforcement [expr int($length/$RSpacing)]

section Fiber $ForceSecID {

# patch rect $matTag $numSubdivY $numSubdivZ $yI $zI $yJ $zJ
patch rect 1 $nrFibers_Y $nrFibers_Z $y1 $z1 $y2 $z2

# layer straight $matTag $numFiber $areaFiber $yStart $zStart $yEnd $zEnd
layer straight 1001 $nrReinforcement $A10 $y1Steel $z1Steel $y2Steel $z1Steel
layer straight 1001 $nrReinforcement $A10 $y1Steel $z2Steel $y2Steel $z2Steel

}

#@@@@@@@@@@@@@@@@@@@@@@@@@@@@@@@@@@@@@@@@@@@@@@@@@@@@@@@@@@@@@@@@@@@@@@@@@@@@@@@
```

```
################################################################################
################################################################################

# Name of file: sectionAggregator.txt
# Function: The setup of a section aggregator

################################################################################
################################################################################

#@@@@@@@@@@@@@@@@@@@@@@@@@@@@@@@@@@@@@@@@@@@@@@@@@@@@@@@@@@@@@@@@@@@@@@@@@@@@@@@@@@


set Ag [expr $length*$width];                      # Gross area of the wall
                                                   # cross section



# Define shear spring

set Poisson 0.2;
set G [expr $E_c/(2*(1+$Poisson))];                # Shear modulus
set factor [expr 0.08];                            # Some factor for uncracked/
                                                   # cracked section


set ks [expr $G*$Ag/1.2/$elLength*$factor];        # Shear stiffness of
                                                   # rectangular wall

uniaxialMaterial Elastic $shearEleID $ks           # Element based on the shear
                                                   # stiffness



# Combine fiber section and shear spring


section Aggregator $AggrSecID $shearEleID Vy −section $ForceSecID;

#@@@@@@@@@@@@@@@@@@@@@@@@@@@@@@@@@@@@@@@@@@@@@@@@@@@@@@@@@@@@@@@@@@@@@@@@@@@@@@@@@@
```

```
#############################################################################################
#############################################################################################

# Name of file: FlexElement.txt
# Function: Creation of the Force−Based Beam−Column Element between
# respective nodes using previously defined cross section.

#############################################################################################
#############################################################################################

#@@@@@@@@@@@@@@@@@@@@@@@@@@@@@@@@@@@@@@@@@@@@@@@@@@@@@@@@@@@@@@@@@@@@@@@@@@@@@@@@@@

set np 7;                              # Number of integration points along
                                       # an element
geomTransf Linear 1;                   # Transformation tag treating the
                                       # element as a column/wall

# element definition

if {$AggregationOnOff == 1} {
set ForceSecID [expr $AggrSecID]
}

# element forceBeamColumn $eleTag $iNode $jNode $numIntgrPts $secTag
# $transfTag <−mass $massDens> <−iter $maxIters $tol> <−integration $intType>

for {set i 1} {$i < $nrNodes} {incr i} {

element forceBeamColumn $i $i [expr $i+1] $np $ForceSecID 1;

}

#@@@@@@@@@@@@@@@@@@@@@@@@@@@@@@@@@@@@@@@@@@@@@@@@@@@@@@@@@@@@@@@@@@@@@@@@@@@@@@@@@@
```

```
################################################################################
################################################################################

# Name of file: LoadCaseGravity.txt
# Function: Application of the self weight of the wall lumped at connecting
# nodes between elements oriented in the global Y direction.

################################################################################
################################################################################

#@@@@@@@@@@@@@@@@@@@@@@@@@@@@@@@@@@@@@@@@@@@@@@@@@@@@@@@@@@@@@@@@@@@@@@@@@@@@@@@@@@

# Self weight of the wall

set g 9.81; #Gravitational constant

set mass [expr $length*$width*$height*$dens_c*$g]
set massOfElementPerNode [expr $mass/($nrElements*2.0)]

# The mass of an element is divided to the two nodes at the end of each element
# the top node recieves  contribution from one element while the others recieve
# contribution from two elements.

pattern Plain 1 Constant {

# load $nodeTag (ndf $LoadValues);       # Second DOF is the global Y direction

load 1 0.0 [expr -$massOfElementPerNode] 0.0;

        for {set i 2} {$i < $nrNodes} {incr i} {

        load $i 0.0 [expr -$massOfElementPerNode*2.0] 0.0;

        }

load [expr int($nrNodes)] 0.0 [expr -$massOfElementPerNode] 0.0;

}

#@@@@@@@@@@@@@@@@@@@@@@@@@@@@@@@@@@@@@@@@@@@@@@@@@@@@@@@@@@@@@@@@@@@@@@@@@@@@@@@@@@
```

```
################################################################################
################################################################################

# Name of file: GravitySolver.txt
# Function: The setup of the solver and relevant features needed to calculate
# the load case for gravity.

################################################################################
################################################################################

#@@@@@@@@@@@@@@@@@@@@@@@@@@@@@@@@@@@@@@@@@@@@@@@@@@@@@@@@@@@@@@@@@@@@@@@@@@@@@@@@

constraints Plain;              # Handling of boundary conditions
numberer Plain;                 # Renumber dof's to minimize band−width
system BandGeneral;             # How to store and solve the system of
                                # equations in the analysis

test NormDispIncr 1.0e−8 6 ;    # Determine if convergence has been achieved
                                # at the end of an iteration step

algorithm Newton;               # Use Newton's solution algorithm: updates
                                # tangent stiffness at every iteration

integrator LoadControl 0.1;     # Determine the next time step for an analysis
analysis Static                 # Define type of analysis static or transient
analyze 10;                     # Perform gravity analysis for 10 steps

#@@@@@@@@@@@@@@@@@@@@@@@@@@@@@@@@@@@@@@@@@@@@@@@@@@@@@@@@@@@@@@@@@@@@@@@@@@@@@@@@
```

```
################################################################################
################################################################################

# Name of file: LateralLoad.txt
# Function: Application of static 2MN force at the top node of the model in
# the global x direction.

################################################################################
################################################################################

#@@@@@@@@@@@@@@@@@@@@@@@@@@@@@@@@@@@@@@@@@@@@@@@@@@@@@@@@@@@@@@@@@@@@@@@@@@@@@@@@@@@

# Set the gravity loads to be constant & reset the time in the domain

loadConst −time 0.0


# Set lateral load pattern with a Linear TimeSeries
pattern Plain 2 "Linear" {

        # Create nodal loads at node 2
        #    nd    FX  FY  MZ
        load [expr int($nrNodes)] 2000000.0 0.0 0.0;
}


#@@@@@@@@@@@@@@@@@@@@@@@@@@@@@@@@@@@@@@@@@@@@@@@@@@@@@@@@@@@@@@@@@@@@@@@@@@@@@@@@@@@
```

```
################################################################################
################################################################################

# Name of file: LateralDisplacement.txt
# Function: Application of reference load of 1N, the displacement control
# integrator will provide multiplicity of the reference load used to provide
# the specified displacement.

################################################################################
################################################################################

#@@@@@@@@@@@@@@@@@@@@@@@@@@@@@@@@@@@@@@@@@@@@@@@@@@@@@@@@@@@@@@@@@@@@@@@@@@@@@@@@@@@

# Set the gravity loads to be constant & reset the time in the domain

loadConst −time 0.0


# Set lateral load pattern with a Linear TimeSeries
pattern Plain 2 "Linear" {

    # Create nodal loads at top node
    #    nd     FX  FY  MZ
    load [expr int($nrNodes)] 1.0 0.0 0.0
}

#@@@@@@@@@@@@@@@@@@@@@@@@@@@@@@@@@@@@@@@@@@@@@@@@@@@@@@@@@@@@@@@@@@@@@@@@@@@@@@@@@@@

################################################################################
################################################################################

# Name of file: LateralRecorders.txt
# Function: Recorder to track the displacement in the x direction at the top
# of the wall.

################################################################################
################################################################################

#@@@@@@@@@@@@@@@@@@@@@@@@@@@@@@@@@@@@@@@@@@@@@@@@@@@@@@@@@@@@@@@@@@@@@@@@@@@@@@@@@@@

# Create a recorder to monitor nodal displacements
recorder Node −file "Filename.out" −time −node [expr int($nrNodes)] −dof 1 disp

# The filename can use variables in the name to identify individual tests.


#@@@@@@@@@@@@@@@@@@@@@@@@@@@@@@@@@@@@@@@@@@@@@@@@@@@@@@@@@@@@@@@@@@@@@@@@@@@@@@@@@@@
```

XXX

```
###############################################################################
###############################################################################

# Name of file: LateralForceSolver.txt
# Function: The setup of the solver and relevant features needed to calculate
# the ultimate displacement of the Flexure−Beam element with a stepped load
# acting on the top node.

###############################################################################
###############################################################################

#@@@@@@@@@@@@@@@@@@@@@@@@@@@@@@@@@@@@@@@@@@@@@@@@@@@@@@@@@@@@@@@@@@@@@@@@@@@@@@@@@

# The analysis part

# Some convergence criteria

set tolAx 1.0e−6;
set iterAx 4000;

initialize;
integrator LoadControl 0.0005;          # Applies a load control to apply the
                                        # load in steps of 0.0005

system SparseGeneral −piv;              # Determines how to store and solve
                                        # the system of equations

test NormUnbalance $tolAx $iterAx 0;    # Convergence criteria

numberer RCM;                           # The numbering of the equations

constraints Plain;                      # Boundary conditions handled with
                                        # Plain constraints

algorithm ModifiedNewton −initial;      # Modified Newton's algorithm: updates
                                        # tangent stiffness

analysis Static;                        # Define analysis static/transient

# perform the lateral load analysis,

analyze 2000                            # Analyze 2000 loadsteps

wipe;                                   # Clears the analysis writing the
                                        # results into the recorder files.

#@@@@@@@@@@@@@@@@@@@@@@@@@@@@@@@@@@@@@@@@@@@@@@@@@@@@@@@@@@@@@@@@@@@@@@@@@@@@@@@@@
```

```
################################################################################
################################################################################

# Name of file: LateralDisplacementSolver.txt
# Function: The setup of the solver and relevant features needed to calculate
# the ultimate force of the Force-Beam element with a stepped displacement
# enforced at the top node.

################################################################################
################################################################################

#@@@@@@@@@@@@@@@@@@@@@@@@@@@@@@@@@@@@@@@@@@@@@@@@@@@@@@@@@@@@@@@@@@@@@@@@@@@@@@@@@@

set currentDisp 0.0;
set ok 0
set dU 0.00001;                                    # Displacement increment

# Change the integration scheme to be displacement control
#                              node dof init Jd min max
integrator DisplacementControl  [expr int($nrNodes)]   1    $dU   1 $dU $dU

while {$ok == 0 && $currentDisp < $maxDisp} {

        set ok [analyze 1]

      # if the analysis fails try initial tangent iteration
      if {$ok != 0} {
          test NormDispIncr 1.0e-6   1000
          algorithm ModifiedNewton -initial
          set ok [analyze 1]

              # Goes back the the Newton algorithm with more loose iteration
              # criteria.

          test NormDispIncr 1.0e-6   10
          algorithm Newton
      }

      set currentDisp [nodeDisp [expr int($nrNodes)] 1]
}

wipe;

#@@@@@@@@@@@@@@@@@@@@@@@@@@@@@@@@@@@@@@@@@@@@@@@@@@@@@@@@@@@@@@@@@@@@@@@@@@@@@@@@@@
```

B.2 Beam on Non-Linear Winkler Foundation program

These programs are used to create a linear wall and BNWF with desired soil and footing properties that are subjected to gravity loads and transient frequency loading.

```
##############################################################################
##############################################################################

# Filename: SoilTest.txt
# Function: A program to create a linear wall resting on a BNWF foundation
# and gravity load analysis.

##############################################################################
##############################################################################

# SI units [m, N, Pa, kg]

##############################################################################


#@@@@@@@@@@@@@@@@@@@@@@@@@@@@@@@@@@@@@@@@@@@@@@@@@@@@@@@@@@@@@@@@@@@@@@@@@@@@@@@@@


wipe; wipeAnalysis;                    # A wipe performed to reset OpenSees
model basic -ndm 2 -ndf 3;             # A two dimensional model using 3
                                       # degrees of freedom

set LengthWall 3.0;                    # Wall dimensions
set WidthWall 0.2;
set HeightWall 5.0;


node 1 0. 0.;                          # Structural nodes
node 2 0. $HeightWall


# Wall properties based on linear attributes

set AWall [expr $WidthWall*$LengthWall]
set EWall [expr 2.5*pow(10,10)]; #————[N/m^2] concrete
set IWall [expr $WidthWall*pow($LengthWall,3)/12.]
```

```
uniaxialMaterial Elastic 1 $EWall;          # Linear material

geomTransf Linear 1;                        # Geometric transformation that
                                            # determines the orientation of
                                            # element.



# Creating the wall

#element elasticBeamColumn $eleTag $iNode $jNode $A $E $Iz $transfTag
element elasticBeamColumn 1 1 2 $AWall $EWall $IWall 1

# Applying mass to the wall

set MWall [expr $LengthWall*$WidthWall*$HeightWall*2400]; # Mass of structure
mass 2 $MWall $MWall 1



#@@@@@@@@@@@@@@@@@@@@@@@@@@@@@@@@@@@@@@@@@@@@@@@@@@@@@@@@@@@@@@@@@@@@@@@@@@@@@@@@@

# Use ShallowFoundationGen command to attach shallow foundation with
# Foundation tag=1 to node 1

#@@@@@@@@@@@@@@@@@@@@@@@@@@@@@@@@@@@@@@@@@@@@@@@@@@@@@@@@@@@@@@@@@@@@@@@@@@@@@@@@@

set FoundationTag 1
#ShallowFoundationGen $FoundationTag $ConectNode $InputFileName $FootCondition
ShallowFoundationGen $FoundationTag 1 "BNWFinput.txt" 5
source Foundation_$FoundationTag.tcl
set MassFooting [expr 0.6*3.0*0.25*2400]
mass 1 $MassFooting $MassFooting 1

#@@@@@@@@@@@@@@@@@@@@@@@@@@@@@@@@@@@@@@@@@@@@@@@@@@@@@@@@@@@@@@@@@@@@@@@@@@@@@@@@@

# Eigen Value Analysis

#@@@@@@@@@@@@@@@@@@@@@@@@@@@@@@@@@@@@@@@@@@@@@@@@@@@@@@@@@@@@@@@@@@@@@@@@@@@@@@@@@

set PI 3.1415926
set lambdax [eigen 1]
set lambda [lindex $lambdax 0]
set omega [expr pow($lambda,0.5)]
set Tn [expr 2*$PI/$omega]
set fn [expr 1/$Tn]
puts "1st mode, Tn=$Tn sec, fn=$fn Hz"
```

```
#@@@@@@@@@@@@@@@@@@@@@@@@@@@@@@@@@@@@@@@@@@@@@@@@@@@@@@@@@@@@@@@@@@@@@@@@@@@@@@@@@

# Gravity load pattern and gravity analysis solver.

#@@@@@@@@@@@@@@@@@@@@@@@@@@@@@@@@@@@@@@@@@@@@@@@@@@@@@@@@@@@@@@@@@@@@@@@@@@@@@@@@@

set gacc 9.81;                            # Gravity acceleration
set deadLoad [expr ($MassFooting+$MWall)*$gacc];


pattern Plain 1 "Linear" {
load 2 0. [expr -$deadLoad] 0.
}



system UmfPack;                           # Storage and the solving method of
                                          # the equations

constraints Plain;                        # Handling of boundary conditions
test NormDispIncr 1.0e-8 40 0;            # Convergence test criteria
algorithm Newton;                         # Non-linear solving method
                                          # updates tangent stiffness.

numberer RCM;                             # Method of umbering of equations
integrator LoadControl 0.1;               # How the load is applied.
analysis Static;                          # Static analysis
analyze 10;                               # Perform 10 steps of analysis


#@@@@@@@@@@@@@@@@@@@@@@@@@@@@@@@@@@@@@@@@@@@@@@@@@@@@@@@@@@@@@@@@@@@@@@@@@@@@@@@@@
```

```
#################################################################################################
#################################################################################################

# Name of file: BNWFinput.txt
# Function: Information about soil properties, footing dimensions and meshing.

#################################################################################################
#################################################################################################

#@@@@@@@@@@@@@@@@@@@@@@@@@@@@@@@@@@@@@@@@@@@@@@@@@@@@@@@@@@@@@@@@@@@@@@@@@@@@@@@@@@@@@@@@

#Input data for foundation 1

#SoilProp $SoilType $c $Phi $Gamma $G $Nu $Crad $Tp
SoilProp 2 0.001 29.0 18849.3 155959410.0 0.25 0.05 0.001



#FootProp $Lf $Bf $Hf $Df $Ef $Wg $beta
FootProp 3.0 0.6 0.25 0.2 25000000000.0 70632 0.0

#MeshProp $Rk $Re $le/L
MeshProp 9.3 0.033 0.02


#@@@@@@@@@@@@@@@@@@@@@@@@@@@@@@@@@@@@@@@@@@@@@@@@@@@@@@@@@@@@@@@@@@@@@@@@@@@@@@@@@@@@@@@@
```

```
###############################################################################
###############################################################################

# Name of file: FrequencyTest.txt
# Function: Creates a sinusoidal load pattern and solves a transient analysis
# for that load case.

###############################################################################
###############################################################################

#@@@@@@@@@@@@@@@@@@@@@@@@@@@@@@@@@@@@@@@@@@@@@@@@@@@@@@@@@@@@@@@@@@@@@@@@@@@@@@


set timestep 0.005;                        # Steps between load applications
set time 5.0;                              # Duration of the load
set subSteps [expr int($time/$timestep)]
set frequency 1.0;                         # Hertz
set period [expr 1.0/$frequency];          # Period time (s)

#@@@@@@@@@@@@@@@@@@@@@@@@@@@@@@@@@@@@@@@@@@@@@@@@@@@@@@@@@@@@@@@@@@@@@@@@@@@@@@

# Recorders

#@@@@@@@@@@@@@@@@@@@@@@@@@@@@@@@@@@@@@@@@@@@@@@@@@@@@@@@@@@@@@@@@@@@@@@@@@@@@@@


recorder Node −time −file "Name1.txt" −node $endFootNodeL_1 −dof 2 disp
recorder Node −time −file "Name2.txt" −node 1 −dof 2 disp



#@@@@@@@@@@@@@@@@@@@@@@@@@@@@@@@@@@@@@@@@@@@@@@@@@@@@@@@@@@@@@@@@@@@@@@@@@@@@@@

# Creation of trigonometric load pattern, to create lateral frequency
# response the load in the pattern can be applied in the first dof.

#@@@@@@@@@@@@@@@@@@@@@@@@@@@@@@@@@@@@@@@@@@@@@@@@@@@@@@@@@@@@@@@@@@@@@@@@@@@@@@

timeSeries Trig 101 0.0 $time $period
pattern Plain 2 101 {
load 2 0. 100000.0 0.
}



#@@@@@@@@@@@@@@@@@@@@@@@@@@@@@@@@@@@@@@@@@@@@@@@@@@@@@@@@@@@@@@@@@@@@@@@@@@@@@@

# Frequency analysis
```

```
#@@@@@@@@@@@@@@@@@@@@@@@@@@@@@@@@@@@@@@@@@@@@@@@@@@@@@@@@@@@@@@@@@@@@@@@@@@@@@@@@@@

set Tol 1.e−8;                           # Convergence tolerance
set maxNumIter 10;                       # Number of iterations that will be
                                         # performed before failure to converge


set printFlag 0;                         # Flag used to print information
set TestType EnergyIncr;                 # Convergence−test type
test $TestType $Tol $maxNumIter $printFlag;



loadConst −time 0.0;                     # Resets time to 0 in the analysis



set algorithmType ModifiedNewton         #Solving method
algorithm $algorithmType;
integrator Newmark 0.5 0.25;             # Transient load integrator control
analysis Transient;                      # Analysis type
set ok [analyze $subSteps $timestep];    # The analysis step by step

if {$ok != 0} {          ;               # If analysis was not successful.

        # Change analysis strategy to try to achieve convergence. These
        # methods are slower than the first one.

        set ok 0;
        set controlTime [getTime];
        while {$controlTime < $time && $ok == 0} {
                set ok [analyze 1 $timestep]
                set controlTime [getTime]
                set ok [analyze 1 $timestep]
                if {$ok != 0} {
                        test NormDispIncr    $Tol 1000   0
                        algorithm Newton −initial
                        set ok [analyze 1 $timestep]
                        test $TestType $Tol $maxNumIter   0
                        algorithm $algorithmType
                }
                if {$ok != 0} {
                        algorithm Broyden 8
                        set ok [analyze 1 $timestep]
                        algorithm $algorithmType
                }
                if {$ok != 0} {
                        algorithm NewtonLineSearch .8
```

```
                    set ok [analyze 1 $timestep]
                    algorithm $algorithmType
              }
        }
};        # Ends if ok !0
```

#@@@

C   Visual Basic code used for result compilation in excel

The results from ANSYS lateral pushover tests generated numerous data files for each node. The following Visual Basic code was used in excel to compile all the text files into a large excel sheet so that the average displacement could be calculated.

```vb
Sub ReadFilesIntoActiveSheet()
    Dim fso As FileSystemObject
    Dim folder As folder
    Dim file As file
    Dim FileText As TextStream
    Dim TextLine As String
    Dim Items() As String
    Dim i As Long
    Dim cl As Range

    ' Get a FileSystem object
    Set fso = New FileSystemObject

    ' get the directory you want
    Set folder = fso.GetFolder("Your Folder Path Here")

    ' set the starting point to write the data to
    Set cl = ActiveSheet.Cells(1, 1)


        ' Loop thru all files in the folder
    For Each file In folder.Files
        ' Open the file
        Set FileText = file.OpenAsTextStream(ForReading)

        ' Read the file one line at a time
        Do While Not FileText.AtEndOfStream
            TextLine = FileText.ReadLine

            ' Parse the line into | delimited pieces
            Items = Split(TextLine, "  ")

            ' Put data on one row in active sheet
            For i = 0 To UBound(Items)
                cl.Offset(0, 0).Value = Items(2)
            Next

            ' Move to next row
            Set cl = cl.Offset(1, 0)
```

```
        Loop

        ' Clean up
        FileText.Close
        Set cl = cl.Offset(-1000, 1)
    Next file

    Set FileText = Nothing
    Set file = Nothing
    Set folder = Nothing
    Set fso = Nothing

End Sub
```

# D FE results of old models with different open and closed coefficients

Initially the importance of the open and closed crack shear transfer coefficient was not known, therefore the study was first conducted using open shear transfer coefficient 0.4 and closed 0.8. Figure 68 shows the results from those tests, they did not agree very well with the ME model results and much resources went into checking if the ME models were correct or not. This was a big obstacle in this study where these analysis took considerable time.
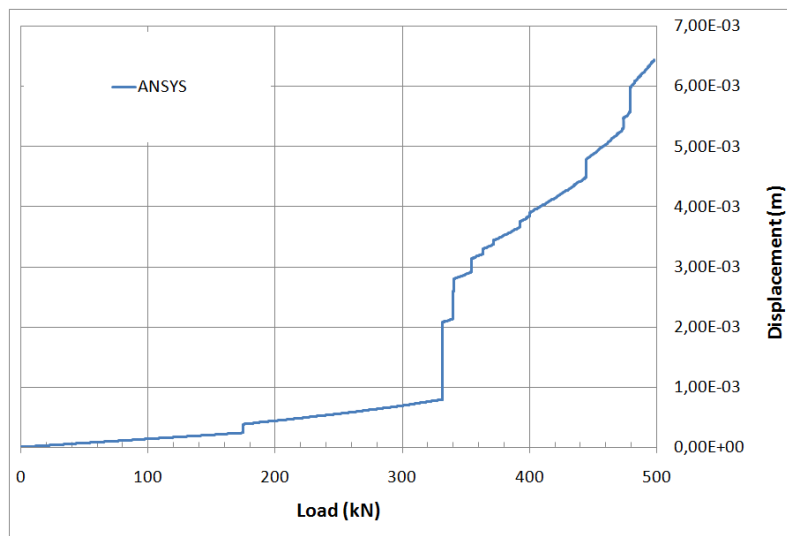
(a) 3.0 m by 3.0 m wall.
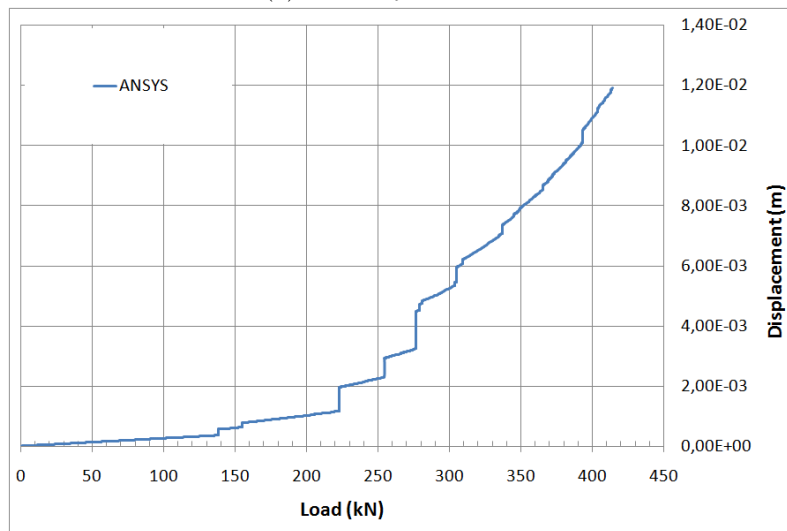
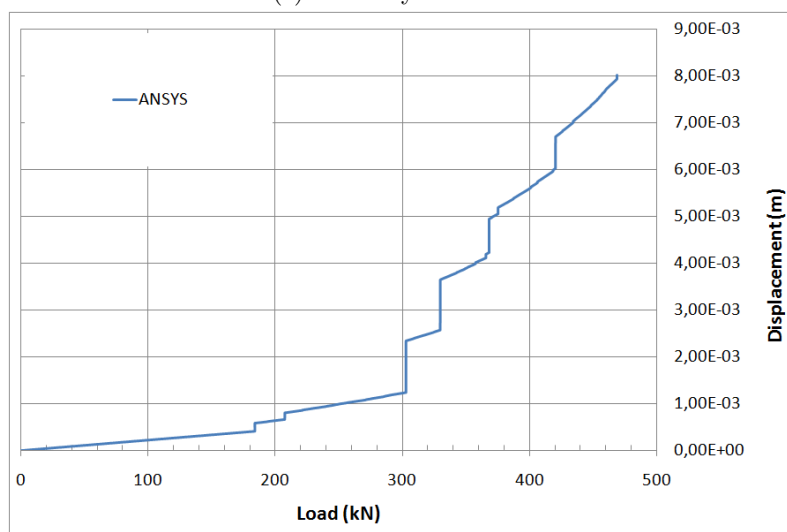(b) 3.0 m by 4.0 m wall.
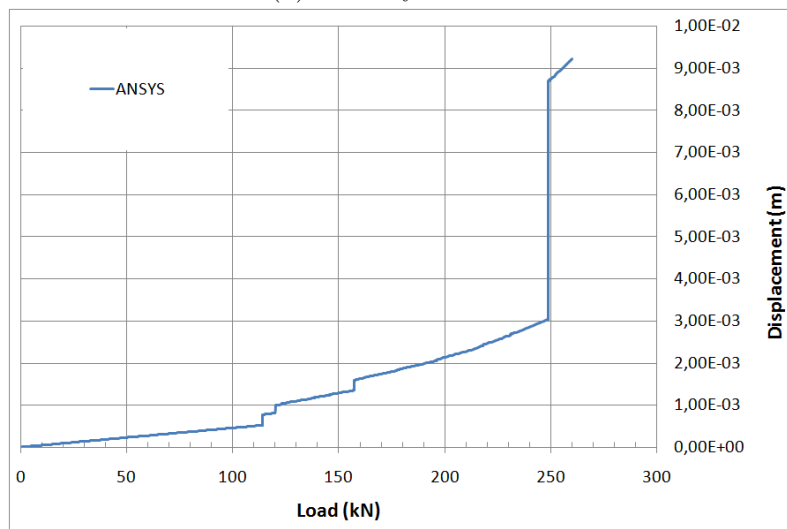
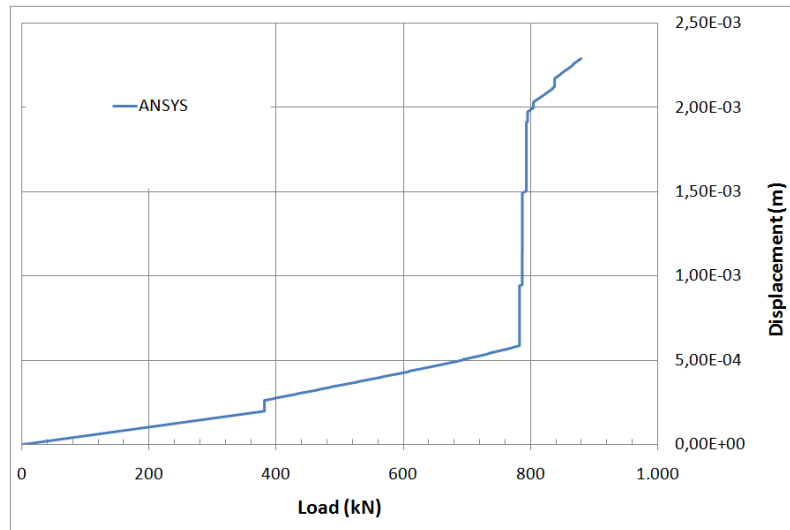(c) 3.0 m by 5.0 m wall.
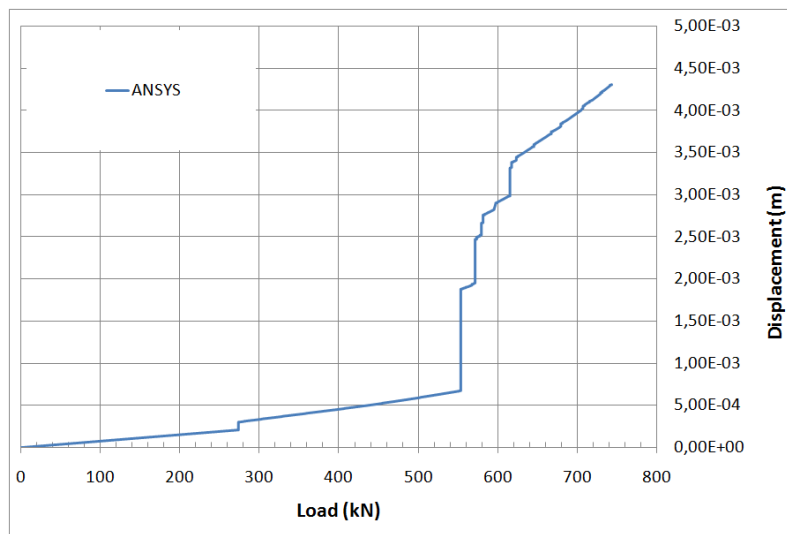
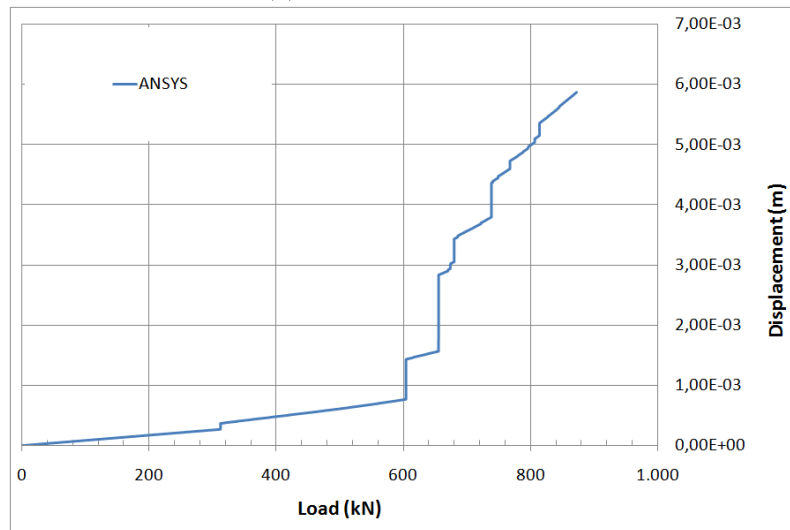(d) 4.0 m by 3.0 m wall.
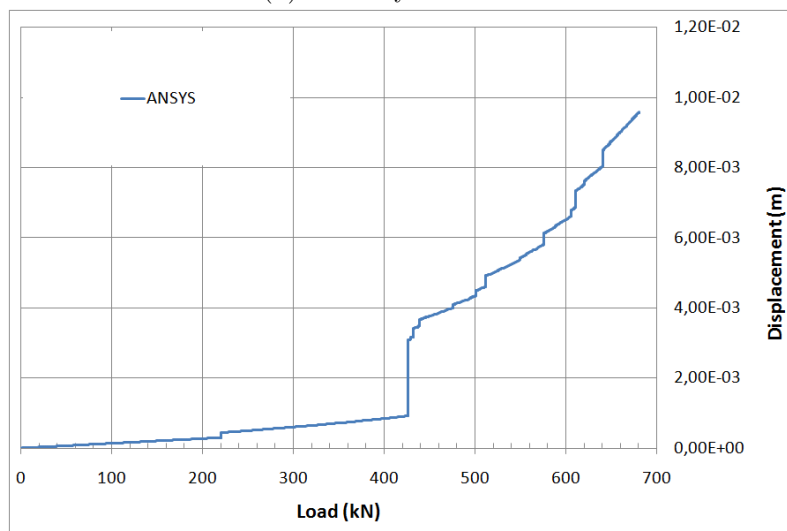
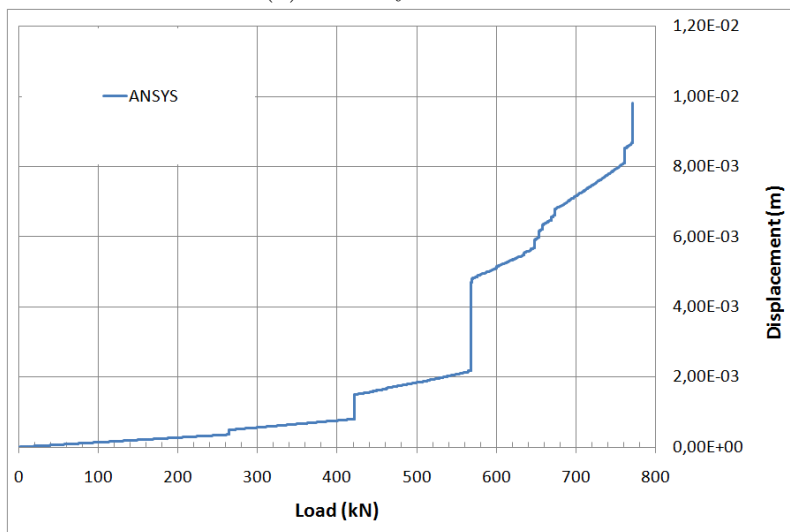(e) 4.0 m by 4.0 m wall.

(f) 4.0 m by 5.0 m wall.

(g) 5.0 m by 3.0 m wall.

(h) 5.0 m by 4.0 m wall.

(i) 5.0 m by 5.0 m wall.

Figure 68: FE model results using open and closed shear transfer coefficients 0.4 and 0.8 respectively.